



Spotlight on Heterogeneity: Measuring and Modelling Stream – Aquifer Interactions

Ph. D. Thesis

presented to the faculty of Sciences of the University of Neuchâtel
to satisfy the requirements for the degree of Doctor of Philosophy in Science

by

Edda Kalbus

Thesis defence date: 13 May 2009

Public presentation date: 29 May 2009

Ph. D. Thesis Evaluation Committee:

Prof. Dr. Mario Schirmer, University of Neuchâtel (co-directeur de thèse)

Prof. Dr. Daniel Hunkeler, University of Neuchâtel

Prof. Dr. Peter Engesgaard, University of Copenhagen

Prof. Dr. François Zwahlen, University of Neuchâtel (directeur de thèse)

IMPRIMATUR POUR LA THESE

Spotlight on Heterogeneity: Measuring and Modelling Stream – Aquifer Interactions

Edda Kalbus

UNIVERSITE DE NEUCHATEL

FACULTE DES SCIENCES

La Faculté des sciences de l'Université de Neuchâtel,
sur le rapport des membres du jury

MM. F. Zwahlen (directeur de thèse), M. Schirmer (co-directeur de thèse),
D. Hunkeler et P. Engesgaard (Copenhagen, DK)

autorise l'impression de la présente thèse.

Neuchâtel, le 25 mai 2009

Le doyen :
F. Kessler

UNIVERSITE DE NEUCHATEL
FACULTE DES SCIENCES
Secrétariat - décanat de la faculté
Rue Emile-Argand 11 - CP 158
CH-2009 Neuchâtel
Felix Kessler

MEINEN ELTERN

Abstract

Interactions between groundwater and streams play an important role for the functioning of stream ecosystems. Most nutrient cycling and stream metabolism takes place in the transition zone between aquifers and streams. Since flow patterns are the major controlling factor for the transformation of dissolved compounds in the transition zone, the characterization and quantification of flow is an important component for integrated river basin management and the protection of both groundwater and surface water resources. The flow pathways in the transition zone commonly display a complex pattern, resulting from heterogeneities in the permeability distribution in the aquifer and in the streambed sediments. A careful selection of measuring methods is therefore required to capture the range of flows as a consequence of subsurface heterogeneities on the one hand, and to obtain representative results on the other hand.

At the Schachtgraben, a small stream in the industrial area of Bitterfeld/Wolfen, Germany, contaminated groundwater discharges into the stream. The general objectives of this study were the determination of water and contaminant fluxes between the contaminated aquifer and the Schachtgraben stream and the investigation of the underlying processes and controlling factors with a focus on subsurface heterogeneity.

A review of measuring methods revealed that numerous methods exist which are either applied in the aquifer, in the surface water, or in the transition zone itself. The methods differ in resolution, sampled volume, and the time scales they represent. A multi-scale approach combining multiple techniques can considerably reduce uncertainties and constrain estimates of fluxes between groundwater and surface water.

For the quantification of water and solute flows at the stream – aquifer interface of the Schachtgraben, two novel approaches were combined into an efficient new methodology: Streambed temperature mapping for determining the spatial distribution and magnitude of groundwater discharge through the streambed, and integral pumping tests for the estimation of average contaminant concentrations and mass flow rates in the groundwater migrating toward the stream. The combination of these methods yielded potential contaminant mass fluxes between aquifer and stream.

The water fluxes between aquifer and stream at the investigated stream reach showed substantial heterogeneity, which is commonly assumed to be a result of a heterogeneous distribution of permeabilities within the connected aquifer. Observed streambed temperatures indicated zones of high or low groundwater discharge and, thus, zones of high or low permeability. Application of a two-dimensional groundwater flow and heat transport model showed that the heterogeneity of the aquifer can be inferred from streambed temperatures. The variance of the logarithm of hydraulic conductivities as input data for a stochastically generated permeability distribution was calibrated with observed streambed temperatures to simulate the observed temperature and groundwater flux distribution in the investigated streambed.

In addition to the properties of the aquifer, the properties of the streambed sediments may further contribute to a heterogeneous distribution of groundwater fluxes through the streambed. Four scenarios with different aquifer and streambed permeability distributions were defined to simulate and assess the impact of aquifer and streambed heterogeneity on the distribution of groundwater fluxes through the streambed. The results showed that the aquifer has a stronger influence on the distribution of groundwater fluxes through the streambed than the streambed itself.

Kurzfassung

Interaktionen zwischen Grundwasser und Flüssen spielen eine wichtige Rolle für Fluss-Ökosysteme. Ein Großteil des Nährstoffkreislaufs findet in der Übergangszone zwischen Aquifer und Fluss statt. Die Verteilung der Wasserströme im Flussbett hat einen maßgeblichen Einfluss auf die Umwandlung von Stoffen in der Übergangszone. Daher leistet die Charakterisierung und Quantifizierung der Fließvorgängen einen wichtigen Beitrag für den Schutz von Wasserressourcen. Die Fließwege in der Übergangszone zeigen oft ein komplexes Muster, das aus der Heterogenität der Durchlässigkeiten im Aquifer und in den Flussbettsedimenten resultiert. Eine sorgfältige Auswahl an Messmethoden ist notwendig um einerseits die Spannweite der Durchflüsse zu erfassen, und andererseits repräsentative Ergebnisse zu erhalten.

Am Schachtgraben, einem kleinen Fluss in der Industrieregion Bitterfeld/Wolfen, Deutschland, fließt kontaminiertes Grundwasser in den Fluss. Ziel dieser Arbeit war die Bestimmung von Wasser- und Stoffflüssen zwischen dem kontaminierten Aquifer und dem Schachtgraben, sowie die Untersuchung der maßgeblichen Prozesse und Einflussfaktoren unter besonderer Berücksichtigung der Untergrund-Heterogenität.

Eine Literaturübersicht über Messmethoden zeigte, dass zahlreiche Methoden existieren, die entweder im Aquifer, im Oberflächengewässer oder direkt in der Übergangszone angewandt werden. Die Methoden unterscheiden sich in ihrer Auflösung, dem Probevolumen, und den Zeitskalen für die sie repräsentativ sind. Die Kombination verschiedener Methoden auf unterschiedlichen Skalen kann zu einer maßgeblichen Reduzierung von Unsicherheiten führen und die Abschätzung von Massenflüssen erheblich verbessern.

Zur Quantifizierung von Wasser- und Stoffflüssen an der Schnittstelle zwischen Grundwasser und Fluss wurden zwei neuartige Methoden zu einer effizienten neuen Vorgehensweise kombiniert: Die Kartierung von Flussbett-Temperaturen zur Bestimmung der räumlichen Verteilung und Größe des Grundwasserzustroms durch das Flussbett, und integrale Pumpversuche zur Abschätzung der durchschnittlichen Schadstoffkonzentrationen im Grundwasser. Die Kombination dieser Methoden ermöglichte die Bestimmung potentieller Schadstoffmassenflüsse zwischen Aquifer und Fluss.

Die Wasserflüsse zwischen Aquifer und Fluss waren durch erhebliche räumliche Heterogenitäten im untersuchten Flussabschnitt gekennzeichnet, was auf eine heterogene Verteilung der Durchlässigkeiten im angeschlossenen Aquifer zurückzuführen ist. Die gemessenen Flussbett-Temperaturen weisen auf Zonen hohen oder niedrigen Grundwasserzustroms hin, und damit auf Zonen hoher oder niedriger Durchlässigkeiten. In einem Grundwasserfluss- und Wärmetransportmodell wurde gezeigt, dass die Heterogenität des Aquifers aus Flussbett-Temperaturen hergeleitet werden kann. Die Varianz der Durchlässigkeitsbeiwerte als Eingangsdaten für die Generierung von stochastisch verteilten Durchlässigkeitsfeldern wurde mit gemessenen Flussbett-Temperaturen kalibriert, um die beobachtete Verteilung von Temperaturen und Durchflüssen im untersuchten Flussbett zu simulieren.

Zusätzlich zu den Aquifereigenschaften können die Eigenschaften der Flussbett-Sedimente ebenso zu einer heterogenen Verteilung von Grundwasserzuflüssen durch das Flussbett beitragen. Vier Szenarien mit unterschiedlichen Verteilungen der Durchlässigkeiten im Aquifer sowie im Flussbett wurden definiert, um den Einfluss der Aquifer- und Flussbettheterogenität auf die Verteilung der Durchflüsse durch das Flussbett zu simulieren und zu untersuchen. Die Ergebnisse zeigten, dass der Aquifer einen stärkeren Einfluss auf die Verteilung der Durchflüsse hat als die Flussbettsedimente selbst.

Résumé

Les interactions entre les eaux souterraines et les cours d'eau jouent un rôle important pour le fonctionnement des écosystèmes fluviaux. La plupart des cycles de nutriments et du métabolisme des cours d'eau à lieu dans la zone de transition entre l'aquifère et le cours d'eau. Puisque les patrons d'écoulement des eaux souterraines sont des facteurs majeurs de contrôle de la transformation des substances dans la zone de transition, la caractérisation et la quantification de ces écoulements sont importantes pour la gestion et la protection des ressources des eaux souterraines et des eaux de surface. Les trajectoires d'écoulement dans la zone de transition présentent communément un motif complexe qui résulte d'hétérogénéités dans la distribution de la perméabilité dans l'aquifère et dans les sédiments du lit des cours d'eau. Une sélection minutieuse des méthodes de mesure est par conséquent nécessaire pour identifier ces trajectoires d'écoulement en fonction de l'hétérogénéité des milieux poreux d'une part et pour obtenir des résultats représentatifs d'autre part.

Le long du petit cours d'eau Schachtgraben dans la zone industrielle de Bitterfeld/Wolfen en Allemagne, des eaux souterraines contaminées se déversent dans ce cours d'eau. Afin de mieux comprendre ce problème de contamination, les objectifs généraux de la présente étude sont de déterminer les flux d'eau et de contaminants entre l'aquifère contaminée et le Schachtgraben ainsi que d'étudier les processus sous-jacents et les facteurs déterminants tout en tenant compte de l'hétérogénéité des milieux.

Un examen des méthodes de mesure révèle que de nombreuses méthodes existent qu'elles peuvent être employées soit pour la caractérisation de l'aquifère, soit pour les eaux de surface ou soit pour la zone de transition elle-même. Les méthodes diffèrent au niveau de leur résolution, du volume d'échantillonnage et des échelles temporelles qu'elles représentent. Une approche multi-échelle qui combine plusieurs techniques peut réduire considérablement les incertitudes et améliorer les estimations des flux entre les eaux souterraines et de surface.

Pour la quantification des flux d'eau et des substances dissoutes à l'interface entre l'aquifère du Schachtgraben et le cours d'eau, deux nouvelles approches ont été combinées dans une nouvelle méthode performante: il s'agit de la mesure des températures du lit de la rivière pour déterminer la distribution spatiale et l'amplitude du déversement des eaux souterraines à travers le lit, et des tests de pompage intégral pour l'estimation des concentrations moyennes des contaminants et des taux de flux de masses dans les eaux souterraines qui migrent vers la rivière. La combinaison de ces méthodes fournit les flux potentiels de masse de contaminants entre l'aquifère et le cours d'eau.

Les flux d'eau entre l'aquifère et le cours d'eau, sur la section étudiée, ont montré une hétérogénéité substantielle qui est associée à la distribution hétérogène des perméabilités au sein de l'aquifère connecté au cours d'eau. Les températures observées dans le lit de la rivière indiquent des zones à haut ou bas écoulement et donc des zones à haute et basse perméabilité. Dans un modèle à deux dimensions d'écoulement des eaux souterraines et de transport de chaleur, il a été montré que l'hétérogénéité de l'aquifère peut être déduite des températures du lit de la rivière. La variance du logarithme des conductivités hydrauliques qui a été utilisée comme donnée d'entrée d'une distribution des perméabilités générée stochastiquement a été calibrée avec les températures du lit observées pour simuler les températures observées et la distribution de flux des eaux souterraines dans le lit étudié.

En plus des propriétés de l'aquifère, les propriétés des sédiments du lit des rivières peuvent aussi contribuer à la distribution hétérogène des flux souterrains à travers le lit. Quatre scénarios

avec différentes distributions des perméabilités de l'aquifère et du lit ont été définis pour simuler et évaluer l'impact de l'hétérogénéité de l'aquifère et du lit sur la distribution des flux d'eau à travers le lit. Les résultats montrent que l'aquifère a une plus forte influence sur la distribution des flux d'eaux souterraines à travers le lit que le lit lui-même.

Contents

1	Introduction	1
1.1	Stream – aquifer interactions	1
1.2	Description of the study site	3
1.2.1	Background	3
1.2.2	Geology	4
1.2.3	Hydrogeology	5
1.2.4	The Schachtgraben stream	6
1.3	Objectives and structure of present thesis	6
2	Measuring methods for groundwater – surface water interactions: a review	9
2.1	Introduction	10
2.2	Direct measurements of water flux	11
2.3	Heat tracer methods	12
2.4	Methods based on Darcy’s Law	14
2.4.1	Hydraulic gradient	14
2.4.2	Hydraulic conductivity	15
2.4.3	Groundwater velocity	17
2.4.4	Porosity	17
2.5	Mass balance approaches	18
2.5.1	Incremental streamflow	18
2.5.2	Hydrograph separation	18
2.5.3	Environmental tracer methods	19
2.5.4	Solute tracer methods	19
2.6	Methods to determine contaminant concentrations	20
2.6.1	Monitoring wells	20
2.6.2	Passive samplers	20
2.6.3	Integral pumping tests	21
2.6.4	Grab samples	21
2.6.5	Seepage meters	21
2.7	Discussion	22
2.7.1	Measurement Scales	22
2.7.2	Groundwater discharge versus hyporheic exchange flow	23
2.7.3	Considerations for choosing appropriate methods	24
2.8	Summary	26

3	Methodology to investigate contaminant mass fluxes at the stream-aquifer interface	27
3.1	Introduction	28
3.2	Study site	29
3.3	Methods	31
3.3.1	Streambed temperature mapping	31
3.3.2	Integral pumping tests	32
3.3.3	Concept of method combination	34
3.4	Results and discussion	35
3.4.1	Results of streambed temperature mapping	35
3.4.2	Results of the integral pumping tests	37
3.4.3	Potential contaminant mass flux to the stream	38
3.5	Conclusions	40
4	How streambed temperatures can contribute to the determination of aquifer heterogeneity	41
4.1	Introduction	42
4.2	Study site	43
4.3	Streambed temperature mapping	43
4.4	Numerical modeling	44
4.4.1	Model set-up	44
4.4.2	Input parameters	46
4.5	Adjusting the aquifer heterogeneity	47
4.6	Discussion	49
4.7	Summary and conclusion	51
5	Influence of aquifer and streambed heterogeneity on the distribution of groundwater discharge	53
5.1	Introduction	54
5.2	Background	55
5.3	Methodology	56
5.3.1	Model set-up	56
5.3.2	Scenarios	58
5.4	Results and discussion	58
5.5	Conclusions	62
6	Summary, conclusions and perspectives	65
6.1	Summary	65
6.1.1	The study site	65
6.1.2	Objectives	65
6.1.3	Review of measuring methods	66
6.1.4	Methods applicable at the study site	66
6.1.5	Contaminant mass fluxes at the stream – aquifer interface	67
6.1.6	Heterogeneity in fluxes through the streambed resulting from aquifer properties	68
6.1.7	Influence of aquifer and streambed heterogeneity on the distribution of fluxes	69
6.2	Conclusions	70

6.3 Perspectives	72
Bibliography	75
Acknowledgements	89
Annex 1 – Integral Pumping Test Data	91
Annex 2 – Injection Logs and Slug Tests	99

List of Figures

1.1	Location of the study site, extent of the groundwater contamination (after <i>Heidrich et al.</i> , 2004a), and position of integral pumping test (IPT) wells and sampling locations of injection logs, slug tests, and temperature profiles.	4
1.2	Cross-section through the subsurface of the study site generated from borehole data. W11 is a groundwater monitoring well.	5
2.1	Spatial measuring scales of the different methods to measure interactions between groundwater and surface water. The spatial scale is given as radius or distance of influence. Dots represent point measurements (pm).	22
2.2	Exchange flows between groundwater and surface water through the hyporheic zone at a riffle-pool-sequence (after <i>Winter et al.</i> , 1998).	24
3.1	Location of the study site and position of the streambed temperature measurements and the integral pumping test (IPT) wells W11, W12, W13, and W14.	30
3.2	Section of the MODFLOW model showing isochrone geometry for the four IPT wells. Samples were collected every 3 h (each isochrone corresponds to a time of sampling), total pumping time was 5 days. The grid was refined around the wells (shaded areas on left-hand side of figure).	34
3.3	Conceptual model of combined method to determine contaminant mass flows at the stream-aquifer interface. (a) Cross-section showing water and contaminant mass flows at the control plane (Q_{CP} , M_{CP}), through the streambed (Q_S , M_S), and below the stream (Q_U , M_U); (b) Plan view showing the subdivision into zones k with average concentrations $C_{av}^{(k)}$ associated with one IPT well, and sections j associated with one temperature profile for calculation of mass flow rates through the streambed $M_S^{(j)}$. Zone $k = 1$ includes sections $j = 1, 2, \dots, 5$; zone $k = 2$ includes sections $j = 6, 7, \dots, 10$	35
3.4	Spatial distribution of groundwater fluxes through the streambed in sections j ($q_z^{(j)}$), average contaminant concentrations in zones k ($C_{av}^{(k)}$) corresponding to the capture zones illustrated by isochrones of wells W11 to W14, and potential contaminant mass fluxes through the streambed in sections j ($J_S^{(j)}$). Values for DCB are given as sum of isomers.	36
3.5	Concentration time series measured at the four IPT wells (W11 to W14) and the Schachtgraben Stream (SG) of (a) MCB, (b) 1,2-DCB, (c) 1,3-DCB, (d) 1,4-DCB.	39

4.1	Study site with location of the injection logs, slug tests (at 2-3 depths at each location) and temperature profiles. The stream section where the temperatures were measured corresponds to the model domain.	44
4.2	a) Conceptual model with grid resolution, boundary conditions and one example of a simulated temperature distribution using the K -field displayed in d. q_z is the vertical groundwater flux through the streambed. b) to d) realizations of K -fields with different variances of $\ln(K)$. Displayed is realization Nr. 1 out of 50 generated realizations for each variance. Vertical exaggeration is approx. 10x	45
4.3	Simulated and observed groundwater fluxes (q_z) and temperatures at a depth of 50 cm below the streambed (T_{50}). Box plots show maximum and minimum (dots), 90 th and 10 th percentile (error bars), 75 th and 25 th percentile (box), arithmetic mean (solid line), and median (dashed line). Simulated data are complete data from 50 realizations with $\sigma_{\ln(K)}^2 = 0.08$ ($n = 11000 \hat{=} 50$ realizations with 220 grid elements each). Observed data are complete data of the two transects ($n = 140$).	48
4.4	Relation between the variance of $\ln(K)$ ($\sigma_{\ln(K)}^2$) and the variance of simulated temperatures at a depth of 50 cm ($\sigma_{T_{50}}^2$). The variance of the measured temperatures at a depth of 50 cm ($\sigma_{T_{50}}^2 = 2.9$) leads to a required variance of hydraulic conductivity of $\sigma_{\ln(K)}^2 = 2.06$	49
4.5	Simulated and observed groundwater fluxes (q_z) and temperatures at a depth of 50 cm below the streambed (T_{50}). Box plots show maximum and minimum (dots), 90 th and 10 th percentile (error bars), 75 th and 25 th percentile (box), arithmetic mean (solid line), and median (dashed line). Simulated data are complete data from 10 selected realizations with $\sigma_{\ln(K)}^2 = 2.16$ ($n = 2200 \hat{=} 10$ realizations with 220 grid elements each). Observed data are complete data of the two transects ($n = 140$).	50
4.6	Distribution of groundwater flux through the streambed with respect to the streambed area (mean flux of 50 realizations per variance; selected = mean flux of the 10 selected realizations with a mean variance of $\sigma_{\ln(K)}^2 = 2.16$).	51
5.1	Model definition and boundary conditions	56
5.2	Observed (top left; after <i>Schmidt et al.</i> (2006)) and simulated (base case and Cases A–D) results showing temperature (colour maps) and flux distributions (white curves) in the streambed (represented by the upper grey zone in Figure 5.1). Temperature data are shown at streambed depths between 0.1 and 0.5 m corresponding to the observations. Simulated results are shown from one example out of ten K -field realizations (the same realization is shown in all scenarios). Vertical exaggeration is approx. 100x.	59
5.3	Box plots of the groundwater discharge through the streambed showing 95 th and 5 th percentile (dots), 90 th and 10 th percentile (error bars), 75 th and 25 th percentile (box), arithmetic mean (solid line), and median (dashed line). Observed data are complete data of the mapping programme ($n = 140$), simulated data are the complete data set from all 10 realizations ($n = 2200$) for each case.	60
5.4	Distribution of groundwater fluxes through the streambed in relation to the streambed area. Bands show the full range between maximum and minimum values of observations and modelling results, respectively.	61

5.5 Standard deviation of groundwater flux through the streambed, $\sigma(q)$, in relation to the connectivity indicator $1/CT_1$ for Case C and Case D. 62

List of Tables

3.1	Comparison of average contaminant concentrations C_{av} obtained from the analytical solution (AS) and CSTREAM (CS).	37
3.2	Contaminant mass fluxes J_{CP} at the four IPT wells obtained from CSTREAM.	38
4.1	Parameters of the numerical model	46
4.2	Input data for FGEN to generate stochastic K -fields from field data	47
5.1	Aquifer and streambed properties of all simulation cases. K = hydraulic conductivity, σ^2 = variance of $\ln(K)$, λ_x and λ_z = correlation lengths in the x- and z-directions.	57

Introduction

1.1 Stream – aquifer interactions

Groundwater and streams are often treated as isolated components of the hydrologic cycle. However, they are closely linked together and interact in many different ways. Streams are commonly hydraulically connected to groundwater, with stream water passing back and forth between the stream channel and the subsurface (*Castro and Hornberger, 1991; Bencala, 1993*). Thus, depletion or degradation of one will affect the other. Contaminated groundwater discharging to streams may result in a long-term deterioration of surface water. Conversely, polluted streams can be a major source of contamination to aquifers. Understanding the interactions between groundwater and surface water is therefore critical for the development of strategies to protect both groundwater and surface water resources and ecosystem functions.

The interactions between groundwater and streams are complex, proceeding on various spatial and temporal scales. Effects of topography, geology, and climate lead to multiple flow systems of different orders of magnitude and of relative, nested hierarchical order (*Tóth, 1963*). Heterogeneities in the hydrogeological and geomorphological characteristics of the catchment and the subsurface result in further diversions of flow pathways. Seasonal variations in the climatic conditions influence the runoff regime and the direction of stream – aquifer interactions. For instance, during conditions of low precipitation, the groundwater maintains the baseflow. More than 90% of the summer discharge in some rivers may come from groundwater (*COM, 2003*). Conversely, during conditions of high precipitation, increased surface runoff and interflow result in higher discharge rates and water levels in streams, leading to infiltration of stream water and recharge of the aquifer. Bank infiltration reduces flood levels and stores water in the subsurface which can later be released to compensate a decrease in stream discharge during dry seasons. Thus, the water exchange between groundwater and streams has a buffering effect on the runoff regimes of streams (*Brunke and Gonser, 1997*).

The transition zone between groundwater and streams plays a critical role in the mediation of interaction processes. It has features of both adjacent hydrological units. Permeable sediments with high substrate stability, saturated conditions, and low flow velocities correspond to the characteristics of terrestrial aquifers. In contrast to aquifers, however, the transition zone may contain some proportion of surface water with other qualities due to the infiltration of stream water into the pore space. Ecologists have termed this area the hyporheic zone (*Schwoerbel,*

1961), an expression which derives from the Greek words for flow (rheo) and under (hypo) and describes the area beneath and adjacent to the stream between the stream channel and the aquifer. From a hydrological point of view, the hyporheic zone can be defined as the part of the streambed sediments where surface water and groundwater mix (*Triska et al.*, 1989). Ecologically, the zone provides habitat for stream organisms and biofilm-forming microorganisms and is characterized by steep gradients of physicochemical parameters. Most of biogeochemical nutrient cycling and stream metabolism take place in the hyporheic zone (*Mulholland and DeAngelis*, 2000; *Pusch and Schwoerbel*, 1994; *Triska et al.*, 1993). Thus, hyporheic functions must be regarded significant for the protection of water resources (*Boulton et al.*, 1998; *Sophocleous*, 2002). As transport, degradation, transformation, precipitation, or sorption of substances may take place in the hyporheic zone, it acts as a filter which buffers against physical and chemical influences between groundwater and surface water (*Brunke and Gonser*, 1997).

The size and activity of the hyporheic zone are largely controlled by the input of heat, oxygen, nutrients, and organic matter through advective transport with the infiltrating stream water (*Mutz et al.*, 2007). Therefore, the vertical surface – subsurface flux (hyporheic exchange) of water plays an important role for the stream metabolism. However, when groundwater discharges to a stream, it may counteract the infiltration of stream water. The spatial extent of the hyporheic zone may be diminished by the groundwater discharge (*Cardenas and Wilson*, 2007) leading to reduced hyporheic functions. Hence, it is necessary to understand the mechanisms of stream – aquifer interactions and investigate the flow rates and pathways at the stream – aquifer interface to enable an assessment of the capacity of the hyporheic zone to transform, degrade, or retain nutrients or contaminants.

Stream – aquifer interactions basically proceed in two ways: groundwater flows through the streambed into the stream (gaining stream), or stream water infiltrates through the sediments into the groundwater (losing stream). Often, a stream is gaining in some reaches and losing in others. The direction of the exchange flow depends on the hydraulic gradient. In gaining reaches, the elevation of the groundwater table is higher than the elevation of the stream stage. Conversely, in losing reaches the elevation of the groundwater table is lower than the elevation of the stream stage. Losing streams can be connected to the groundwater by a saturated zone or can be disconnected from the groundwater system by an unsaturated zone when the groundwater table is below the streambed. Seasonal variations in precipitation patterns as well as single precipitation events can alter groundwater tables and stream stages and thereby cause temporal changes in the direction and magnitude of exchange flows.

Observations of the elevation of the stream stage and the groundwater table in a near-by monitoring well deliver information whether a stream reach is generally in gaining or losing conditions. However, heterogeneities of the subsurface can lead to zones of groundwater discharge within net-losing reaches and vice versa. Anyway, the groundwater discharge through the streambed is commonly not uniformly distributed over the reach length, but rather occurs in locally distinct discharge areas.

One major influence on the distribution of groundwater fluxes through the streambed is the heterogeneity in permeability of the connected aquifer. Alluvial deposits are stratigraphically complex, commonly displaying a high degree of heterogeneity in their sediment properties (*Mi-all*, 1996). Values of hydraulic conductivity may range over several orders of magnitude. The spatial arrangement of high- and low-permeability zones has considerable effects on the distribution of flow paths between aquifers and streams (*Wroblicky et al.*, 1998; *Dahm et al.*, 1998; *Winter et al.*, 1998). Another strong effect may result from the streambed properties. Also

streambed deposits commonly display substantial heterogeneities in the distribution of permeabilities, leading to preferential flow paths. High-discharge zones in the streambed may therefore occur where highly permeable deposits in the streambed are connected to underlying highly permeable zones in the aquifer (Conant, 2004). On the other hand, colmation of the streambed due to intrusion of fine sediments into the pore spaces may significantly reduce water fluxes through the streambed. However, in gaining stream reaches, the upwelling groundwater counteracts siltation (Schaelchli, 1993), so that the influence of colmation is more pronounced in losing streams.

The distribution of water fluxes through the streambed may further be altered by hyporheic exchange flows. Hyporheic exchange is induced by discontinuities in stream slope and water depth resulting from riffle-pool sequences or obstacles on the streambed such as large cobbles, wood pieces, or natural bedforms (e.g., gravel bars, ripples) (Thibodeaux and Boyle, 1987; Savant *et al.*, 1987). Pressure gradients at these discontinuities lead to downwelling of stream water into the sediments, replacing interstitial water. The infiltrated stream water travels for some distance as underflow beneath the streambed surface and returns to the stream at some low-pressure zone downstream.

The heterogeneities of the aquifer and streambed properties and, in addition, the heterogeneities of the streambed morphology result in a very complex pattern of flow pathways and fluxes through the streambed. However, the flow patterns are the major controlling factor of the physicochemical gradients at the stream – aquifer interface (Brunke and Gonser, 1997). It is, therefore, essential to characterize and quantify the flow between groundwater and streams in order to take advantage of the processes occurring in the streambed with respect to the protection and management of water resources. Nevertheless, the interactions are difficult to observe and measure, because they take place mainly in the subsurface and are characterized by substantial heterogeneities on various spatial and temporal scales.

1.2 Description of the study site

1.2.1 Background

The study site is located in the industrial area of Bitterfeld/Wolfen, about 130 km south of Berlin, Germany. This region is one of the oldest industrial centres of Germany (Heidrich *et al.*, 2004a,b). In the 1890s, the first chemical plants were constructed in this region because of the large lignite deposits found near-by. Low-cost lignite, potash deposits, water supply from the Mulde river, and good railway connections attracted the chemical industry (Derlien *et al.*, 1999). Initially, the chemical production focused on producing and manufacturing chlorine, sodium hydroxide, aluminium, and magnesium (Walkow, 2000). Later, the production was extended to nearly all sectors of organic chemistry comprising about 5000 different substances over the years.

Waste products were usually disposed in abandoned mining pits near-by without installation of bottom sealings. Today, about 20 dumping sites are known in the Bitterfeld region (Heidrich *et al.*, 2004a). Moreover, time-worn manufacturing facilities, war damages, inappropriate handling and transport of hazardous chemicals, and missing environmental protection measures contributed to the large-scale contamination of soils and aquifers. 3200 potentially contaminated sites were identified in the Bitterfeld/Wolfen area, 269 of which with a high risk potential

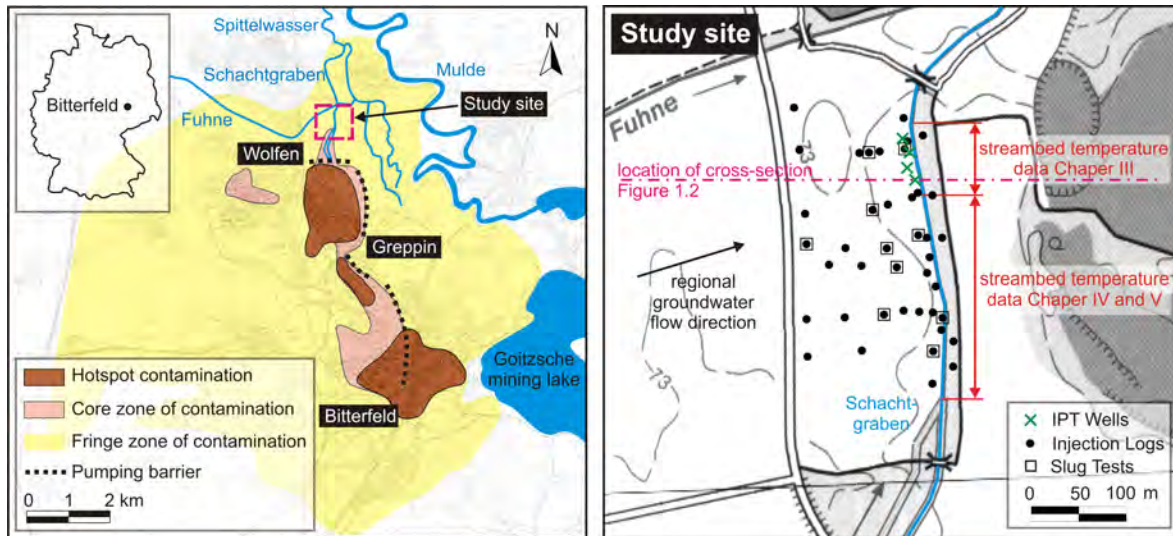


Figure 1.1. Location of the study site, extent of the groundwater contamination (after *Heidrich et al.*, 2004a), and position of integral pumping test (IPT) wells and sampling locations of injection logs, slug tests, and temperature profiles.

(*Derlien et al.*, 1999). The aquifer contamination has an estimated extent of 25 km² directly affecting more than 200 million m³ of groundwater (*Weiss et al.*, 2001). The main contaminants in the groundwater are volatile halogenated hydrocarbons, monoaromatic hydrocarbons such as BTEX or chlorinated benzenes and phenols, hexachlorocyclohexanes, polychlorinated biphenyls, dioxins, and a variety of other substances.

After the German reunification in 1990, most of the production plants were closed down and demolished, others were modernized and new companies were settled. The pumping of groundwater to lower the groundwater table for lignite mining has ceased and some of the mining pits have been flooded for recreation purposes. This caused a rise in groundwater levels and the general flow regime changed to the quasi-natural runoff regime with the main groundwater flow direction towards the Mulde river. The contamination of soils and aquifers has since been investigated and continues to be monitored within the framework of the Ecological Mega Project (ÖGP - Ökologisches Großprojekt) (*Lücke*, 2002). Around the core zones of contamination, pumping barriers have been installed to contain the contamination. However, the groundwater contamination has already expanded beyond the pumping barriers (Figure 1.1). In the north-east of the industrial area, several small streams interact with the aquifer and receive the contaminated groundwater.

1.2.2 Geology

The study region is located in the centre of the Halle-Wittenberg clod which basically consists of Permian rocks. The general geological profile is as follows (*Eismann*, 2002): The pre-quatarnary is formed by kaolinised porphyric rock. The solid rock surface lies at about 80 – 100 m below ground surface. Above the Paleozoic rocks are the Upper Eocene layers (clay, sand, gravel) with localized lignite seams. Then follows the Middle Oligocene Rupel clay at about 60 m below ground surface, which covers the entire study area. The overlying layer consists of Micaceous

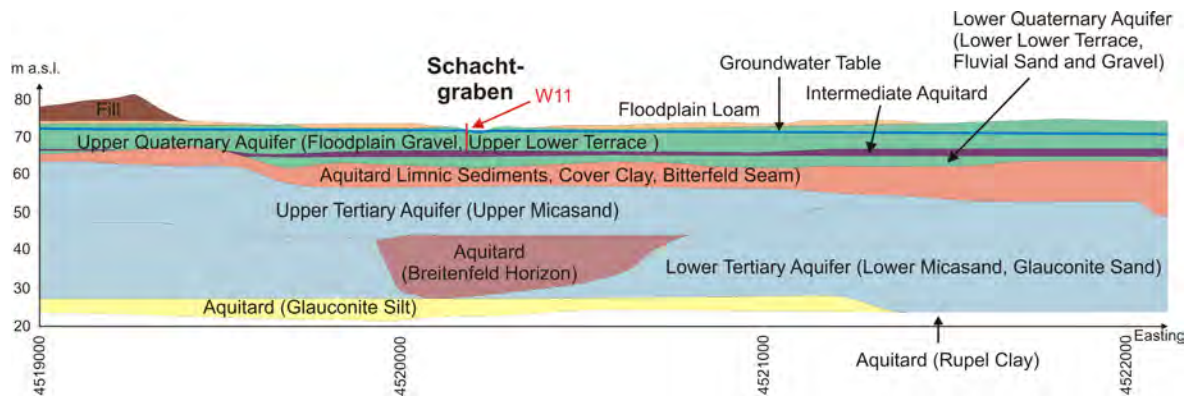


Figure 1.2. Cross-section through the subsurface of the study site generated from borehole data. W11 is a groundwater monitoring well.

sand, followed mostly by the Miocene Bitterfeld seam. The Pleistocene layers consist of Saalian fluvial sand and gravel with localized clay and till deposits. The uppermost layer is formed by Holocene humose sands. At the industrial sites, the upper layer has widely been excavated and replaced by various construction materials. Due to the extensive open-cast lignite mining, the geological structures are widely disturbed. Quaternary and Tertiary rocks have been excavated and the lignite has been exploited down to the Upper Oligocene Micaceous sands. The open-cast mining craters were filled with excavation material or municipal and industrial waste.

The stratigraphy at the study site was determined from a borehole data base containing 296 boreholes within an area of 17 km². A cross-section through the subsurface of the study site as determined from the borehole data is displayed in Figure 1.2.

1.2.3 Hydrogeology

The relevant layers with respect to water resources are the Tertiary and Quaternary deposits. The main aquifer is within the Bitterfeld Micasand Complex and has a thickness of up to 50 m. It consists of fine to medium sands with a mean hydraulic conductivity (K) of about 10^{-4} to 10^{-5} m s^{-1} . It is confined by a layer of Rupel Clay which is about 15 m thick with a hydraulic conductivity of $10^{-11} \text{ m s}^{-1}$. The overlying layer is, or was, respectively, the Bitterfeld Seam Complex, which is considered an aquitard. It is followed by the Quaternary aquifer which consists of Pleistocene sands and gravels ($K = 6 \times 10^{-4} \text{ m s}^{-1}$) of about 15 m thickness. Due to lignite mining, the Quaternary and Tertiary aquifers are locally connected. An intermediate aquitard consisting of silt, clay, and peat separates the Quaternary aquifer locally into two horizons. In the North of the study region, an Elsterian channel system determines the hydrogeological conditions. Fine-grained carbonaceous moraine deposits reach down to the Rupel clay layer and lead to reduced transmissivities.

1.2.4 The Schachtgraben stream

Our investigations were conducted at the Schachtgraben stream (Fig. 1.1). The stream is part of the Mulde river system which belongs to the Elbe basin. The Schachtgraben is a man-made stream which had originally been constructed for drainage water discharge from the open-cast lignite mines. Later, it was also used for waste water discharge from the chemical industry over a period of three decades until 1990. During this time, water levels in the stream were presumably higher than the groundwater table, leading to an infiltration of contaminated stream water and accumulation of contaminants in the streambed sediments. Today, water table elevations in the aquifer are generally higher than the Schachtgraben water level, so that the Schachtgraben can be classified as a generally gaining stream.

The Schachtgraben partially penetrates the Quaternary alluvial aquifer (Figure 1.2). At the study site, this aquifer is locally subdivided into two horizons. The unconfined shallow horizon, which is connected to the Schachtgraben, consists of sandy gravel. The streambed is composed of crushed rock. The interstices of the coarse crushed rock grains are filled with allochthonous, sandy, alluvial material. The stream has an average width of 3 m and an average water depth of 0.6 m. The mean discharge is $0.2 \text{ m}^3 \text{ s}^{-1}$ at a slope of 0.0008 m m^{-1} .

The dominant contaminants in the Quaternary aquifer at the study site, which is connected to the Schachtgraben, are chlorinated benzenes. The contamination source is believed to be in the southern part of the former Bitterfeld Chemical Works facilities (*Heidrich et al.*, 2004a), about 3.5 km south of the study site. Along the Schachtgraben, the contamination is predominantly diffuse. However, the contaminant distribution as well as the properties of the aquifer and streambed sediments may be locally very heterogeneous. A major challenge, therefore, is a careful selection of measuring methods in combination with modelling efforts to reliably determine water and contaminant mass fluxes between aquifer and stream in the complex setting of the study site.

1.3 Objectives and structure of present thesis

The general objectives of this study were the determination of water and solute fluxes between the contaminated aquifer at the study site and the Schachtgraben stream and the investigation of the underlying processes and controlling factors with a focus on subsurface heterogeneity. Appropriate measuring and modelling approaches should be selected and applied which, on the one hand, capture small-scale heterogeneities and allow an assessment of the full range of fluxes between aquifer and stream, and, on the other hand, provide robust and representative flux estimates. The selected approaches should furthermore be generally applicable to various hydrogeological settings.

The first step involved a literature review of currently available field methods for measuring groundwater–surface water interactions (Chapter II). This enabled the selection of methods appropriate for the study purpose and applicable at the study site.

Chapter III describes a methodology for the estimation of the mass flux of contaminants between groundwater and surface water. Two novel measuring methods were combined to an efficient new methodology for quantifying water and solute flows at the stream - aquifer interface: Streambed temperature mapping for determining the spatial distribution and magnitude of groundwater discharge through the streambed and integral pumping tests for the estimation of

average contaminant concentrations and mass flow rates in the groundwater migrating towards the stream.

Heterogeneous distributions of aquifer properties constitute a major challenge for a reliable estimation of water and solute flow pathways and mass flow rates. Substantial heterogeneity of groundwater discharge was observed at the study stream. Therefore, a further objective was to find a methodology to use high-resolution streambed temperature measurements for the calibration of a stochastic groundwater flow model (Chapter IV) to enable a realistic representation of the distribution of groundwater discharge.

The heterogeneity of the groundwater discharge to a stream may not only be a result of the heterogeneous distribution of aquifer properties, but may also be influenced by the properties of the streambed sediments. Another objective, therefore, was to investigate the influence of the heterogeneity of both the aquifer and the streambed sediments on the distribution of fluxes through the streambed (Chapter V). In numerical simulations, different combinations of aquifer and streambed heterogeneity were used to evaluate which of these hydrological units has a stronger influence on the flux distribution.

Chapter VI contains a summary of the previous chapters, presents the main outcomes and conclusions of the present study and gives recommendations for future research.

**Measuring methods for groundwater – surface water interactions:
a review**

This chapter is published as:

Kalbus, E., Reinstorf, F. and Schirmer, M. (2006): Measuring methods for groundwater – surface water interactions: a review. *Hydrology and Earth System Sciences*, 10, 873-887.

Abstract. Interactions between groundwater and surface water play a fundamental role in the functioning of riparian ecosystems. In the context of sustainable river basin management it is crucial to understand and quantify exchange processes between groundwater and surface water. Numerous well-known methods exist for parameter estimation and process identification in aquifers and surface waters. Only in recent years has the transition zone become a subject of major research interest; thus, the need has evolved for appropriate methods applicable in this zone. This article provides an overview of the methods that are currently applied and described in the literature for estimating fluxes at the groundwater – surface water interface. Considerations for choosing appropriate methods are given including spatial and temporal scales, uncertainties, and limitations in application. It is concluded that a multi-scale approach combining multiple measuring methods may considerably constrain estimates of fluxes between groundwater and surface water.

2.1 Introduction

Surface water and groundwater have long been considered separate entities, and have been investigated individually. Chemical, biological and physical properties of surface water and groundwater are indeed different. In the transition zone a variety of processes occur, leading to transport, degradation, transformation, precipitation, or sorption of substances. Water exchange between groundwater and surface water may have a significant impact on the water quality of either of these hydrological zones. The transition zone plays a critical role in the mediation of interactions between groundwater and surface water. It is characterized by permeable sediments, saturated conditions, and low flow velocities, thus resembling the characteristics of terrestrial aquifers. In streams, however, the zone may contain some proportion of surface water due to the infiltration of stream water into the pore space, conferring on it features of the surface water zone as well. Ecologists have termed this area the hyporheic zone (*Schwoerbel*, 1961) and highlighted the significance of exchange processes for the biota and metabolism of streams (*Hynes*, 1983; *Brunke and Gonser*, 1997). For the protection of water resources it is crucial to understand and quantify exchange processes and pathways between groundwater and surface water. Particularly in case of contamination, it is fundamental to know the mass flow rates between groundwater and surface water for the implementation of restoration measures. *Woessner* (2000) stressed the need for hydrogeologists to extend their focus and investigate near-channel and in-channel water exchange, especially in the context of riparian management.

Interactions between groundwater and surface water basically proceed in two ways: groundwater flows through the streambed into the stream (gaining stream), and stream water infiltrates through the sediments into the groundwater (losing stream). Often, a stream is gaining in some reaches and losing in other reaches. The direction of the exchange flow depends on the hydraulic head. In gaining reaches, the elevation of the groundwater table is higher than the elevation of the stream stage. Conversely, in losing reaches the elevation of the groundwater table is lower than the elevation of the stream stage. A special case of losing streams is the disconnected stream, where the groundwater table is below the streambed and the stream is disconnected from the groundwater system by an unsaturated zone. Seasonal variations in precipitation patterns as well as single precipitation events can alter groundwater tables and stream stages and thereby cause changes in the direction of exchange flows. On a smaller scale, water flow into and out of the streambed may be induced by pressure variations on the streambed caused by geomorphological features such as pool-riffle sequences, discontinuities in slope, or obstacles on the streambed (*Thibodeaux and Boyle*, 1987; *Savant et al.*, 1987; *Hutchinson and Webster*, 1998). Also, a relocation of sediment grains on the streambed may lead to a trapping of stream water in the sediment interstices and a release of interstitial water to the stream (*Elliott and Brooks*, 1997). The interactions, however, are complex. *Sophocleous* (2002) presented a comprehensive outline of the principal controls and mechanisms of groundwater – surface water exchange.

Hydrogeologists and surface water hydrologists traditionally have approached the interface between groundwater and surface water from their particular perspective. In the literature a variety of techniques to identify and quantify exchange flows are described which originate from the respective disciplines of water research. Our aim was to bring together these different perspectives and approaches in order to study the stream-aquifer system as a whole. The range of available techniques to determine interactions between groundwater and surface water is broad. Depending on the study purpose, methods have to be chosen which are appropriate for

the respective spatial and temporal scale. If processes or flow paths are the study focus, other methods are needed than for the quantification of regional groundwater flow to develop management schemes. Numerical modelling, which is an indispensable tool for watershed management, relies on the determination of parameters representing the flow conditions for the selected model scale. Thus, the proper choice of methods is critical for the usefulness of measurement results. As *Sophocleous* (2002) pointed out, the determination of water fluxes between groundwater and surface water is still a major challenge due to heterogeneities and the problem of integrating measurements at various scales.

Scanlon et al. (2002) presented an overview of techniques for quantifying groundwater recharge on different space and time scales. Some of these methods can equally be applied to measure groundwater discharge to streams and recharge through the streambed. *Landon et al.* (2001) compared instream methods for measuring hydraulic conductivity aiming at determining the most appropriate techniques for use in sandy streambeds.

The purpose of this paper is to provide an overview of the methods that are currently state-of-the-art for measuring interactions between groundwater and surface water. The focus is on the estimation of water fluxes at the stream-aquifer interface. It is intended for readers starting to work on the investigation of interactions between groundwater and surface water who might have varying backgrounds in the different disciplines of hydrology. Therefore, each method is briefly described and references for further information are given. The methods are grouped into direct measurements of water flux, heat tracer methods, methods based on Darcy's Law, and mass balance approaches. Since the contamination of aquifers and streams is of growing concern worldwide, methods to determine contaminant concentrations for the estimation of contaminant mass fluxes between groundwater and stream water are also presented. With respect to the study purpose, the suitability of the different methods and their applicability on different space and time scales are discussed. Modelling approaches, such as inverse modelling to determine hydraulic conductivities, are not covered in this study. The special case of disconnected streams with an unsaturated zone between streambed and aquifer is omitted in this review and, thus, methods typically applied in the unsaturated zone are not discussed.

2.2 Direct measurements of water flux

Direct measurements of water flux across the groundwater – surface water – interface can be realized by seepage meters. Bag-type seepage meters as proposed by *Lee* (1977) consist of a bottomless cylinder vented to a deflated plastic bag. The cylinder is turned into the sediment, and as water flows from the groundwater to the surface water, it is collected in the plastic bag. From the collected volume, the cross section area of the cylinder, and the collection period the seepage flux can be calculated. In case of surface water seeping into the sediment, a known water volume is filled into the plastic bag prior to the installation and from the volume loss the infiltration rate is calculated. These bag-type seepage meters have been used extensively in lakes, estuaries, reservoirs, and streams (e.g., *Lee and Cherry*, 1978; *Woessner and Sullivan*, 1984; *Isiorho and Meyer*, 1999; *Landon et al.*, 2001).

Murdoch and Kelly (2003) discussed that, despite the simplicity of applying bag-type seepage meters, their performance is far from simple. Particularly in streams, water flowing over the collection bag may affect the hydraulic head in the bag, or may distort or fold the bag and lead to decreased or increased flux measured by the seepage meter. *Libelo and MacIntyre* (1994)

proposed to cover the collection bag with a rigid container to isolate it from pressure gradients resulting from the movement of the stream water. *Kelly and Murdoch (2003)* presented a modification of a seepage meter fitted with a piezometer along the axis of the pan (a piezo-seep meter). A manometer was used to measure the difference in hydraulic head between the piezometer screen and the inside of the pan. A pump was temporarily attached to the pan and the pumping flow rate was correlated to the head differential between piezometer and pan. This permitted the estimation of fluxes into the seepage meter pan from the head differential measured under ambient conditions.

Various types of automated seepage meters have been developed that overcome problems related to the collection bags. They are based on the same principle of isolating and covering a part of the groundwater – surface water interface with a chamber open at the bottom, but abandon the use of collection bags and instead deploy instruments to continuously record the water flow rate through the outlet tube. Devices to measure the flow rate include, for instance, the heat pulse meter (*Taniguchi and Fukuo, 1993; Krupa et al., 1998*) that is based on the relationship between the travel time of a heat pulse in the flow tube and the flow velocity; the ultrasonic meter (*Paulsen et al., 2001*) that relates the travel time of an ultrasonic signal through the flow tube to the flow velocity; the dye-dilution meter (*Sholkovitz et al., 2003*) based on the principle that the rate at which a dyed solution is diluted by the inflow or outflow of water is directly proportional to the seepage flow rate; and the electromagnetic meter (*Rosenberry and Morin, 2004*) that measures the voltage induced by water passing through an electromagnetic field, which is proportional to the flow velocity. These modifications enable a monitoring of seepage variations with time.

Seepage meters are based on a simple concept and inexpensive to construct. They are useful for the detection of groundwater discharge or recharge zones. To obtain representative average seepage fluxes, however, measurements at many locations are required. In streams, the fluxes measured with a seepage meter might not entirely be attributed to groundwater discharge, but include shallow throughflow or hyporheic exchange flow (see Sect. 2.7.2). The seepage meters themselves constitute obstacles to the stream flow that might induce interstitial flow into the seepage meter pan.

2.3 Heat tracer methods

The difference in temperature between groundwater and surface water can be used to delineate groundwater discharge or recharge zones and quantify water fluxes at the groundwater – surface water interface. Groundwater temperatures are relatively stable throughout the year. In contrast, stream temperatures vary strongly on a daily and seasonal basis. Therefore, gaining reaches are characterized by relatively stable sediment temperatures and damped diurnal variations in surface water temperatures, whereas losing reaches are characterized by highly variable sediment and surface water temperatures (*Winter et al., 1998*). This permits an identification of the general character of the flow regime by recording temperature time series in the stream and the surrounding sediments (*Constantz, 1998; Constantz and Stonestrom, 2003*).

Time series of temperature profiles document the penetration of cyclic temperature changes into the streambed. Because water is heated and cooled at the surface, downward moving water causes a deeper penetration of cyclic temperature changes. Conversely, upward moving water leads to less penetration of cyclic temperature changes because the upwelling groundwater has

a relatively constant temperature. The maximum and minimum temperatures of a complete cycle form a temperature envelope enclosing all measured temperature profiles. This envelope is compressed toward the streambed surface in case of upwelling groundwater. Downwelling stream water lets the envelope expand downward (*Constantz and Stonestrom, 2003*).

Heat transport in the subsurface is a combination of advective heat transport (i.e., heat transport by the flowing water) and conductive heat transport (i.e., heat transport by heat conduction through the solid and fluid phase of the sediment). It can be described by a heat transport equation (*Domenico and Schwartz, 1998*) which is analogous to the advection-dispersion equation for solute transport in groundwater. Various analytical and numerical solutions have been developed for the heat transport equation (e.g., *Carslaw and Jaeger, 1959; Suzuki, 1960; Bredehoeft and Papadopolus, 1965; Stallman, 1965; Turcotte and Schubert, 1982; Silliman et al., 1995*). Using these solutions, seepage rates through the streambed can be calculated from the temperature profiles measured beneath the stream (e.g., *Constantz et al., 2001, 2002; Taniguchi et al., 2003; Becker et al., 2004*). A popular procedure is to adjust hydraulic conductivities in a numerical model until seepage rates cause a match between measured and modelled temperatures (*Stonestrom and Constantz, 2004*). The thermal properties of streambed sediments are almost independent of texture and vary only little between different streambeds; hence, they can be obtained from literature values (*Constantz and Stonestrom, 2003*). In contrast, hydraulic properties are highly variable. Streambed temperatures are very sensitive to the hydraulic conditions, which makes heat a useful tool for the estimation of fluxes through streambed sediments.

A different approach to estimate water fluxes through the streambed using streambed temperatures was taken by *Conant (2004)* and *Schmidt et al. (2006)*. They measured temperatures in the streambed at many locations within a short time period. The underlying assumption was that variations in temperature are attributed to spatial variations in water flux through the streambed and not to temporal changes during the measurement period. *Conant (2004)* mapped the temperatures at a certain depth in the streambed and developed an empirical relation between fluxes obtained from minipiezometer data and streambed temperatures. *Schmidt et al. (2006)* measured streambed temperatures simultaneously at five depths and inferred fluxes from the temperature profiles using a one-dimensional analytical solution (*Bredehoeft and Papadopolus, 1965*) of the heat transport equation with the average surface water temperature during the measurement period and the constant groundwater temperature as boundary conditions.

A heat balance equation was used by *Becker et al. (2004)* to calculate groundwater discharge from measurements of stream temperature and streamflow. They divided the stream into reaches corresponding to temperature measurement points and set up a balance equation where the stream temperature is a function of the groundwater discharge rate, the difference in stream water and groundwater temperature, streamflow, and additional heat gains and losses through the stream surface.

Temperature is a robust and relatively inexpensive parameter to measure. Measurements are quick and easy to perform, making temperature-based methods very attractive for detailed delineations of groundwater discharge or recharge zones with high resolutions.

For further information on the use of heat as a groundwater tracer, the reader is referred to the comprehensive review by *Anderson (2005)*.

2.4 Methods based on Darcy's Law

Methods based on Darcy's Law generally correspond to the methods used to study groundwater movement in terrestrial aquifers. They typically require measurements of the components of the Darcy equation (Darcy, 1856):

$$q = -K \frac{dh}{dl} \quad (2.1)$$

where q is specific discharge [L/T], K is hydraulic conductivity [L/T], h is hydraulic head [L] and l is distance [L]. The specific discharge has the dimensions of a velocity, or a flux, and is also known as Darcy velocity or Darcy flux. Groundwater velocity, i.e., the flow velocity between two points in the aquifer as can be observed, for instance, by tracer methods, includes the porosity of the aquifer material:

$$v = \frac{q}{n} \quad (2.2)$$

where v is groundwater velocity [L/T], q is Darcy flux [L/T] and n is porosity [-]. Hence, the determination of water flux in the subsurface typically requires information on the hydraulic gradient and hydraulic conductivity, or groundwater velocity and porosity.

2.4.1 Hydraulic gradient

Measuring the water level in wells and piezometers installed in the fluvial plain is the standard method to determine hydraulic head (Freeze and Cherry, 1979). A piezometer is basically a tube or pipe that is inserted into the sediment to measure the hydraulic head at a certain point in the subsurface. The direction of local groundwater flow can be determined from the differences in hydraulic head between individual piezometers installed in groups (at least three in a triangular arrangement). In case of horizontal flow, the hydraulic gradient can be calculated from the difference in hydraulic head and the horizontal distance. For the vertical components of groundwater flow, which are particularly important to understand the interaction between groundwater and surface water, a piezometer nest may be installed, with two or more piezometers set in the same location at different depths. The hydraulic gradient can then be calculated from the difference in hydraulic head and the vertical distance. Furthermore, vertically distributed piezometer data can be used to draw lines of equal hydraulic head for the construction of a flow field map showing the groundwater flow behaviour in the vicinity of a surface water body.

Installed directly in the streambed, piezometers deliver information whether a stream reach is gaining or losing by a comparison of piezometer and stream water level. Assuming vertical flow beneath the streambed, the hydraulic gradient is obtained from the difference of the water level in the piezometer and the stream, and the depth from the sediment surface to the centre of the piezometer screen (Freeze and Cherry, 1979). Baxter *et al.* (2003) described an installation technique for minipiezometers which permits obtaining a large number of measurements in gravel and cobble streambeds.

The piezometer method provides point measurements of hydraulic head. The equipment is quick and easy to install, and measurement analysis is straightforward. Therefore, this method

is appropriate for small-scale applications and allows a detailed survey of the heterogeneity of flow conditions in the subsurface. Groundwater movement, however, is subject to temporal variations. Therefore, all measurements of hydraulic head at a study site should be made approximately at the same time, and the resulting contour and flow field maps are representative only of that specific time (*Winter et al.*, 1998). Pressure transducers and data loggers installed in the piezometers or pressure probes buried in the saturated subsurface may facilitate observing temporal variations in hydraulic head.

2.4.2 Hydraulic conductivity

Grain size analysis

From the grain size distribution of a sediment sample, an estimate of hydraulic conductivity can be derived employing empirical relations between hydraulic conductivity and some statistical grain size parameters such as geometric mean, median, effective diameter, etc. (e.g., *Hazen*, 1892; *Schlichter*, 1905; *Terzaghi*, 1925; *Beyer*, 1964; *Shepherd*, 1989). *Alyamani and Sen* (1993) proposed to relate hydraulic conductivity to the initial slope and intercept of the grain size distribution curve. During the determination of grain size distribution, the sediment structure and stratification are destroyed. Hence, these relations yield a value of hydraulic conductivity that represents neither the vertical nor the horizontal hydraulic conductivity and is not representative of the true hydraulic properties of the subsurface. Grain size analysis, however, delivers information about the subsurface material and the hydraulic conductivity values can be used as a first estimation for the design of further applications such as slug and bail tests.

Permeameter tests

For laboratory permeameter tests a sediment sample is enclosed between two porous plates in a tube. In case of a constant-head test, a constant-head potential is set up and a steady discharge flows through the system. Hydraulic conductivity can be calculated following Darcy's law. In a falling-head test, the time needed for the hydraulic head to fall between two points is recorded. Hydraulic conductivity is calculated from the head difference, the time, and the tube and sample geometry (*Hvorslev*, 1951; *Freeze and Cherry*, 1979; *Todd and Mays*, 2005). Depending on the direction of flow through the sediment sample in the experiment, directional hydraulic conductivity may be obtained. It is, however, difficult to take and transport samples from streambed sediments without disturbing the packing and orientation of the sediment grains, which may influence measurement results.

To obtain the vertical hydraulic conductivity of the streambed, in situ permeameter tests can be performed using a standpipe pressed into the sediment (*Hvorslev*, 1951). The standpipe is open at the bottom, so that a sediment column is laterally enclosed by the pipe. The pipe is filled with water and as the water level falls, the hydraulic head in the pipe and the time is recorded at two stages (falling-head permeameter test). Hydraulic conductivity is calculated from the difference in hydraulic head, the time difference, and the length of the sediment column in the standpipe. Alternatively, the water level in the pipe is held constant by injecting water, and the measured injection rate is used for test analysis (constant-head permeameter test). *Chen* (2000) proposed a variation of the standpipe method to obtain hydraulic conductivities in any desired direction by using an L-shaped pipe. Using a pipe with an angle of 90° , horizontal

hydraulic conductivity can be calculated. An L-shaped pipe with any angle greater than 90° delivers hydraulic conductivity along any oblique direction.

Horizontal hydraulic conductivities of the streambed may be obtained from a constant-head injection of water through a screened piezometer (*Cardenas and Zlotnik, 2003*). From the test geometry, the injection rate, and the operational head, hydraulic conductivity can be calculated.

In situ permeameter tests provide point measurements of hydraulic conductivity directly in the streambed. Performance and analysis are quick and easy, so that it can be useful for a detailed survey of the heterogeneity of streambeds.

Slug and bail tests

Slug and bail tests are based on introducing/removing a known volume of water (or a solid object) into/from a well or piezometer, and as the water level recovers, the head is measured as a function of time. The hydraulic properties of the subsurface are determined following the methods of *Hvorslev (1951)*, *Cooper et al. (1967)*, *Bouwer and Rice (1976)*, or *Hyder et al. (1994)*, among others. Analysis methods for partially penetrating wells in unconfined formations are most appropriate for the estimation of streambed hydraulic conductivities (e.g., *Springer et al., 1999*; *Landon et al., 2001*; *Conant, 2004*). *Butler (1998)* provided a comprehensive summary of slug and bail test performance and analysis methods. Slug and bail tests are quick and easy to perform with inexpensive equipment. In contrast to pumping tests, only one well or piezometer is needed to perform a slug and bail test. Care has to be taken concerning sufficient well development, proper test design, and appropriate analysis procedures in order to obtain reliable results (*Butler, 1998*). This method provides point measurements of hydraulic conductivity, albeit the scale of measurement is slightly larger than in permeameter tests. It is appropriate for process studies or for investigating heterogeneities.

Pumping tests

A pumping test to determine hydraulic conductivity requires the existence of a pumping well and at least one observation well (piezometer) in the capture zone. The well is pumped at a constant rate and drawdown in the piezometer is measured as a function of time. The hydraulic properties of the subsurface are determined using one of several available methods, e.g. the methods of *Theis (1935)*, *Cooper and Jacob (1946)*, *Chow (1952)*, *Neuman (1975)*, or *Moench (1995)*, among others. However, for the determination of streambed hydraulic conductivities to analyse groundwater – surface water interactions the application of pumping tests is problematic because of the boundary conditions. *Kelly and Murdoch (2003)* described a theoretical analysis for pumping tests in submerged aquifers assuming a constant-head boundary as upper boundary condition. The lower boundary condition can either be a no-flow boundary in case the stream is underlain by bedrock or a low-conductivity formation, or a constant-head boundary in case the stream is underlain by higher conductivity materials. Pumping tests provide hydraulic conductivity values that are averaged over a large subsurface volume. Thus, these values are more representative for the entire subsurface body than conductivities obtained by point measurements. Results are less sensitive to heterogeneities in the subsurface material and preferential flow paths. However, the installation of wells and piezometers is costly and may not be justified in all cases.

A piezo-seep meter (*Kelly and Murdoch, 2003*) as described in Sect. 2.2 may provide an alternative for pumping tests to estimate streambed hydraulic conductivities. As water is pumped from a seepage meter pan, hydraulic conductivity may be obtained from the head gradient measured at a piezometer fixed to the pan, the flow rate, and the cross-sectional area of the pan. This approach yields measurements of vertical hydraulic conductivities at shallow streambed depths. Contrary to conventional pumping tests, the test radius is small. The equipment is relatively inexpensive and easy to install, permitting tests at many locations to delineate the spatial distribution of streambed hydraulic conductivities.

2.4.3 Groundwater velocity

Groundwater velocity may be estimated by introducing a conservative tracer, e.g. a dye, such as uranine, or a salt, such as calcium chloride, to a well, and recording the travel time for the tracer to arrive at a downstream observation well. The groundwater velocity can then be computed from the travel time and distance data (*Freeze and Cherry, 1979*). Because groundwater velocities are usually small, the wells need to be close together in order to obtain results in a reasonable time span. Thus, only a small portion of the flow field can be observed by this method. Furthermore, the flow direction should be precisely known, otherwise the tracer plume may miss the downstream well. Multiple downstream wells along a control plane can help to overcome this problem. Another problem arises if stratification of the subsurface leads to different travel times in different layers. In this case, the applicable average groundwater velocity in the subsurface is difficult to determine (*Todd and Mays, 2005*). Alternatively, a tracer dye is added to a well and mixed with the contained water (borehole dilution test). While water flows into and out of the well, the tracer concentration is measured continuously. From the tracer dilution curve, groundwater velocity can be derived. This type of tracer test is particularly useful to determine the flow velocity in the streambed assuming that flow from a well near a stream is directed exclusively towards the stream (*Todd and Mays, 2005*).

Both tracer methods can also be used to infer hydraulic conductivity following Darcy's Law if the hydraulic gradient and porosity are known.

On a very small scale, the flow velocity in streambed sediments may be determined using the method proposed by *Mutz and Rohde (2003)*. A small amount of tracer dye is injected into the streambed using a syringe. After a few hours a sediment core is taken around the injection point and is deep-frozen. Dividing the frozen sediment core longitudinally uncovers the movement of the tracer plume in the sediment. The flow direction can then be observed and the flow velocity can be calculated from the distance the tracer plume has travelled and the duration of exposure. This method gives velocity estimates on a scale of a few centimetres. It requires the visibility of the tracer plume in the sediment core and is limited to use in light-coloured, fine sediments.

2.4.4 Porosity

The porosity of a sediment sample can be determined by relating the bulk mass density of the sample to the particle mass density. The bulk mass density is the oven-dried mass divided by the field volume of the sample. The particle mass density is the oven-dried mass divided by the volume of the solid particles, which can be determined by a water-displacement test (*Freeze and Cherry, 1979*).

2.5 Mass balance approaches

The underlying assumption of mass balance approaches to study groundwater – surface water interactions is that any gain or loss of surface water or any change in the properties of surface water can be related to the water source, and, therefore, the groundwater component can be identified and quantified.

2.5.1 Incremental streamflow

Measurements of streamflow discharge in successive cross-sections enable the determination of groundwater – surface water exchange by computing the differences in discharge between the cross sections. Streamflow discharge can be measured by various methods, including the velocity gauging method deploying any type of current meter (*Carter and Davidian, 1968*), or gauging flumes (*Kilpatrick and Schneider, 1983*). Another option is the dilution gauging method (*Kilpatrick and Cobb, 1985*), where a solute tracer is injected into the stream and the tracer breakthrough curves at successive cross sections are recorded. The volumetric discharge can then be inferred from the measurements. *Zellweger (1994)* compared the performance of four ionic tracers to measure streamflow gain or loss in a small stream.

With the velocity gauging method, the net exchange of groundwater with stream water is captured, but it is not possible to identify inflow and outflow components of surface water exchange. *Harvey and Wagner (2000)* suggest a combination of the velocity gauging method and the dilution gauging method to estimate groundwater inflow and outflow simultaneously. They propose “injecting a solute tracer at the upstream of the reach, measuring stream volumetric discharge at both reach end points by the dilution gauging method, and then additionally measuring discharge at the downstream end using the velocity gauging method. Groundwater inflow rate is estimated from the difference between the dilution gauging measurements at the downstream and upstream ends of the reach (divided by the reach length). In contrast, the net groundwater exchange is estimated by the difference between the velocity gauging estimate at the downstream end of the reach and the dilution gauging estimate at the upstream end of the reach (divided by reach length). The final piece of information that is needed, the groundwater outflow rate, is estimated by subtracting the net exchange rate from the groundwater inflow rate.” (*Harvey and Wagner, 2000*).

To estimate groundwater discharge from incremental streamflow, measurements should be performed under low flow conditions so that one can assume that any increase in streamflow is due to groundwater discharge and not due to quickflow resulting from a rainfall event. This method provides estimates of the groundwater contribution to streamflow averaged over the reach length, making it insensitive to small-scale heterogeneities. The seepage flow rates should be significantly higher than the uncertainties inherent in the measurements, which constrains the spatial resolution of the method.

2.5.2 Hydrograph separation

An estimation of the groundwater contribution to streamflow can be realized by separating a stream hydrograph into the different runoff components, such as baseflow and quickflow (e.g., *Chow, 1964; Linsley et al., 1988; Hornberger et al., 1998; Davie, 2002*), and then assuming

that baseflow represents groundwater discharge into the stream (e.g., *Mau and Winter, 1997; Hannula et al., 2003*).

The validity of the underlying assumptions of the separation techniques is critical for the performance of hydrograph separation as a tool to determine groundwater-surface water interactions (*Halford and Mayer, 2000*). Furthermore, in cases where drainage from bank storage, lakes or wetlands, soils, or snowpacks contributes to stream discharge, the assumption that baseflow discharge represents groundwater discharge may not hold (*Halford and Mayer, 2000*). The limited number of stream gauging stations constrains the resolution of this method. Results are usually averaged over long stream reaches.

2.5.3 Environmental tracer methods

Tracer-based hydrograph separation using isotopic and geochemical tracers provides information on the temporal and spatial origin of streamflow components. Stable isotopic tracers, such as stable oxygen and hydrogen isotopes, are used to distinguish rainfall event flow from pre-event flow, because rain water often has a different isotope composition than water already in the catchment (*Kendall and McDonnell, 1998*). Geochemical tracers, such as major chemical parameters (e.g., sodium, nitrate, silica, conductivity) and trace elements (e.g. strontium), are often used to determine the fractions of water flowing along different subsurface flowpaths (*Cook and Herczeg, 2000*). Generally, to separate the streamflow components, mixing models (*Pinder and Jones, 1969*) or diagrams (*Christophersen and Hooper, 1992*) based on the conservation of mass are applied. Numerous applications under different hydrological settings using various tracers have been documented (e.g., *Pinder and Jones, 1969; Hooper and Shoemaker, 1986; McDonnell et al., 1990; Laudon and Slaymaker, 1997; Ladouche et al., 2001; Carey and Quinton, 2005*). The main drawbacks of tracer-based hydrograph separation are that event and pre-event waters are often too similar in their isotope composition and that the composition is often not constant in space or time (*Genereux and Hooper, 1998*).

Tracer-based hydrograph separation yields groundwater discharge rates from reach to catchment scale. On a smaller scale, the differences in concentrations of environmental tracers between groundwater and surface water can be used to identify and delineate zones of groundwater discharge or recharge, provided that the differences are sufficiently large. Stable hydrogen and oxygen isotopes are widely used, because groundwater is generally less enriched in deuterium and ^{18}O than surface water (*Coplen et al., 2000; Hinkle et al., 2001; Yehdeghoa et al., 1997*). Numerous other geochemical and isotopic tracers have been used to study interactions between groundwater and surface water, including alkalinity (*Rodgers et al., 2004*), electrical conductivity (*Harvey et al., 1997*), or isotopes of radon (*Cook et al., 2003; Wu et al., 2004*), chlorofluorocarbons (*Cook et al., 2003*), strontium (*Negrel et al., 2003*), and radium (*Kraemer, 2005*). For further information on the use of geochemical and isotopic tracers in catchment hydrology, the reader is referred to the books by *Clark and Fritz (1997); Kendall and McDonnell (1998)*, or *Cook and Herczeg (2000)*, among others. As all researchers working with environmental tracers point out, a combination of various tracers and hydrologic data yields the most reliable results.

2.5.4 Solute tracer methods

Besides dilution gauging, solute tracers are also used to study the interaction between stream water and interstitial water in the streambed sediments. The temporary detainment of stream

water in the sediment voids or in any other stagnant pockets of water, such as eddies or at the lee side of obstacles, is referred to as transient storage (*Bencala and Walters, 1983*). It is usually studied by injecting a conservative tracer into the stream and fitting a model to the tracer breakthrough curves which yields the determination of the storage zone size and exchange rate (*Runkel, 1998*). Studies using solute tracers and the transient storage approach to characterize surface-subsurface water exchange have been presented by *D'Angelo et al. (1993)*; *Harvey and Bencala (1993)*; *Morrice et al. (1997)*, and *Hart et al. (1999)*, among others. However, surface storage and storage in the streambed sediments are lumped together in this approach and the identification of the actual subsurface component is often difficult (*Runkel et al., 2003*).

2.6 Methods to determine contaminant concentrations

2.6.1 Monitoring wells

By collecting subsurface water samples from monitoring wells or piezometers the contaminant concentration can be estimated. In order to obtain reliable results, the monitoring wells should be closely spaced along transects across the contaminant plume. Multi-level monitoring wells help in creating a three-dimensional integration of contaminant concentrations (e.g., *Borden et al., 1997*; *Pitkin et al., 1999*; *Conant, 2004*). A dense grid of monitoring wells can give very detailed information about the distribution of contaminants. However, for large study sites this method becomes impractical.

2.6.2 Passive samplers

The accumulation of groundwater contaminants by passive samplers provides an alternative to the conventional snap-shot-sampling in monitoring wells (*Bopp et al., 2004*). Over the past few years, this technique was extensively developed and a variety of passive sampling devices has evolved. In general, these devices can be divided into four groups: water filled devices, solvent filled devices, semipermeable membrane devices, and solid-sorbent filled devices. Contaminants are collected by diffusion and/or sorption over extended periods of time. After sampling using these devices, contaminants are removed from the receiving phases or whole samplers by solvent extraction or thermodesorption and analysed chemically (*Schirmer et al., 2005*). The state-of-the-art of passive sampling techniques is summarized in review articles by *Namiesnik et al. (2005)*; *Stuer-Lauridsen (2005)*, and *Vrana et al. (2005)*, for example. Further developments of passive sampling devices allow a combined chemical and toxicological analysis of the samples (*Bopp, 2004*), and combined contaminant and water flux measurements (*Hatfield et al., 2004*; *De Jonge and Rothenberg, 2005*).

The accumulation of contaminants over an entire sampling period enables time-averaged measurements which are less sensitive to daily fluctuations. Furthermore, very low contaminant concentrations can be detected in this way. Long-term monitoring using passive samplers is time- and cost-efficient, since only a few field trips and sample analyses are required (*Bopp et al., 2004*). Transport and storage of large sample volumes is not necessary, which again reduces costs and, moreover, the risk of degradation of labile substances prior to the analysis (*Kot et al., 2000*). The problem of the disposal of highly contaminated purged groundwater is avoided and changes in flow regimes are circumvented, both being typical problems associated

with sampling through pumping. Furthermore, volatile organic compounds, which often get lost during purging, can also be detected (*Powell and Puls, 1997*).

Passive samplers can be applied in the aquifer, in the surface water, or in the transition zone. Frequent changes in flow direction, however, which are often observed in the transition zone, might be problematic for the calculation of mass fluxes.

2.6.3 Integral pumping tests

The issue of heterogeneity of the contaminant distribution in the subsurface is addressed by using the integral pumping test method (*Schwarz et al., 1998; Teutsch et al., 2000; Ptak et al., 2000; Bauer et al., 2004; Bayer-Raich et al., 2004*). This method consists of one or more pumping wells along a control plane perpendicular to the mean groundwater flow direction. The wells are operated with a constant discharge for a time period of up to several days. During pumping, concentrations of target contaminants are measured in the pumped groundwater. From the concentration time series, the concentration distribution along the control plane and thus the presence of contaminant plumes can be determined. Furthermore, contaminant mass flow rates along the control plane and the representative average contaminant concentration in the well capture zone can be computed. The method provides integral measurements over a large subsurface volume and is, therefore, less prone to heterogeneity effects of the subsurface and the contaminant distribution than point measurements. However, the disposal of the large volumes of contaminated groundwater that is pumped out of the wells during the test can be costly. The application of integral pumping tests near streams is problematic due to the boundary conditions and the influence of pumped stream water. However, it may provide reliable estimates of the contaminant concentration in the groundwater that approaches a stream and potentially discharges to the surface water.

2.6.4 Grab samples

The contaminant concentration in the surface water can simply be determined by analysing water samples from discrete grab or bottle samples. The main drawbacks of this method are that large sample volumes are often needed when contaminants are present at only trace levels, and that only snapshots of contaminant levels at the time of sampling are provided (*Vrana et al., 2005*). Automated sampling systems can facilitate sample collection for long-term monitoring.

2.6.5 Seepage meters

Seepage water collected in a collection bag of a seepage meter (*Lee, 1977*), as described in Sect. 2.2, can be sampled and analysed for the contaminant concentration.

2.7 Discussion

2.7.1 Measurement Scales

Various approaches and techniques to measure the interaction between groundwater and surface water have been outlined above. The methods differ in resolution, sampled volume, and the time scales they represent. The spatial measurement scales of the different methods (Figure 2.1) have to be considered for the integration of diverse measurements at a study site. Densely spaced point measurements may deliver detailed information on the heterogeneity of the measured parameter, but the reaches between the measurement locations remain unknown. Therefore, there is a risk to miss extreme values of the parameter distribution which may affect computed results. Methods that integrate over large sample volumes provide reliable estimates of average values but do not enable a detailed characterization of the spatial heterogeneity of the respective parameter. Often, the choice of methods constitutes a trade-off between resolution of heterogeneities and sampled volume (*Rubin et al., 1999*).

In general, most methods applied in the subsurface provide point estimates of the respective parameter, whereas most methods applied to the surface water represent larger sample volumes. Measurements of hydraulic head, grain size analysis, and permeameter tests are point measurements. In slug and bail tests and tracer tests, the portion of sampled aquifer volume is larger, on the scale of meters around the sample point. Pumping tests operate on the largest scale among the methods applied in the subsurface, typically on the scale of tens of meters up to kilometers. Measurements of the temperature gradient in the streambed provide point estimates of flux. Seepage meter measurements yield flux estimates over the diameter of the seepage pan, usually less than one meter. Incremental streamflow measurements result in groundwater discharge

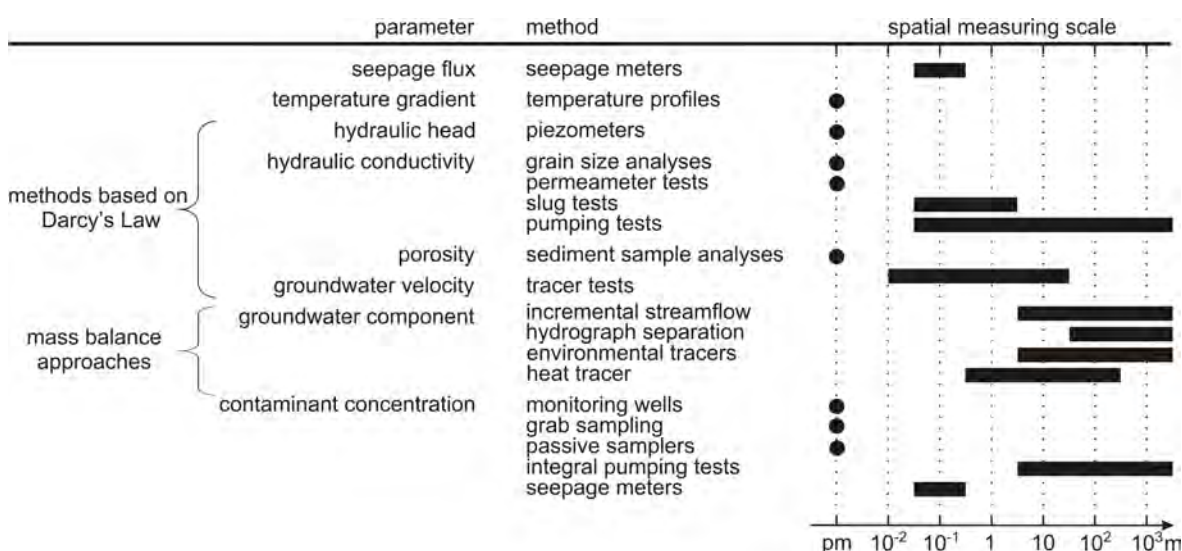


Figure 2.1. Spatial measuring scales of the different methods to measure interactions between groundwater and surface water. The spatial scale is given as radius or distance of influence. Dots represent point measurements (pm).

estimates averaged over the reach length between measurement transects, ranging from several meters to hundreds of meters. The same applies to environmental and heat tracer methods aiming at identifying the groundwater contribution to streamflow. Solute tracer methods for the estimation of transient storage also operate on the reach scale. Hydrograph separation delivers information on the groundwater discharge upstream of a gauging station and, therefore, enables the calculation of discharge rates averaged over the upstream length. Concerning contaminant concentration, grab sampling from piezometers or from the surface water, passive samplers and seepage meters provide point measurements of contaminant concentration, whereas integral pumping tests yield concentrations averaged over a large subsurface volume.

For measurements conducted in heterogeneous media, such as the subsurface, the measurement scale on which a selected technique operates may have a significant influence on the results, which has clearly been demonstrated for hydraulic conductivity in numerous studies. As *Rovey and Cherkauer* (1995) point out, hydraulic conductivity generally increases with test radius, because with a larger test radius the chance to encounter high-conductivity zones in a heterogeneous medium increases.

The scale-dependency of measurements in heterogeneous media implies that even a dense grid of point measurements may deliver results that are considerably different from those obtained from larger-scale measurements, because the importance of small heterogeneities, such as narrow high-conductivity zones, may be underestimated. A better representation of the local conditions including the effects of scale on measurement results can be achieved by conducting measurements at multiple scales within a single study site.

The various methods also differ in the time scale they represent. The majority of techniques deliver parameter estimates at a certain point in time. Only seepage meters and passive samplers collect water volume and contaminant mass, respectively, over a time period from hours to weeks and, thus, yield time-averaged fluxes. Hydrograph separation gives estimates of the groundwater contribution to streamflow averaged over the duration of the recorded hydrograph, typically from several years to decades. Automated sampling methods or data loggers, however, can help breaking down measurement time steps to intervals that allow for observations of temporal variations. In particular, parameters that can be measured simply using probes, such as pressure or temperature, are suitable for long-term monitoring.

2.7.2 Groundwater discharge versus hyporheic exchange flow

Exchange processes between streams and groundwater do not only comprise groundwater discharging to a stream or stream water infiltrating into the aquifer, but also include downwelling of stream water into the sediment and re-emerging to the stream further downstream (Figure 2.2). These small-scale exchange processes are driven by pressure variations caused by geomorphologic features such as pool-riffle sequences, discontinuities in slope, or obstacles on the streambed (*Thibodeaux and Boyle*, 1987; *Savant et al.*, 1987; *Hutchinson and Webster*, 1998). This implies that water discharging through the streambed into the stream can either be groundwater, or re-emerging surface water, or a mixture of both. *Harvey and Bencala* (1993) found that the gross inflow (groundwater + subsurface flow) of water to their study stream exceeded the net inflow (groundwater only) by nearly twofold. Thus, methods to determine water flux in the shallow streambed, such as seepage meters or shallow streambed piezometers, may result in discharge rates that may not necessarily be attributed to groundwater discharge. Qualitative methods, such as heat or environmental tracers, may additionally be used to eluci-

date the origin of the water. Solute tracer methods based on the transient storage approach may help estimate the hyporheic flow component.

2.7.3 Considerations for choosing appropriate methods

The study goal plays a decisive role for the choice of appropriate methods to characterize groundwater – surface water interactions. The objective of the research project defines the required measurement scale which in turn constrains the possible methods. A regional assessment of water resources or the fate and transport of pollutants requires information on a large scale, requiring methods that represent a large sample volume, such as pumping tests or surface water methods. Equally, if the impact of groundwater discharge on surface water quality or vice versa is of concern, measurements on a large scale may be more appropriate. In contrast, investigations of the spatial variation of exchange processes and flow paths between groundwater and surface water require measurements that allow for high spatial resolutions, such as temperature profiles or piezometer methods. If temporal variations or trends are of concern, long-term monitoring of certain parameters may be required. Automated sampling methods and probes coupled with data loggers are most suitable for that purpose.

The choice between methods on a similar scale may be more of an operational character, considering factors such as accessibility of the study site, portability of the equipment, and financial and human resources, among others. *Landon et al.* (2001) compared instream methods for measuring hydraulic conductivity in sandy streambeds (in situ permeameter tests, seepage meters coupled with hydraulic head measurements, slug tests, grain size distribution) and found that the spatial variability of hydraulic conductivity was greater than the variability of hydraulic conductivity between different methods. They concluded that the method used may matter less than making enough measurements to characterize spatial variability.

Uncertainties inherent in the different techniques may be taken into account when selecting methods to study groundwater – surface water interactions. Measurements of hydraulic conductivity are generally characterized by high uncertainties, because hydraulic conductivity can vary over several orders of magnitude. Hence, flux estimates based on the Darcy equation are inherently inaccurate, which relates to the majority of methods applied in the aquifer and the transition zone. Hydrograph separation is based on the assumptions that stream discharge can

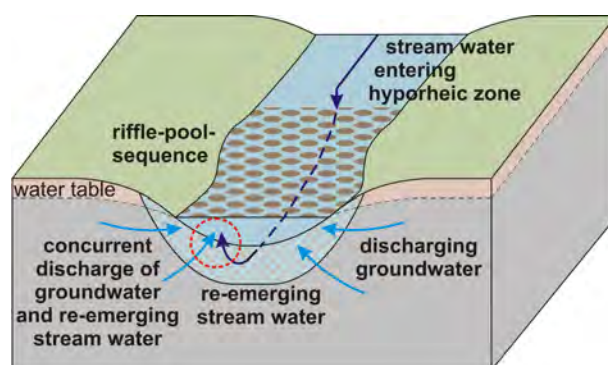


Figure 2.2. Exchange flows between groundwater and surface water through the hyporheic zone at a riffle-pool-sequence (after *Winter et al.*, 1998).

be directly correlated to groundwater recharge. Several factors are neglected in this approach, such as evapotranspiration and bank storage, leading to considerable uncertainties (*Halford and Mayer, 2000*). Tracer-based hydrograph separation further assumes that pre-event water and event water are clearly different in isotopic or chemical composition and that the composition is constant in space and time; both being conditions that are often not met (*Genereux and Hooper, 1998*). Similarly, environmental and heat tracer measurements in the surface water rely on clearly pronounced and stable differences between groundwater and surface water, incorporating some degree of uncertainty. Flux estimates based on temperature gradients in the streambed are calculated on the assumption of vertical flow beneath the stream, which may not be true in the vicinity of the river banks or because of influences of hyporheic water movement as described before. Furthermore, the influence of daily fluctuations in surface water temperature may create some error. Flux measurements made by conventional seepage meters may be influenced by the resistance of the collection system to streamflow (*Murdoch and Kelly, 2003*). The accuracy of contaminant concentrations from water samples is influenced by the handling of the samples and the detection sensitivity of the analysis methods. Passive flux meter measurements may further be affected by competitive sorption or rate-limited sorption, and by fluctuations in flow direction in case of long-term measurements. The evaluation of integral pumping tests requires information on aquifer properties which may already be uncertain. In conclusion, inaccuracies are inherent in all methods to determine interactions between groundwater and surface water, so that an analysis of uncertainties along with any measurement is indispensable.

Because of the limitations and uncertainties associated with the various methods, any attempt to characterize stream-aquifer interactions may benefit from a multi-scale approach combining multiple techniques. For instance, flux measurements in the transition zone alone may not suffice to clearly identify the groundwater component, while isotope concentrations alone may also lead to misinterpretations. Also, integrating point measurements may not be a valid substitute for measurements on a larger scale due to the scale-effects of measurements in heterogeneous media. Therefore, measurements on multiple scales are recommended to characterize the various processes and include different factors controlling groundwater-surface water exchange. Furthermore, a combination of measurements of physical and chemical properties may help identify water sources and subsurface flow paths. For instance, *Becker et al. (2004)* combined current meter measurements with a stream temperature survey to both identify zones of groundwater discharge and calculate groundwater inflow to the stream; *Constantz (1998)* analysed diurnal variations in streamflow and stream temperature time series of four alpine streams to quantify interactions between stream and groundwater; *James et al. (2000)* combined temperature and the isotopes of O, H, C, and noble gases to understand the pattern of groundwater flow; *Harvey and Bencala (1993)* used hydraulic head measurements and solute tracers injected into the stream and the subsurface to identify flow paths between stream channel and aquifer and to calculate exchange rates; *Storey et al. (2003)* used hydraulic head measurements, salt tracers injected into the subsurface, and temperature measurements in the stream and subsurface to trace the flow paths in the hyporheic zone; *Ladouche et al. (2001)* combined hydrological data, geochemical and isotopic tracers to identify the components and origin of stream water. An elaborate combination of methods can considerably reduce uncertainties and constrain flux estimates.

2.8 Summary

Measuring interactions between groundwater and surface water is an important component for integrated river basin management. Numerous methods exist to measure these interactions which are either applied in the aquifer, in the surface water, or in the transition zone itself.

The methods differ in resolution, sampled volume, and the time scales they represent. Often, the choice of methods constitutes a trade-off between resolution of heterogeneities and sampled subsurface volume. Furthermore, the measurement scale on which a selected technique operates may have a significant influence on the results, leading to differences between estimates obtained from a grid of point measurements and estimates obtained from large-scale techniques. Therefore, a better representation of the local conditions including the effects of scale on measurement results can be achieved by conducting measurements at multiple scales at a single study site.

Attention should be paid to distinguish between groundwater discharge and hyporheic exchange flow. Small-scale flow measurements in the shallow streambed may not suffice to make this distinction, so that additional measurements to identify the water source are recommended.

The study goal plays a decisive role in choosing appropriate methods. For regional investigations large-scale techniques may be more suitable, whereas process studies may require measurements which enable high resolution. All methods have their limitations and uncertainties. However, a multi-scale approach combining multiple techniques can considerably reduce uncertainties and constrain estimates of fluxes between groundwater and surface water.

New methodology to investigate potential contaminant mass fluxes at the stream-aquifer-interface by combining integral pumping tests and streambed temperatures

This chapter is published as:

Kalbus, E., Schmidt, C., Leschik, S., Reinstorf, F., Balcke, G. U., and Schirmer, M. (2007): New methodology to investigate potential contaminant mass fluxes at the stream-aquifer-interface by combining integral pumping tests and streambed temperatures. *Environmental Pollution*, 148, 808-816.

Abstract. The spatial pattern and magnitude of mass fluxes at the stream-aquifer interface has important implications for the fate and transport of contaminants in river basins. Integral pumping tests were performed to quantify average concentrations of chlorinated benzenes in an unconfined aquifer partially penetrated by a stream. Four pumping wells were operated simultaneously for a time period of five days and sampled for contaminant concentrations. Streambed temperatures were mapped at multiple depths along a 60 m long stream reach to identify the spatial patterns of groundwater discharge and to quantify water fluxes at the stream-aquifer interface. The combined interpretation of the results showed average potential contaminant mass fluxes from the aquifer to the stream of $272 \mu\text{g m}^{-2} \text{d}^{-1}$ MCB and $71 \mu\text{g m}^{-2} \text{d}^{-1}$, respectively. This methodology combines a large-scale assessment of aquifer contamination with a high-resolution survey of groundwater discharge zones to estimate contaminant mass fluxes between aquifer and stream.

3.1 Introduction

The spatial pattern and magnitude of mass fluxes at the stream-aquifer interface has important implications for the fate and transport of contaminants in river basins. Polluted stream water may infiltrate into the aquifer and affect groundwater quality, or contaminated groundwater may discharge to the stream and cause a long-term deterioration of surface water quality. In perennial streams, groundwater provides the base flow, i.e., the water that feeds the stream throughout the year. In many rivers, more than 50% of the annual flow is derived from groundwater. During low-flow periods in summer, more than 90% of the discharge in some rivers may come from groundwater (COM, 2003). Thus, contaminant transport from groundwater to surface water may directly affect related aquatic and terrestrial ecosystems.

In recent years, research has focused increasingly on the investigation of interaction processes between groundwater and surface water. Interactions are complex (Sophocleous, 2002) and are driven by various geomorphologic and hydrogeologic controls (e.g., Woessner, 2000; Kasahara and Wondzell, 2003; Storey et al., 2003; Gooseff et al., 2006). Both aquifers and streambed sediments can be highly heterogeneous systems where characteristics change on small spatial and temporal scales. Malcolm et al. (2003) found substantial variability in streambed chemistry at fine (<10 m) spatial scales and over the course of hydrological events. These changing conditions may influence the exchange of water and solutes at the stream-aquifer interface, which may have important implications for the stream ecology. The nature of the hydrochemical response was found to vary among stream locations depending on the strength of local groundwater influence (Malcolm et al., 2003). Conant (2004) found that the near-river zone strongly modified the distribution, concentration, and composition of a tetrachloroethene groundwater plume prior to discharging into the surface water. They concluded that variations in the contaminant plume itself as well as the composition of streambed sediments and biodegradation processes caused the complex concentration distribution in the streambed. Therefore, a detailed investigation of the streambed is recommended when studying contaminant transport at the stream-aquifer interface, particularly with respect to the impact of the spatial distribution of contaminants on the interstitial habitat.

There has been a growing consensus among technical groups and regulatory agencies (API, 2002, 2003; ITRC, 2003; EPA, 2003; NRC, 2004) that contaminant mass fluxes and contaminant mass flow rates should be used as alternate performance metrics instead of maximum concentration levels for site assessment and remediation design at contaminated sites (e.g., Jawitz et al., 2005; Basu et al., 2006). For a determination of contaminant mass flow rates, groundwater flow rates and average contaminant concentrations are required. To obtain groundwater flow rates through the streambed, various methods exist that provide different spatial resolutions (for a review see, e.g., Kalbus et al., 2006). For investigations with high spatial resolution, Schmidt et al. (2006) presented a very promising method that is based on measurements of streambed temperature profiles. Average contaminant concentrations have traditionally been investigated by point-scale measurements at monitoring wells. Due to the usually heterogeneous composition of both the subsurface and the contaminant distribution in the source zones this approach may lead to highly unreliable results and would require a large number of closely spaced monitoring wells, particularly when investigating groundwater contamination at a long stream reach. A new integral pumping test (IPT) method has recently been developed, which is based on the evaluation of concentration time series measured during pumping from a well (Teutsch et al., 2000; Bockelmann et al., 2001). This method overcomes the problem of heterogeneous

contaminant distributions, since a large aquifer volume is involved in the evaluation.

This paper presents the results of an investigation of contaminant mass flux at the stream-aquifer interface within the EU-project AquaTerra. In the framework of AquaTerra, the river-sediment-soil-groundwater system as a whole is investigated in order to provide the scientific basis for an improved river basin management. Within the subproject FLUX, fluxes from groundwater to surface water, and vice versa, are assessed on various scales. A crucial point is the quantification of water and solute mass fluxes between groundwater and surface water at the river subcatchment and catchment scale.

The objective of this study is to provide a methodology for the estimation of the mass flux of contaminants between groundwater and surface water. We hypothesize that a combination of two novel approaches constitutes an efficient new methodology for quantifying water and solute flows at the stream-aquifer interface: Streambed temperature mapping for determining the spatial distribution and magnitude of groundwater discharge through the streambed combined with integral pumping tests for the estimation of average contaminant concentrations and mass flow rates in the groundwater migrating toward the stream. An advantage of this methodology is that it does not require sophisticated measurement devices. We use simple analytical solutions for the estimation of both groundwater discharge and average contaminant concentrations that can be applied to typical situations of aquifers connected to streams. Both methods individually have proved to provide reliable data in previous studies (*Béland-Pelletier et al.*, 2001; *Schmidt et al.*, 2006), and a combination may therefore constitute an efficient alternative to conventional piezometer studies. This methodology, however, neglects degradation and sorption of the contaminants on the passage through the streambed. Simplifying assumptions had to be made for the current state of the work. The methodology enables the quantification of the total contaminant mass that is discharged to the stream excluding degradation and/or sorption, which we termed “potential” contaminant mass flux through the streambed.

3.2 Study site

The study site is located in the industrial area of Bitterfeld/Wolfen, about 130 km south of Berlin, Germany. This region is one of the oldest industrial centres of Germany (*Heidrich et al.*, 2004a,b), where a century of chemical production resulted in a regional aquifer contamination with an estimated extent of 25 km² affecting more than 200 million m³ of groundwater (*Weiss et al.*, 2001). The main contaminants are volatile halogenated hydrocarbons, monoaromatic hydrocarbons such as BTEX or chlorinated benzenes and phenols, hexachlorocyclohexanes, polychlorinated biphenyls, dioxins, and a variety of other substances.

Investigations were conducted at a 60 m long section of the Schachtgraben Stream (Figure 3.1). The stream is part of the Mulde River system which belongs to the Elbe basin. The Schachtgraben is a man-made stream which had originally been constructed for wastewater discharge from open-cast lignite mines. The streambed is composed of a 0.6 m thick crushed rock layer on top of a clay layer. The stream is about 3 m wide and has an average water depth of 0.6 m. The slope is 0.0008 m m⁻¹, and the mean annual discharge is 0.2 m³ s⁻¹.

The Schachtgraben partially penetrates a Quaternary alluvial aquifer. This aquifer is locally subdivided into two horizons by a silt/clay/peat layer that serves as a local aquitard. The unconfined shallow horizon, which is connected to the Schachtgraben, consists of sandy gravel with a mean hydraulic conductivity of 5×10⁻⁴ m s⁻¹ and an effective porosity of 0.25. The mean

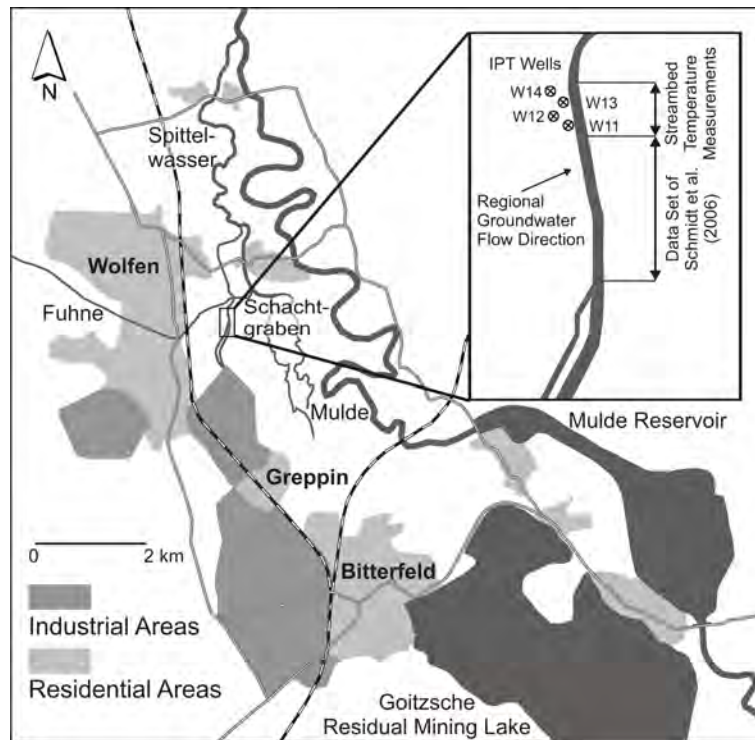


Figure 3.1. Location of the study site and position of the streambed temperature measurements and the integral pumping test (IPT) wells W11, W12, W13, and W14.

saturated thickness is 7.83 m with its base at about 11 m below ground surface. The regional groundwater flow direction is from southwest to northeast towards the Mulde River. The average gradient at the study site is $4 \times 10^{-3} \text{ m m}^{-1}$. Water table elevations in the aquifer are generally higher than the Schachtgraben water level, so that the Schachtgraben can be considered a gaining stream. The streambed, however, has been constructed with a clay layer to avoid infiltration of wastewater into the aquifer. Preliminary investigations suggested, though, that it is not completely impermeable, but rather shows distinct zones of discharging groundwater. Most of the groundwater flows underneath the Schachtgraben and transports contaminants towards the Mulde River. However, some of the groundwater discharges to the Schachtgraben and releases the contaminants to the stream, where they are quickly transported to the receiving rivers.

The dominant contaminants in the Quaternary aquifer are chlorinated benzenes. The contamination source is believed to be in the southern part of the former Bitterfeld Chemical Works facilities (Heidrich *et al.*, 2004a), about 3.5 km south of the study site. Contamination at the study site is predominantly diffuse. Contaminant distributions, however, may be locally heterogeneous. In the Schachtgraben, contamination levels are generally higher than in the surrounding aquifer, because the stream receives polluted drainage water from a landfill in a former open-cast lignite mine and from unknown sources in the area of the former chemical plants.

3.3 Methods

3.3.1 Streambed temperature mapping

Background

The concept of streambed temperature mapping implies that spatial differences in streambed temperature can be attributed to spatial differences in water fluxes and are not a result of temporal variations (Conant, 2004). Aquifer temperatures remain nearly constant at the mean annual air temperature at a sufficient depth, whereas stream water temperatures vary seasonally and diurnally. In summer, for instance, stream water temperatures are higher than groundwater temperatures. Relatively cold temperatures in the streambed then indicate groundwater discharge zones. Temperature measurements in the streambed can be used to quantify water fluxes between aquifer and stream by solving the heat transport equation (Anderson, 2005). Analytical solutions to solve the heat transport equation for water flux were developed in the 1960s (Suzuki, 1960; Stallman, 1965; Bredehoeft and Papadopolus, 1965). Assuming that water flow in the streambed is at steady-state and essentially vertical, i. e. $\vec{q}(x, y, z) = q_x\vec{i} + q_y\vec{j} + q_z\vec{k}$ with $q_z = q_z(x, y)$, the water flux at each measurement location (x, y) can be estimated from the observed temperatures $T(x, y, z)$ at depth z applying (Bredehoeft and Papadopolus, 1965):

$$\frac{T(x, y, z) - T_0}{T_L - T_0} = \frac{\exp\left(\frac{q_z(x, y)\rho_f c_f}{K_{fs}}z\right) - 1}{\exp\left(\frac{q_z(x, y)\rho_f c_f}{K_{fs}}L\right) - 1} \quad (3.1)$$

where $T(x, y, z)$ is the streambed temperature at depth z and horizontal location x, y ; T_0 is the stream water temperature; T_L is the aquifer temperature; q_z is the vertical specific discharge; $\rho_f c_f$ is the volumetric heat capacity of the fluid; K_{fs} is the thermal conductivity of the solid-fluid system; and L is the depth of the aquifer temperature measurement T_L . Streambed temperatures are measured simultaneously at multiple depths below the streambed surface at each horizontal location x, y . Eq. 3.1 is solved for q_z using a least square optimization. The calculated q_z at the location x, y minimizes the error between the temperature profile at x, y (consisting of temperature observations at multiple depths) and the simulated temperature profile (Schmidt et al., 2006). The assumption of streambed temperatures being at steady-state is valid for measurements at a sufficient depth below the influence of diurnal variations for the finite time of a mapping programme, which has been confirmed by Conant (2004) and Schmidt et al. (2006). Diurnal oscillations of surface water temperatures do not significantly influence the temperatures at 0.15 m or deeper below the streambed surface in a gaining stream. The total groundwater discharge Q_s through a given area of the streambed S can be estimated from:

$$Q_s = \int_S q_z(x, y) dS \quad (3.2)$$

Field application

Streambed temperatures were measured during a two days mapping campaign on 24 and 25 July 2006 along a longitudinal transect of 60 m length (Figure 3.1). The stream section corresponds to the location where the integral pumping tests were performed as described below. Measurements were spaced at intervals of roughly 3 m in the centre of the channel cross-section. We used a multilevel stainless steel temperature probe (TP 62, Umwelt Elektronik GmbH, Geislingen, Germany) to measure streambed temperatures simultaneously at depths of 0.10 m, 0.15 m, 0.20 m, 0.30 m, and 0.50 m below the streambed surface at each location. At these depths, the temperature measurements were within the crushed rock layer and did not reach the underlying clay layer. The temperature probe required about two to five minutes to equilibrate. Stream water temperatures were monitored continuously using a self-containing Stowaway TidbiT temperature logger (Onset Computer Corporation, Pocasset, Massachusetts). Groundwater temperatures were also monitored continuously with temperature probes (HT575, Hydrotechnik GmbH, Wangen, Germany) placed directly in the aquifer. For a detailed description of the field methods and the analytical model the reader is referred to *Schmidt et al.* (2006), since we followed precisely their methodology. Furthermore, we included their data set, which was collected adjacent to our study site (Figure 3.1) in our calculations.

3.3.2 Integral pumping tests

Background

The integral pumping test (IPT) method (*Teutsch et al.*, 2000; *Bockelmann et al.*, 2001) was applied to estimate the average contaminant concentrations C_{av} and mass fluxes J_{CP} over control planes (CP) within the Quaternary aquifer next to the stream. The advantage of the IPT method, compared to conventional methods, is that a large aquifer volume is investigated through pumping and therefore estimates are more representative than those from conventional contaminant sampling at monitoring wells. The first analytical solution for the evaluation of IPTs, for the case of circular isochrones was derived by *Schwarz* (2002). A generalization of Schwarz's solution, which accounts for non-circular isochrones and effects of retardation/sorption is given in *Bayer-Raich et al.* (2004, 2006). A number of IPT evaluations have been described in previous studies (e.g., *Bockelmann et al.*, 2001, 2003; *Bauer et al.*, 2004; *Rügner et al.*, 2004; *Ptak et al.*, 2004; *Jarsjö et al.*, 2005). However, this is the first study where (a) the IPT was applied for the quantification of the total potential contaminant mass flow to a stream and (b) all wells were pumped simultaneously.

IPT design, performance and evaluation

Four wells were drilled along a control plane perpendicular to the mean local groundwater flow direction. They were fully screened and completely penetrated the shallow Quaternary aquifer. The wells were spaced at intervals of 15 m to fully cover the control plane by the expected capture zones for the selected pumping rate and test duration (Figure 3.2). All wells were pumped simultaneously with a constant pumping rate of 1 L s^{-1} per well over a test duration of 5 days (120 hours) from 24 to 29 October 2005. Water samples were taken every three hours from all wells and from the Schachtgraben. Additionally, water level, electrical conductivity, oxygen

content, pH, and temperature were monitored at each pumping well and in the stream (electrical conductivity: WTW TetraCon 325; oxygen: WTW CellOx 325; pH and temperature: WTW SenTix 41; Wissenschaftlich-Technische Werkstätten GmbH, Weilheim, Germany). Drawdown and recovery of piezometric heads were recorded at the beginning and end of the pumping test. Groundwater levels were also monitored at a nearby test plot equipped with pressure probes (HT575, Hydrotechnik GmbH, Wangen, Germany). For design of the IPT and simulation of flow during pumping, we set up a numerical flow model using MODFLOW-96 (McDonald and Harbaugh, 1996). Mean aquifer thickness b , gradient, hydraulic conductivity K and effective porosity n_e were estimated from field data (see Sect. 3.2) and assigned to the grid cells assuming a homogeneous aquifer. The capture zone of each well $V_W(t)$ is defined as the aquifer volume containing all groundwater extracted at the well up to time t . For definition of the geometry of $V_W(t)$, we used particle tracking with the code MODPATH 3.0 (Pollock, 1994).

The stream was not included in the MODFLOW model used for the numerical evaluation of the IPTs. Preliminary simulations indicated that the influence of the river on the shape of the isochrones was of minor importance at this site. Average contaminant concentrations were computed for each well using the analytical solution as a first approximation (Bayer-Raich et al., 2006):

$$C_{av}(t_n) = \frac{1}{\sqrt{t_n}} \sum_{i=1}^n C_w(t_i) (\sqrt{t_n - t_{i-1}} - \sqrt{t_n - t_i}) \quad (3.3)$$

where $C_{av}(t_n)$ is the average concentration for undisturbed conditions (i.e. before pumping) along the CP defined by the width of the capture zone at time t_n ; $C_w(t_i)$ is the concentration at the well at the pumping time t of sample number i ; and n is the total number of samples. This solution is valid, in theory, only for the case of circular isochrones. To verify the accuracy of the calculated average concentrations, we compared C_{av} obtained from Eq. 3.3 to C_{av} obtained numerically through the code CSTREAM (Bayer-Raich, 2004), which accounts for the irregular shape of the isochrones shown in Figure 3.2.

Sample analysis

Water samples, filled to the brim into glass bottles, were transported and stored under cooled conditions. Analyses were carried out within 24 h. Automated sample extraction was performed via headspace solid phase micro-extraction (SPME, 85 μm polyacrylate coating, Supleco, Taufkirchen, Germany) using 4 mL samples in 10 mL GC vials provided with 1.5 g NaCl. The SPME fibre was allowed to absorb for 25 min before desorption (250 °C) into a gas chromatograph (Varian 3400 CX, Darmstadt, Germany) equipped with an HP-5MS column (Hewlett-Packard, Waldbronn, Germany) and a flame ionization detector (FID). Chromatographic separation was assisted by a temperature gradient from 40 °C - 280 °C. Helium served as carrier gas. External calibration was done using authentic standards (Supelco) diluted in methanol and spiked to the GC vials. Detection limits were 0.15 $\mu\text{g L}^{-1}$ for monochlorobenzene and 0.20 $\mu\text{g L}^{-1}$ for all other di- and trichlorobenzenes. For validation of the signal stability throughout the test series, a validation standard was measured every eight samples and the results of the respective samples were corrected for the recovery of this standard. The standard deviation for a 2 $\mu\text{g L}^{-1}$ validation standard varied between 11 and 12% for all chlorinated benzenes based on a total of 20 validation standards measured throughout the 120 h sampling period. Thus, the contribution to variations in the contaminant concentrations by the detection method was minor.

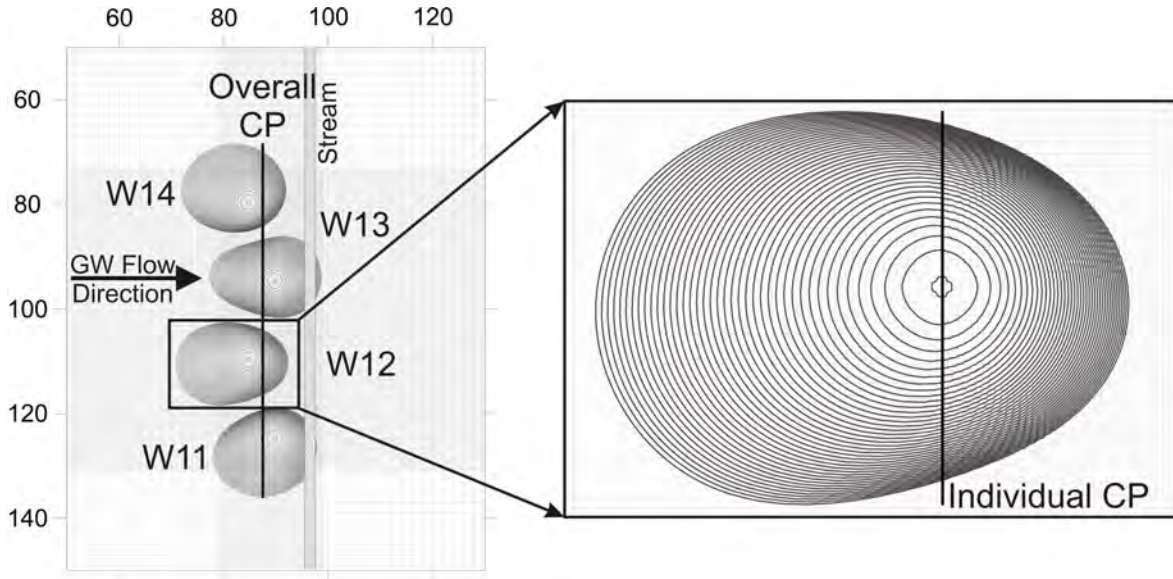


Figure 3.2. Section of the MODFLOW model showing isochrone geometry for the four IPT wells. Samples were collected every 3 h (each isochrone corresponds to a time of sampling), total pumping time was 5 days. The grid was refined around the wells (shaded areas on left-hand side of figure).

3.3.3 Concept of method combination

The integral pumping test method provides estimates of average contaminant concentrations and mass fluxes along a control plane, which in our case was parallel to the stream. Thus, it yields the total contaminant mass flow through the aquifer that is approaching the stream. The streambed temperature observations enable the detection of permeable zones in the streambed and provide estimates of groundwater fluxes to the stream. This helps to separate the groundwater flow (Q_{CP}) into the proportion flowing underneath the stream (Q_U) and the proportion discharging to the stream (Q_S) with $Q_{CP} = Q_U + Q_S$ as indicated in Figure 3.3(a). Assigning the average contaminant concentration C_{av} [$\mu\text{g L}^{-1}$] as determined by the IPT method to the proportion discharging to the stream, the contaminant mass flow rate to the stream M_S [$\mu\text{g d}^{-1}$] or the contaminant mass flux J_S [$\mu\text{g m}^{-2} \text{d}^{-1}$] can be computed.

For estimation of total mass flows, we subdivided the stream into zones with each zone k being associated with one IPT well. The zones k were further subdivided into sections j associated with one temperature profile. Assigning the average concentration $C_{av}^{(k)}$ [$\mu\text{g L}^{-1}$] obtained from the IPT in zone k to the water flux $q_z^{(j)}$ [$\text{L m}^{-2} \text{d}^{-1}$] at the section j of the streambed, the mass flow rate $M_S^{(j)}$ [$\mu\text{g d}^{-1}$] and the mass flux $J_S^{(j)}$ [$\mu\text{g m}^{-2} \text{d}^{-1}$] for section j are obtained from

$$M_S^{(j)} = Q_S^{(j)} C_{av}^{(k)} \quad (3.4)$$

$$J_S^{(j)} = q_z^{(j)} C_{av}^{(k)} \quad (3.5)$$

where k is the zone including section j , as indicated in Figure 3.3(b). For instance, zone $k = 2$ comprises sections $j = 6, 7, \dots, 10$. The total mass flow rate for the entire streambed

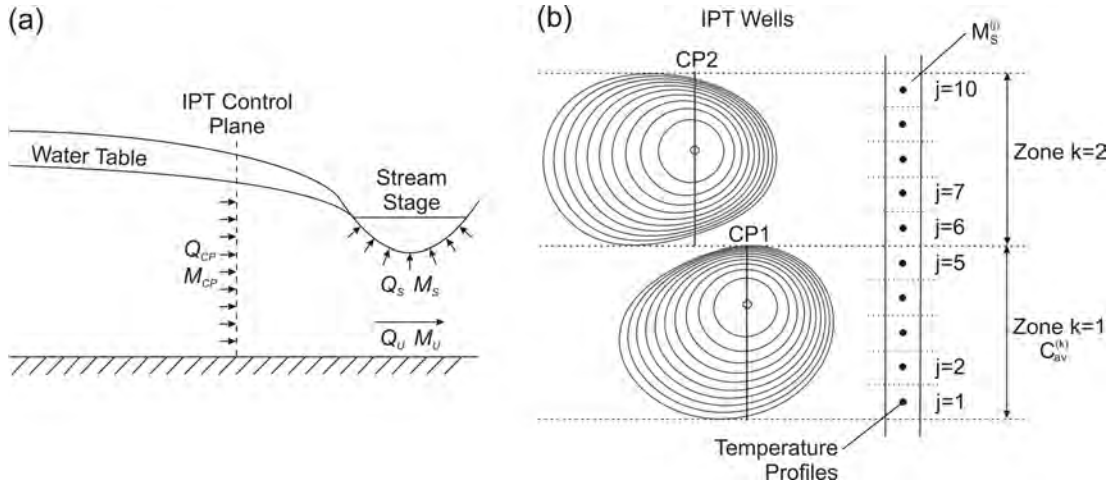


Figure 3.3. Conceptual model of combined method to determine contaminant mass flows at the stream-aquifer interface. (a) Cross-section showing water and contaminant mass flows at the control plane (Q_{CP} , M_{CP}), through the streambed (Q_S , M_S), and below the stream (Q_U , M_U); (b) Plan view showing the subdivision into zones k with average concentrations $C_{av}^{(k)}$ associated with one IPT well, and sections j associated with one temperature profile for calculation of mass flow rates through the streambed $M_S^{(j)}$. Zone $k = 1$ includes sections $j = 1, 2, \dots, 5$; zone $k = 2$ includes sections $j = 6, 7, \dots, 10$.

is then computed by adding up the mass flow rates of each section as

$$M_S = \sum_{j=1}^m M_S^{(j)} \quad (3.6)$$

where m is the total number of sections.

3.4 Results and discussion

3.4.1 Results of streambed temperature mapping

Observed stream water temperatures ranged from 17.3 to 23.5 °C during the measurement campaign. Streambed temperatures were rather high, showing only little spatial variability throughout the observed reach. At a depth of 0.50 m below streambed surface, temperatures varied between 15.4 and 18.4 °C. At the shallow depth of 0.10 m, temperatures ranged from 18.9 to 22.8 °C.

Water fluxes were computed at each temperature profile from Eq. 3.2. To obtain q_z from Eq. 3.1, the average stream water temperature during the measurement campaign of 19.9 °C was used as quasi-steady-state upper boundary condition T_0 (Schmidt *et al.*, 2006). The lower boundary condition T_L was represented by the groundwater temperature of 11 °C at a depth L of 4.0 m. K_{fs} was not measured for this study. However, it can be reliably estimated, because thermal conductivities of water-saturated sediments vary only within a small range (Stonestrom and Constantz, 2003). K_{fs} was set to $2 \text{ J s}^{-1} \text{ m}^{-1} \text{ K}^{-1}$, assuming that this value is representative for

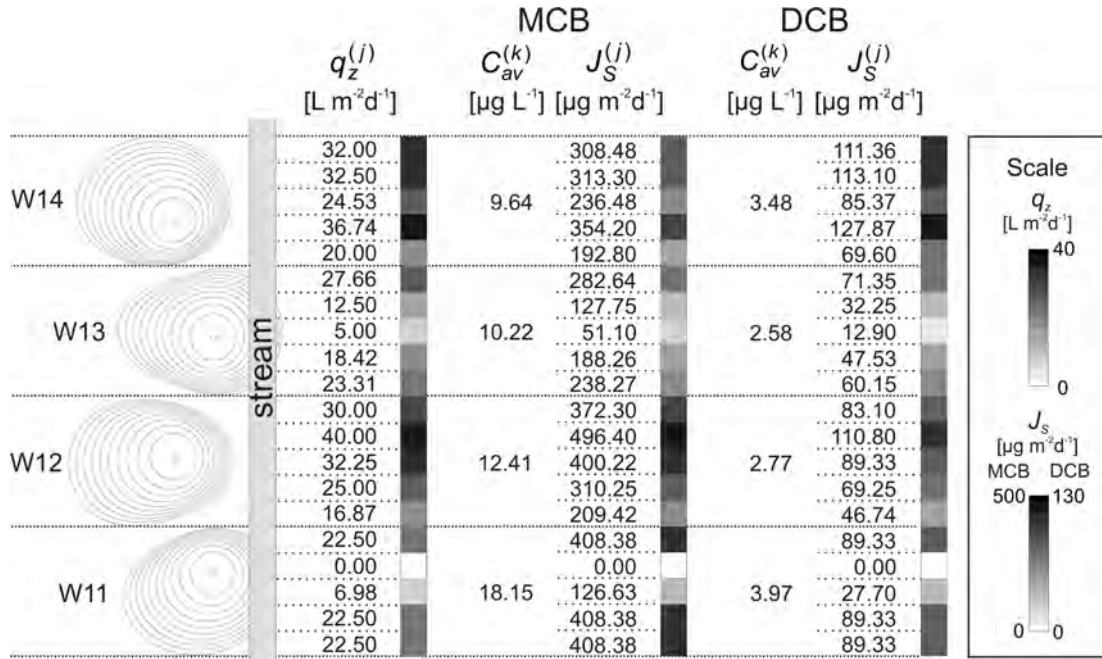


Figure 3.4. Spatial distribution of groundwater fluxes through the streambed in sections j ($q_z^{(j)}$), average contaminant concentrations in zones k ($C_{av}^{(k)}$) corresponding to the capture zones illustrated by isochrones of wells W11 to W14, and potential contaminant mass fluxes through the streambed in sections j ($J_S^{(j)}$). Values for DCB are given as sum of isomers.

each temperature profile. *Schmidt et al.* (2006) showed that fluxes calculated by using this value matched well with fluxes obtained from Darcy’s Law calculations from streambed piezometer data. The volumetric heat capacity of water $\rho_f c_f$ is given as $4.19 \times 10^{-6} \text{ J m}^{-3} \text{ K}^{-1}$. Calculated groundwater fluxes through the streambed ranged from 0 to $40 \text{ L m}^{-2} \text{ d}^{-1}$ (Figure 3.4) with an average of $22.7 \text{ L m}^{-2} \text{ d}^{-1}$. Total daily groundwater discharge over the investigated reach length of 60 m and a stream width of 3 m (Eq. 3.2) was 4061 L d^{-1} .

The characteristics of groundwater discharge estimated in this study were significantly different from the results obtained from *Schmidt et al.* (2006) in the summer of 2005 at an adjacent upstream reach (Figure 3.1). Contrary to the findings of *Schmidt et al.* (2006), we did not observe spatially distinct high-discharge sections, nor did we detect any sections of downwelling stream water. In their study, calculated water fluxes ranged from $-10.0 \text{ L m}^{-2} \text{ d}^{-1}$ (surface water enters the streambed) to $455.0 \text{ L m}^{-2} \text{ d}^{-1}$ (groundwater discharges to the stream), which is more than tenfold the range of our results. The discharge of groundwater to the stream showed high spatial heterogeneity. Only 20% of the length of the observed stream reach contributed 50% of total groundwater discharge. Four of the 140 measurement locations showed a discharge exceeding $200 \text{ L m}^{-2} \text{ d}^{-1}$ and thereby contributed about 10% of the total groundwater discharge at the observed reach (*Schmidt et al.*, 2006). In our study, 15 of the 20 sections contributed 4-8% each to the total groundwater discharge, resulting in a relatively homogenous distribution of groundwater discharge through the streambed. Of the remaining five sections, one contributed 9% to the total groundwater discharge and the other four sections contributed less than 4%.

Table 3.1. Comparison of average contaminant concentrations C_{av} obtained from the analytical solution (AS) and CSTREAM (CS).

Contaminant	C_{av} [$\mu\text{g L}^{-1}$]							
	W11		W12		W13		W14	
	AS	CS	AS	CS	AS	CS	AS	CS
MCB	18.150	17.908	12.410	12.411	10.220	10.258	9.642	9.689
1,2-DCB	1.662	1.641	1.168	1.168	1.039	1.044	1.448	1.462
1,3-DCB	1.707	1.687	1.244	1.232	1.147	1.166	1.420	1.434
1,4-DCB	0.601	0.598	0.360	0.355	0.395	0.399	0.614	0.621

Average groundwater discharge over the observed reach length ($q_z = 22.7 \text{ L m}^{-2} \text{ d}^{-1}$) was only 40% of the value obtained by *Schmidt et al.* (2006) ($q_z = 58.2 \text{ L m}^{-2} \text{ d}^{-1}$). Because of the dry summer of 2006 the groundwater table was lower than in the summer of 2005. The hydraulic gradient between the Schachtgraben and the aquifer was also only 40% of the gradient in the summer of 2005, which corresponds to the smaller average flux in the 2006 campaign.

3.4.2 Results of the integral pumping tests

The standard parameters measured in the pumped water from the IPT wells remained stable throughout the test duration, while parameters measured in the stream water showed strong variations. pH-values in the wells varied from 6.19 to 6.42 (stream: 6.61 to 7.20), temperatures varied from 10.7 to 11.9°C (stream: 13.5 to 16.2°C), electrical conductivity varied from 1325 to 1523 $\mu\text{S cm}^{-1}$ (stream: 1817 to 2650 $\mu\text{S cm}^{-1}$), and oxygen concentration varied from 0.10 to 0.82 mg L^{-1} (stream: 2.90 to 5.88 mg L^{-1}). The values measured in the stream were considerably different from those measured in the groundwater. Since all parameters in the pumped water remained stable during the entire pumping duration, we concluded that no or negligibly little stream water was drawn to the pumping wells, even though the capture zones were expected to extend beyond the stream banks.

Tri- and tetrachlorobenzenes were found only in concentrations close to the detection limit, so that the following analysis focuses on monochlorobenzene (MCB) and dichlorobenzene (DCB). Measured concentration time series of MCB and DCB-isomeres at the four IPT wells and the Schachtgraben are depicted in Figure 3.5. Contaminant concentrations remained quite stable in the four wells during the pumping duration. Only at well W11 a slight increase in MCB concentration was observed. In the Schachtgraben, concentrations varied strongly. As proven by validation standards, these variations were not related to the analysis method; we assume that they resulted from the pumping schedule of the landfill drainage.

The measured concentration time series correspond to the characteristic plume scenario 4 in *Bockelmann et al.* (2001), indicating that the wells are located within a wide plume with an insignificantly varying contaminant concentration. We evaluated the concentration time series using both the analytical solution (Eq. 3.3) and the particle tracking numerical algorithm CSTREAM (*Bayer-Raich et al.*, 2004). Both methods yield average contaminant concentrations in the aquifer along the CP. Table 3.1 shows computed average contaminant concentrations obtained from Eq. 3.3 in comparison with those obtained from CSTREAM for each of the

four wells. Deviations between the results were less than 1%. Thus, the assumption of circular isochrones for the analytical solution seems to be suitable for computing average concentrations from the concentration time series measured in our study area, and the application of the simple analytical solution produces satisfactory results. This was also found in another study in Linz (Austria), where differences between the analytical solution and CSTREAM were less than 12% for average concentrations (Table 6 in *Bauer et al.*, 2004). However, for mass flow rates the differences were up to 100% in their study. Therefore, we used CSTREAM for calculating average contaminant mass flows along the control plane, accounting for irregular isochrone shapes. Individual control plane lengths of the well capture zones varied from 15.6 to 16.9 m. Average mass fluxes of MCB ranged from 1705 to 3138 $\mu\text{g m}^{-2} \text{d}^{-1}$, increasing from well W14 to well W11 (Table 3.2). Mass fluxes of DCB isomers were one order of magnitude smaller than those of MCB and less variable between the wells.

3.4.3 Potential contaminant mass flux to the stream

The potential contaminant mass flux to the stream was calculated from the average contaminant concentrations obtained from the IPT and the groundwater flux to the stream obtained from the temperature observations as described in Sect. 3.3.3. For simplicity, we used the average concentrations computed with the analytical solution (Eq. 3.3) as displayed in Table 3.1. The potential contaminant mass flux through the streambed varied between 0 and 496.40 $\mu\text{g m}^{-2} \text{d}^{-1}$ for MCB and between 0 and 127.75 $\mu\text{g m}^{-2} \text{d}^{-1}$ for DCB (sum of isomers) (Figure 3.4), with mean values of 272 $\mu\text{g m}^{-2} \text{d}^{-1}$ MCB and 71 $\mu\text{g m}^{-2} \text{d}^{-1}$ DCB, respectively. The total contaminant mass flow rate at the observed reach of 60 m length and 3 m width was 48.9 mg d^{-1} MCB and 12.8 mg d^{-1} DCB. These values are representative only for the time of the streambed temperature mapping campaign. As discussed before, the small gradient between the water table and stream stage in the dry summer of 2006 resulted in small groundwater fluxes to the stream and thus small potential contaminant mass fluxes. The values of q_z and J_S shown in Figure 3.4 are only approximately 40% of the values at the average gradient. Hence, long-term average contaminant mass fluxes may be at 680 $\mu\text{g m}^{-2} \text{d}^{-1}$ MCB and 178 $\mu\text{g m}^{-2} \text{d}^{-1}$ DCB, respectively, calculated with the average gradient.

Contaminant concentrations in the aquifer were found to be relatively constant. We assume that the entire aquifer penetrated by the Schachtgraben is characterized by contamination levels on the order of magnitude as determined through the IPT. Concentrations may decrease with distance from the source area and may increase closer to the source area, but the results from the IPT can be used as an approximation to calculate total contaminant mass flow from the aquifer. We further assume that mean groundwater discharge through the streambed as obtained from

Table 3.2. Contaminant mass fluxes J_{CP} at the four IPT wells obtained from CSTREAM.

Contaminant	J_{CP} [$\mu\text{g m}^{-2} \text{d}^{-1}$]			
	W11	W12	W13	W14
MCB	3138	2190	1792	1705
1,2-DCB	288	206	182	257
1,3-DCB	296	217	204	252
1,4-DCB	105	63	70	109

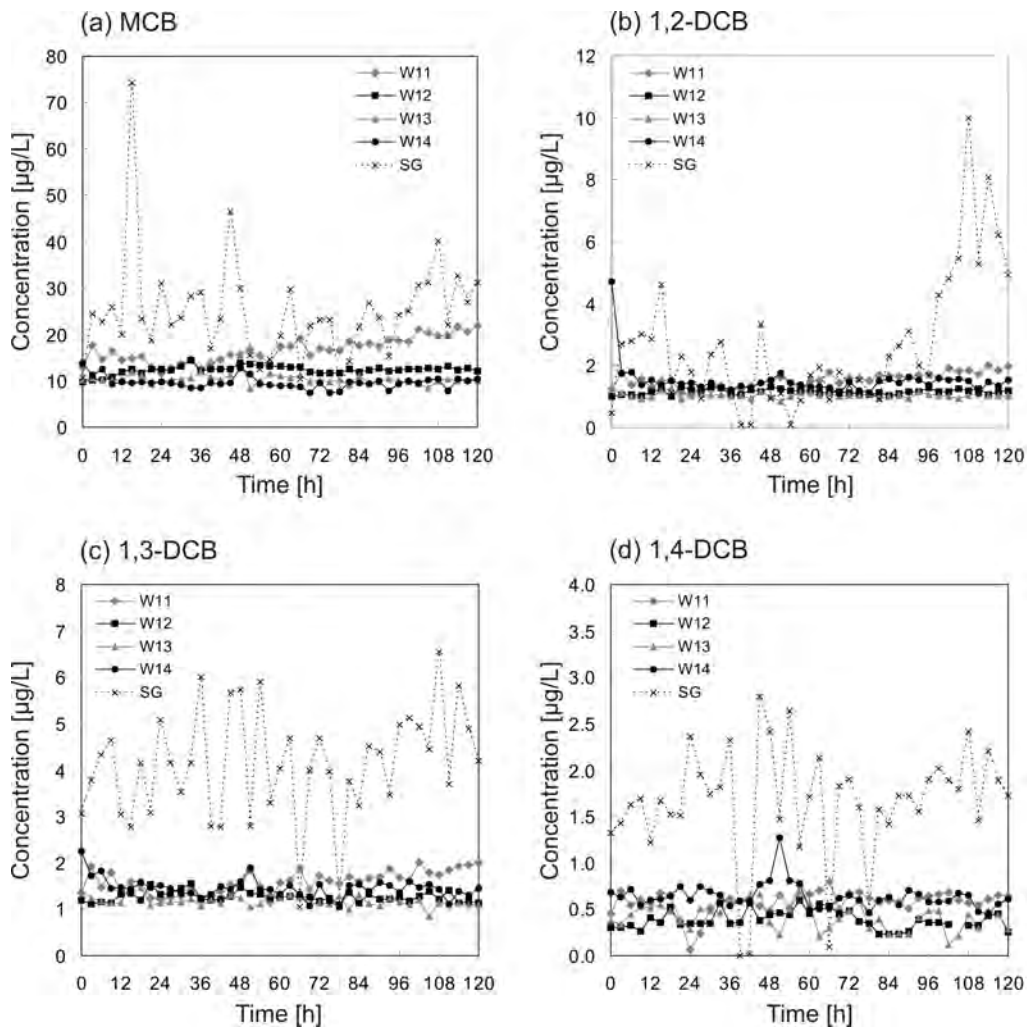


Figure 3.5. Concentration time series measured at the four IPT wells (W11 to W14) and the Schachtgraben Stream (SG) of (a) MCB, (b) 1,2-DCB, (c) 1,3-DCB, (d) 1,4-DCB.

the temperature measurements is applicable to the entire stream length of 3200 m, because the hydraulic conditions do not change significantly upstream or downstream of the observed reach. The hydraulic gradient between stream and aquifer during the measurement campaign of *Schmidt et al.* (2006) corresponds to the long-term mean, so that we used their value of mean groundwater flux to the stream for the following calculation. With a mean groundwater flux to the stream of $58.2 \text{ L m}^{-2} \text{ d}^{-1}$ and an average contaminant concentration of $12.61 \mu\text{g L}^{-1}$ MCB and $3.21 \mu\text{g L}^{-1}$ DCB (sum of isomers), respectively, the total potential release of contaminants through the entire streambed length of 3200 m was estimated to be 7.05 g MCB and 1.79 g DCB per day.

These numbers might be reduced if biodegradation and sorption processes were considered. Chlorinated benzenes are degraded aerobically and adsorbed to soil depending on the organic matter content (*Malcolm et al.*, 2004). Microorganisms colonizing the streambed interstitials may degrade the contaminants using oxygen delivered by downwelling stream water. Streambed sediments are often rich in organic matter, which could enhance adsorption on the passage

through the streambed and thus reduce the released contaminant mass. Future work is needed to include these influences in the methodology presented here.

A verification of our calculations of contaminant discharge to the stream was not possible within the framework of the present project, since the stream water was more heavily polluted than the groundwater and contaminant concentrations varied strongly with time. In the future, the stream may receive cleaner water from surface runoff and then the still ongoing discharge of contaminants through the groundwater may have adverse impacts on the stream water quality and related ecosystems.

3.5 Conclusions

The methodology presented in this study combines a large-scale (tens of meters) assessment of aquifer contamination with a high-resolution survey of groundwater discharge zones in the streambed. Using the integral pumping test (IPT) method, representative average contaminant concentrations in the aquifer were estimated using measurements of concentration time series obtained from pumping wells. The magnitude of groundwater discharge to the stream was estimated using temperature observations in the streambed. A sampling programme of only seven days (five days for the IPT and two days for the temperature mapping) was sufficient to enable a reliable determination of average concentrations and groundwater discharge rates. By combining these methods, we developed a new methodology that permits an efficient quantification of the potential mass fluxes and flow rates of chlorinated benzenes from the contaminated aquifer to the stream. Further research is needed to include the effects of degradation and sorption processes on the contaminant mass flux through the streambed. We believe that the methodology presented here can provide a useful basis for further studies to evaluate the environmental impact of large-scale contaminated aquifers on connected stream ecosystems. It is applicable in any regions where seasonal temperature variations result in temperature gradients between groundwater and surface water.

How streambed temperatures can contribute to the determination of aquifer heterogeneity

This chapter is a translation of an article published in German as:

Kalbus, E., Schmidt, C., Reinstorf, F., Krieg, R., and Schirmer, M. (2008): Wie Flussbett-Temperaturdaten zur Ermittlung der Aquifer-Heterogenität beitragen können (How streambed temperatures can contribute to the determination of aquifer heterogeneity). *Grundwasser*, 13, 91-100.

Some parts are also published in:

Kalbus, E., Schmidt, C., Molson, J., Reinstorf, F. and Schirmer, M. (2008): Groundwater-surface water interactions at the contaminated mega-site Bitterfeld, Germany. In: *GQ07: Securing Groundwater Quality in Urban and Industrial Environments. Proceedings of the 6th International Groundwater Quality Conference held in Fremantle, Western Australia, December 2007*. IAHS Publication, 324, 491-498, IAHS Press, Wallingford.

Abstract. The groundwater discharge to a stream may show small-scale heterogeneities caused by the structure of the connected aquifer. The spatial pattern of the groundwater discharge can be investigated by temperature measurements in the streambed. Thus, the heterogeneity of the hydraulic conductivity (K) of an aquifer can be inferred from measured streambed temperatures. A flow and heat transport model of a stream-aquifer system was set up including stochastic K -fields generated from the mean and variance of K data obtained from direct-push measurements. Yet, the simulated streambed temperatures did not cover the range of measured temperatures. Therefore, the relation between the distribution of streambed temperatures and the variance of K was used to calibrate the variance of K such that the distribution of measured temperatures could be reproduced by the model. This study showed that methods based on heat as a parameter for measuring and calibration constitute a valuable supplement to traditional subsurface exploration techniques.

4.1 Introduction

The natural interaction between groundwater and surface water is an important part of the terrestrial water cycle. In the transition zone, besides the exchange of water and solutes between the hydrologic units, also various transformation and retention processes take place. So far, these processes are poorly understood on the field scale. Several studies have shown that the interaction between groundwater and surface water directly impacts the microbial activity and diversity in the near-stream zone, the nutrient and carbon dynamics (*Hinkle et al.*, 2001; *Meißner et al.*, 2005; *Hlavacova et al.*, 2005) as well as the retention and transport of contaminants in the streambed (*Conant et al.*, 2004; *Kalbus et al.*, 2007; *Schmidt et al.*, 2008b).

To investigate and understand the spatial patterns and temporal dynamics of the relevant processes, it is essential to know the spatial patterns of water exchange. However, the water exchange between groundwater, streambed, and stream water may show small-scale heterogeneities (<1 m) and may therefore be difficult to capture. The main reasons for these small-scale heterogeneities are variations in hydraulic conductivity of the streambed sediments (*Cardenas et al.*, 2004) and the shallow aquifer sediments (*Storey et al.*, 2003).

Apart from hydraulic methods such as streambed-piezometers and seepage meters, the natural difference in temperature between groundwater and surface water has been used in many studies as a tracer to detect and quantify water fluxes between groundwater and surface water (*Kalbus et al.*, 2006). Overviews of the theory and application of heat as a natural tracer can be found in *Stonestrom and Constantz* (2003) and *Anderson* (2005). The theoretical background and first application studies were published already in the 1960s (*Suzuki*, 1960; *Stallman*, 1965; *Bredehoeft and Papadopolus*, 1965).

The underlying idea of these methods is based on the interplay between heat conduction and advective heat transport with the flowing water. In winter, for instance, the temperature in the surface water is lower than the groundwater temperature, which corresponds approximately to the average annual air temperature. Streambed temperatures close to the groundwater temperature therefore indicate zones of groundwater discharge to the stream. In most field applications, time series of temperatures in the surface water, the streambed sediments, and the groundwater are recorded and the water flow velocity is determined by inversion of the heat-diffusion-advection equation (e.g., *Silliman et al.*, 1995; *Constantz et al.*, 2002; *Land and Paull*, 2001; *Keery et al.*, 2007). Besides temperature time-series, a spatially high-resolving mapping of streambed temperatures can also be used to quantify the water exchange between aquifer and stream. The temperatures are recorded only at one point in time at each sampling location. The advantage of this methodology is the large number of sampling locations which enables a very detailed investigation of spatial heterogeneities (*Conant*, 2004; *Schmidt et al.*, 2006, 2007).

Only few authors have coupled temperature data to groundwater flow models as an additional parameter for model calibration. *Bravo et al.* (2002) used aquifer temperature data to simultaneously calibrate hydraulic conductivities and the Neumann boundary conditions of a numerical flow model. *Bense and Kooi* (2004) coupled vertical temperature profiles to a flow model to represent lateral changes of the vertical groundwater flow around a fault zone. *Ferguson* (2007) investigated the influence of subsurface heterogeneity on heat transport and temperature distribution in an aquifer and the implications for the use of geothermal energy. In the present work, a mapped streambed temperature data set of *Schmidt et al.* (2006) is used which represents the heterogeneity of the groundwater discharge to a stream. We assume that

the heterogeneity of the groundwater discharge is a result of the heterogeneity of the aquifer. Zones of high groundwater discharge in a stream are therefore connected to highly permeable zones in the underlying aquifer. Various authors confirmed the influence of aquifer heterogeneity on the spatial patterns of groundwater - surface water interactions (*Wroblicky et al.*, 1998; *Conant*, 2004; *Fleckenstein et al.*, 2006). Conversely, we hypothesize that the heterogeneity of the aquifer properties, expressed as the variance of hydraulic conductivity, can be inferred from streambed temperature data. For the description of aquifer heterogeneity in stream-aquifer models, stochastic approaches are useful tools (*Fleckenstein et al.*, 2006).

In the present study we show that streambed temperature data can be used to calibrate the distribution of hydraulic conductivity as input data for a stochastic stream-aquifer model, which enables a realistic representation of the heterogeneity of the groundwater discharge to the stream. In a numerical flow and heat transport model of the streambed and the connected aquifer, the distribution of hydraulic conductivity (K) is represented by stochastically generated K -fields. The mean and variance of K data obtained from direct-push measurements are used as input data for the K -field generation. By adjusting the variance of the input data and comparing simulated and observed streambed temperature distributions, the required variance to cause the observed heterogeneity of groundwater discharge and temperature distribution in the streambed can be determined. K -fields generated with the adjusted variance constitute realistic parameter sets and can then be used for further applications of the numerical model.

4.2 Study site

The study site is located in the industrial area of Bitterfeld/Wolfen, Saxony-Anhalt (Germany). In the framework of the EU-Project AquaTerra, numerous field investigations of water exchange and contaminant transport between groundwater and an artificial stream, the Schachtgraben, have been performed (*Schmidt et al.*, 2006; *Kalbus et al.*, 2007; *Schmidt et al.*, 2008a). The Schachtgraben partially penetrates a Quaternary alluvial aquifer with a saturated thickness of about 8 m. Its base is at 11 m below the surface. The stream can be characterized as a gaining stream since the water table elevation is generally higher than the water level in the stream. The regional groundwater flow direction is from south-west to north-east. Therefore, the sampling points for the investigation of the aquifer were placed at the western (upstream) side of the stream (Figure 4.1).

4.3 Streambed temperature mapping

For the mapping of streambed temperatures, the temperatures are recorded at each sampling location (x, y) at the depth z . Based on the measured temperatures $T(x, y, z)$ the flow velocity of the discharging groundwater can be determined (*Schmidt et al.*, 2006, 2008a) using a one-dimensional analytical solution of the heat-advection-diffusion equation, assuming that the groundwater flow through the streambed is vertical and at steady state (*Bredehoeft and Papadopolus*, 1965).

At the Schachtgraben, streambed temperatures were mapped in the summer of 2005 along a 220 m long stream reach (*Schmidt et al.*, 2006). The measurements were spaced at intervals of roughly 3 m. Two parallel longitudinal transects were mapped with a total number of 140

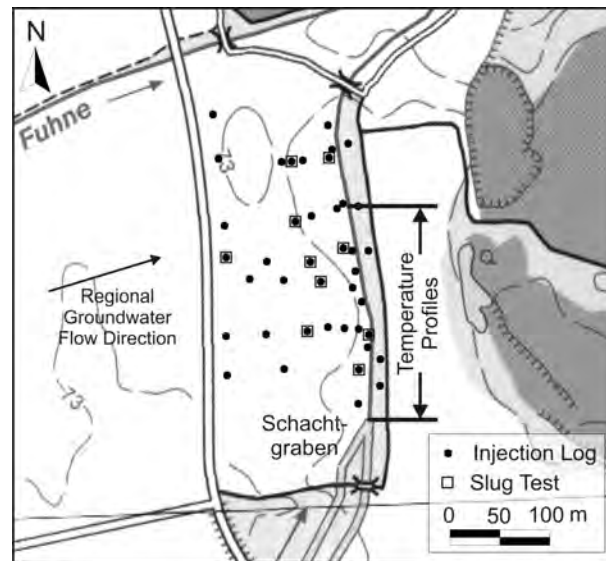


Figure 4.1. Study site with location of the injection logs, slug tests (at 2-3 depths at each location) and temperature profiles. The stream section where the temperatures were measured corresponds to the model domain.

sampling locations. The streambed temperatures were measured simultaneously at five depths (0.10 m, 0.15 m, 0.20 m, 0.30 m, and 0.50 m) below the streambed surface at each sampling location. Stream water and groundwater temperatures were recorded continuously during the mapping programme and served as upper and lower boundary conditions for the calculation of groundwater fluxes. The mean surface water temperature during the 5-day sampling programme of 18.4°C was used as upper boundary condition. The lower boundary condition was represented by the constant groundwater temperature at a depth of 4 m of 11°C which was measured in a monitoring well close to the stream.

4.4 Numerical modeling

4.4.1 Model set-up

A two-dimensional groundwater flow and heat transport model of the streambed and the connected aquifer was set up using the finite-element numerical model code HEATFLOW (Molson *et al.*, 1992). The model domain corresponds to the length of the investigated stream section and the saturated thickness of the aquifer (220 m × 8 m) and represents a vertical longitudinal profile through the streambed to the underlying aquitard (Figure 4.2). Horizontally, the model grid has 220 elements with a grid length of 1.0 m. In the vertical direction, the model grid consists of 65 layers with the layer thickness varying from 0.2 m at the lower boundary to 0.05 m at the upper boundary. The top 1.0 m was modelled with a layer thickness of 0.05 m to resolve the streambed temperature measurements in the model. The upper boundary represents the streambed surface. Altogether the model consists of 220 × 65 = 14300 elements.

For the calculation of groundwater fluxes from the measured temperature profiles, vertical

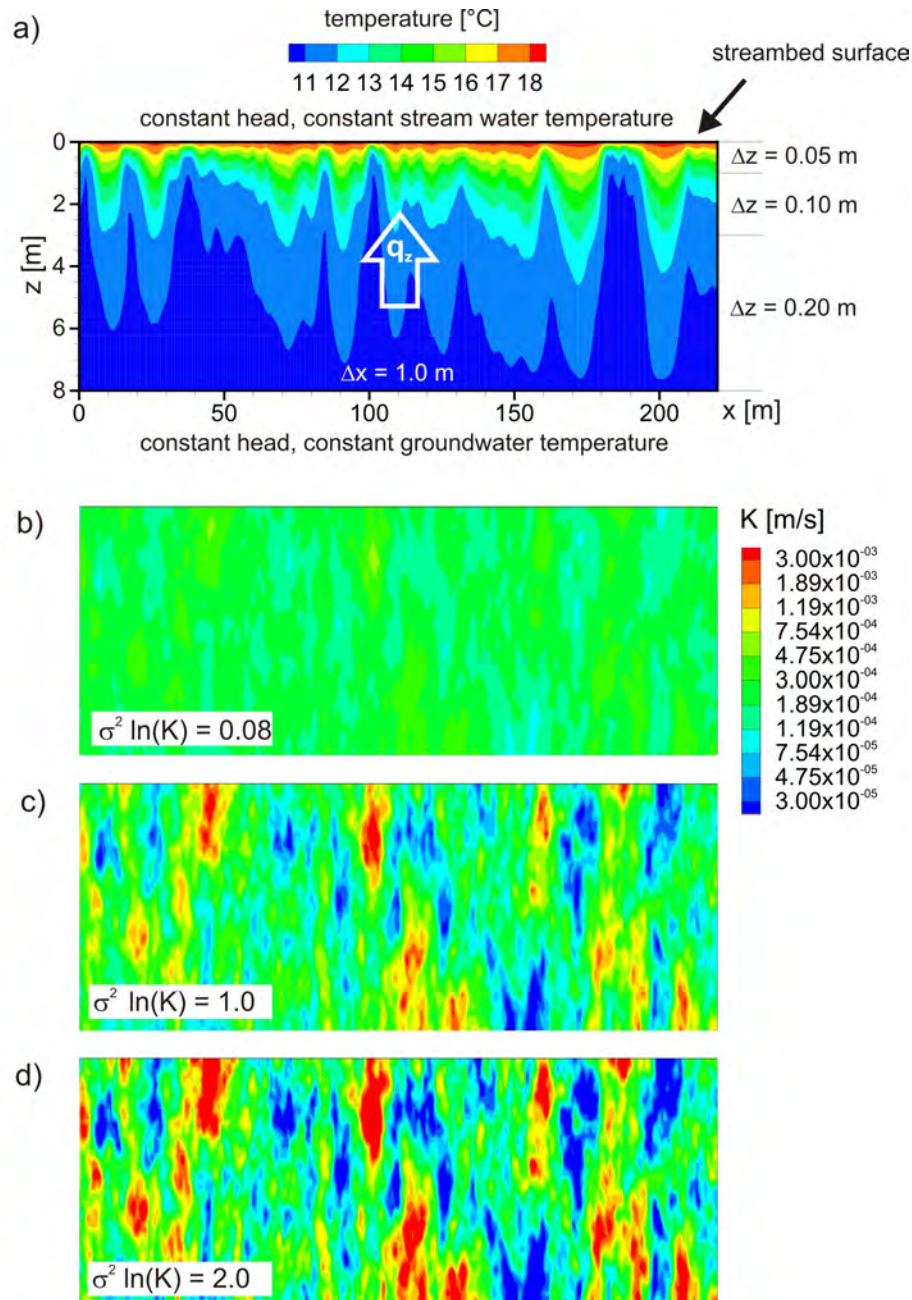


Figure 4.2. a) Conceptual model with grid resolution, boundary conditions and one example of a simulated temperature distribution using the K -field displayed in d. q_z is the vertical groundwater flux through the streambed. b) to d) realizations of K -fields with different variances of $\ln(K)$. Displayed is realization Nr. 1 out of 50 generated realizations for each variance. Vertical exaggeration is approx. 10x

flow was assumed for the application of the analytical solution, which is a common assumption for temperature-based methods to quantify groundwater discharge (Suzuki, 1960; Hatch *et al.*, 2006; Keery *et al.*, 2007). The assumption of vertical flow lines applies ideally to the centre of the streambed if groundwater flows towards the stream from both sides. Deviations to the vertical flow direction are difficult to detect with temperature measurements, since the temperature profiles are particularly sensitive to vertical water flow (Schmidt *et al.*, 2007). For the numerical model we also assumed vertical flow, which allows to represent the problem in a two-dimensional system. The boundary conditions are assumed to be at steady state. Upper and lower boundaries are constant-head boundaries (Dirichlet boundary condition), left and right boundaries are no-flow boundaries (Neumann boundary condition). The hydraulic gradient was chosen such that for a homogeneous parameter distribution the modelled groundwater flux equalled the mean flux calculated from the measured temperature profiles ($q_{z\text{mean}} = 58.2 \text{ L m}^{-2} \text{ d}^{-1}$). Analogous to the estimation of groundwater discharge rates from the measured temperature profiles, the mean stream water temperature during the mapping programme (18.4 °C) was set as the upper temperature boundary condition, and the constant temperature of the groundwater at a depth of 8 m (10.9 °C) as the lower temperature boundary condition.

4.4.2 Input parameters

The parameters in Table 4.1 were homogeneously distributed in the model, except the hydraulic conductivity. A heterogeneous distribution of K was achieved by stochastically generating K -fields using the code FGEN (Robin *et al.*, 1993). The algorithm generates three-dimensional random fields of real variables on a regular grid by performing an inverse Fourier transform after Gutjahr (1989). Input data for FGEN were the mean and variance of $\ln(K)$ and the correlation lengths in each direction (Table 4.2). The generated K -fields are not spatially conditioned to field data, so that an exact spatial representation of the groundwater discharge is not possible. The range and distribution of groundwater discharge, however, can be investigated with these K -fields.

Aquifer K data were estimated by a combination of direct-push injection logging (DPIL, Dietrich *et al.*, 2008) and direct-push pneumatic slug tests (Butler *et al.*, 2000). At 41 sampling locations (Figure 4.1), profiles of relative permeability (K_{DPIL} ratio) were recorded in the saturated zone with a vertical spacing of 30 cm to a depth of 10-12 m (position of aquitard layer) with the DPIL method, resulting in a total number of 1292 values. The recorded profiles provided information about the vertical variations in the K_{DPIL} ratio and thus of vertical

Table 4.1. Parameters of the numerical model

Parameter	Value
hydraulic conductivity (K)	$2.109 \times 10^{-4} \text{ m s}^{-1}$
thermal conductivity of the saturated sediments	$2 \text{ J s}^{-1} \text{ m}^{-1} \text{ }^\circ\text{C}^{-1}$
effective porosity	0.25
matrix specific heat	$800 \text{ J kg}^{-1} \text{ }^\circ\text{C}^{-1}$
matrix density	2630 kg m^{-3}
specific heat of water	$4174 \text{ J kg}^{-1} \text{ }^\circ\text{C}^{-1}$
density of water	1000 kg m^{-3}

Table 4.2. Input data for FGEN to generate stochastic K -fields from field data

Parameter	Value
mean $\ln(K)$	-8.46
variance of $\ln(K)$	0.08
correlation length in x -direction	6.0 m
correlation length in y -direction	4.0 m
correlation length in z -direction	1.5 m

variations in K . To obtain absolute values of K , direct-push pneumatic slug tests were performed at 2-3 depths at 10 DPIL locations (Figure 4.1) and evaluated following the method of *Butler and Garnett* (2000). The K data obtained from the slug tests (29 values) were used in a regression analysis between K_{DPIL} ratios and slug-test K estimates (*Dietrich et al.*, 2008). With the regression equation, all K_{DPIL} ratios were transformed into K estimates. From all K estimates, the mean and variance were calculated and the correlation lengths in x -, y -, and z -direction were determined by variogram-analysis. The x -direction matches the flow direction of the stream and corresponds to the regional direction of the glaciofluvial deposits. Assuming that the heterogeneity of the groundwater discharge mainly results from the heterogeneity of the aquifer (*Wroblicky et al.*, 1998; *Conant*, 2004), the streambed was not parameterized separately; it was represented as one unit together with the aquifer.

The extent of the generated K fields with FGEN should cover several correlation lengths in each direction to avoid periodicity (*Robin et al.*, 1993). Therefore, we generated at first a three-dimensional K -field which was substantially larger than the model domain. From this field we used a two-dimensional vertical section corresponding to the model domain. Since FGEN requires a regular grid, we interpolated the generated grid with a vertical spacing of 0.1 m to the irregular grid of the HEATFLOW model with a vertical spacing changing from 0.2 m at the bottom to 0.05 m at the top using the GMS software (Environmental Modeling Systems, Inc.). The input data (mean and variance of $\ln(K)$) are varied randomly around the input value during the generation of the realizations, so that the resulting realizations differ slightly in mean and variance of $\ln(K)$. However, the mean values of both parameters from all realizations match the input values.

4.5 Adjusting the aquifer heterogeneity

Initially, the model was run with 50 realizations of K -fields generated with the variance of $\ln(K)$ obtained from the DPIL data ($\sigma_{\ln(K)}^2 = 0.08$). Figure 4.2 b) shows one example of a K -field realization. The model results were compared with the data obtained from the temperature measurements. We used only the temperatures at a depth of 50 cm below the streambed for the following comparison, since these are not influenced by diurnal variations in stream water temperature (*Schmidt et al.*, 2006). It was found that the range of simulated groundwater fluxes was much smaller than the range of fluxes determined from the temperature profiles (Figure 4.3). The range of simulated streambed temperatures at a depth of 50 cm below the streambed was also much smaller than the range of measured temperatures. We concluded that the variance of $\ln(K)$ obtained from the DPIL data was too small to represent the heterogeneity

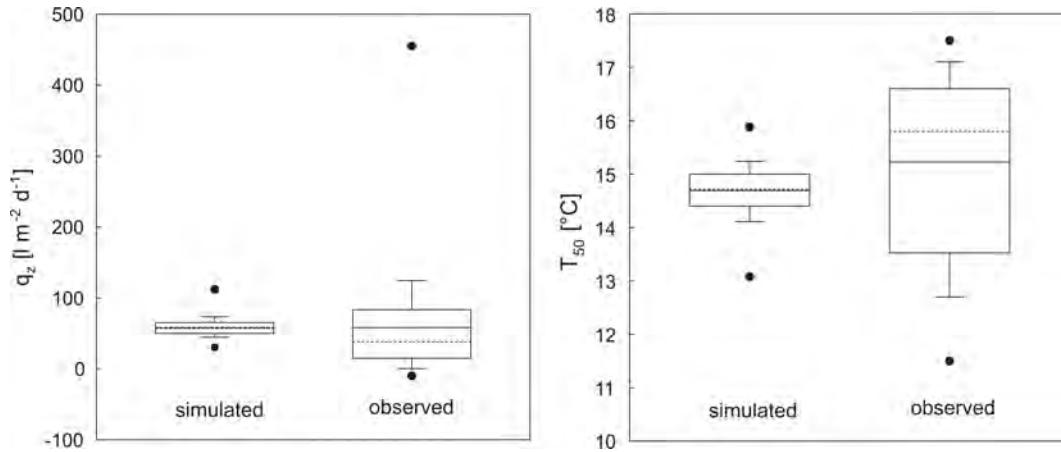


Figure 4.3. Simulated and observed groundwater fluxes (q_z) and temperatures at a depth of 50 cm below the streambed (T_{50}). Box plots show maximum and minimum (dots), 90th and 10th percentile (error bars), 75th and 25th percentile (box), arithmetic mean (solid line), and median (dashed line). Simulated data are complete data from 50 realizations with $\sigma_{\ln(K)}^2 = 0.08$ ($n = 11000 \cong 50$ realizations with 220 grid elements each). Observed data are complete data of the two transects ($n = 140$).

of the groundwater flux to the stream in the model. One explanation might be that the horizontal spacing of the DPIL data (15–50 m) was not sufficiently small to resolve the heterogeneities responsible for the strong variations in groundwater fluxes and streambed temperatures. Another reason could be that we did not fully capture some shallow low-permeability layers of the aquifer. The entire screen of the slug test equipment must be within a low-permeability layer to correctly estimate the hydraulic conductivity. As soon as parts of the screen are located in a layer of higher permeability, this layer will be included in the slug test which will give wrong results. The screen of our slug test equipment was 60 cm long, which was possibly too much to correctly perform slug tests in some of the shallow low-permeability layers identified from the DPIL. Therefore, only few slug test K estimates of low-permeability layers were available, leading to a poor correlation between the slug test K estimates and the K_{DPIL} ratios. Thus, the full range of K values was presumably not covered with the measurements, even though the DPIL were performed with a high vertical resolution of 30 cm.

In the next step, we generated K fields with the same mean $\ln(K)$ and correlation lengths as before, but with variances of $\ln(K)$ varying between 0.1 and 2.6. From the simulation results with these K -fields we plotted the variances of $\ln(K)$ versus the variances of the simulated temperatures at a depth of 50 cm (Figure 4.4). The plot shows a strong linear relation from which the variance of $\ln(K)$ required to induce the variance of measured temperatures at a depth of 50 cm can be determined ($\sigma_{\ln(K)}^2 = 2.06$). This relation is of course only valid for the given input parameters (hydraulic gradient, temperature of stream water and groundwater, mean K , correlation lengths).

Subsequently, we selected those realizations for which the simulated results matched best the observed values. We compared arithmetic mean and variance of the groundwater flux q_z and arithmetic mean and variance of the temperature at a depth of 50 cm, permitting a deviation of 10% from the mean and variance of the observed values. Ten realizations remained with a mean $\sigma_{\ln(K)}^2 = 2.16$, matching well the required variance determined from Figure 4.4 ($\sigma_{\ln(K)}^2$

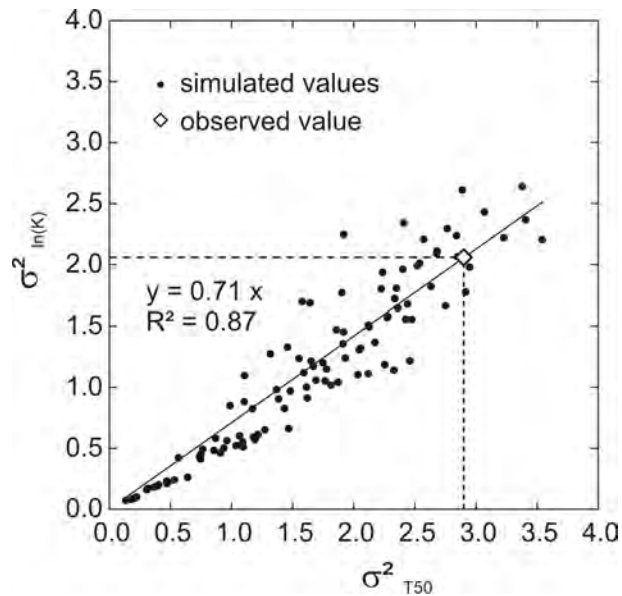


Figure 4.4. Relation between the variance of $\ln(K)$ ($\sigma^2_{\ln(K)}$) and the variance of simulated temperatures at a depth of 50 cm (σ^2_{T50}). The variance of the measured temperatures at a depth of 50 cm ($\sigma^2_{T50} = 2.9$) leads to a required variance of hydraulic conductivity of $\sigma^2_{\ln(K)} = 2.06$.

= 2.06). The range of measured groundwater fluxes and streambed temperatures could be well reproduced with the selected realizations of K -fields (Figure 4.5). The distribution of the groundwater flux in relation to the streambed area is displayed in Figure 4.6. Apparently, the distribution obtained from the simulations with the selected K -fields is in good agreement with the observed distribution.

The K -fields of the selected 10 realizations can now be used for further model applications. A closer analysis of these fields could help to better understand the relation between the distribution of K and the patterns of groundwater discharge to the stream. Furthermore, a larger number of realizations could be generated and selected with the presented methodology to obtain sufficient realizations for a Monte Carlo Analysis.

4.6 Discussion

Measured streambed temperature data were used to calibrate the heterogeneity of an aquifer connected to a stream in a numerical model. The variance of the mean K value obtained from field data, which was used as input data for the generation of stochastically distributed fields of hydraulic conductivity, was varied to find the required value. Through this approach, K -fields could be selected as input data for a flow and heat transport model which were appropriate to simulate the distribution of streambed temperatures and groundwater discharge rates as observed in the field. Simulated mean values as well as maxima and minima were in good agreement with measured values (Figure 4.5). The simulated distribution of fluxes in relation to the streambed area also matched well the observed distribution (Figure 4.6). From this figure it is apparent that with increasing heterogeneity a larger proportion of the groundwater discharge to the stream occurs through a smaller streambed area and the proportion of streambed area

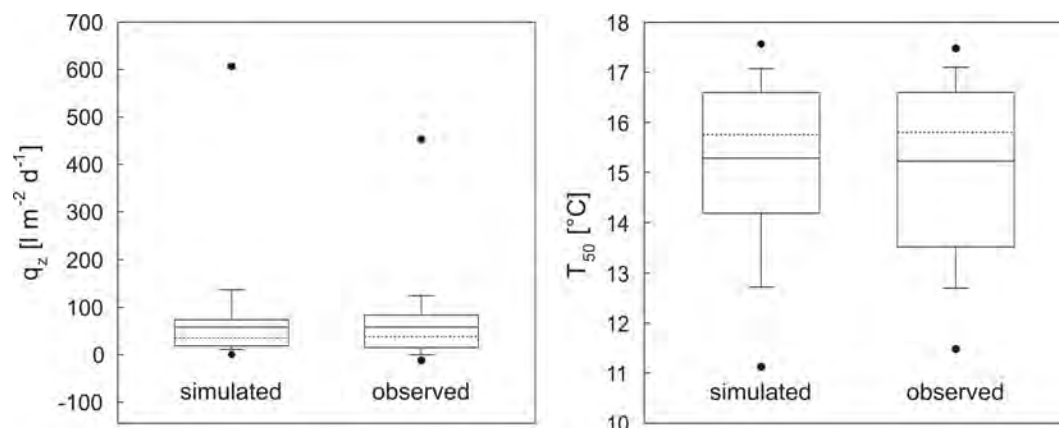


Figure 4.5. Simulated and observed groundwater fluxes (q_z) and temperatures at a depth of 50 cm below the streambed (T_{50}). Box plots show maximum and minimum (dots), 90th and 10th percentile (error bars), 75th and 25th percentile (box), arithmetic mean (solid line), and median (dashed line). Simulated data are complete data from 10 selected realizations with $\sigma_{\ln(K)}^2 = 2.16$ ($n = 2200 \pm 10$ realizations with 220 grid elements each). Observed data are complete data of the two transects ($n = 140$).

which is not contributing to the groundwater discharge increases. This is also evident from the fact that at about 10% of the streambed no groundwater discharge could be detected and therefore 100% of the total discharge occurs at 90% of the streambed area. Small variances of $\ln(K)$ lead to a uniform distribution of the groundwater discharge along the entire streambed area. Thus, the heterogeneity of the aquifer has a significant influence on the heterogeneity of the groundwater discharge through the streambed. Since the groundwater discharge rates vary on a very small scale, the heterogeneities of the aquifer have to be correspondingly small-scale. A very dense grid of sampling points would be necessary to capture these small-scale changes in aquifer properties, which would require considerable measurement efforts and financial resources. Observations of streambed temperature profiles offer the opportunity to easily and quickly obtain additional parameters to significantly improve estimations of aquifer heterogeneity from traditional techniques.

The approach presented in this paper is suitable for small streams that are well connected to the underlying aquifer and whose streambed properties are not considerably different from the aquifer properties. The illustrated relation between the variance of $\ln(K)$ and the variance of temperatures at a certain streambed depth is only valid for the given conditions. A larger mean groundwater flux (due to a larger mean K or a larger gradient) would lead to a larger variance of groundwater fluxes and a larger variance of temperatures. This is true until the groundwater flux is so high that the streambed temperatures approach the groundwater temperatures (Schmidt *et al.*, 2007). In case the mean groundwater discharge is so high that the streambed temperatures are equal to the groundwater temperature, a further increase in groundwater discharge would lead to a decrease in variance of temperatures, since the streambed temperatures cannot be higher in summer (stream water warmer than groundwater) or lower in winter (stream water colder than groundwater) than the groundwater temperature. The order of magnitude of groundwater discharge at which this effect occurs is at about 400 to 800 $\text{L m}^{-2} \text{d}^{-1}$, depending on the boundary conditions. Furthermore, the temperature gradient between stream water and groundwater influences the temperature distribution in the streambed. A larger temperature gradient results in larger variances of the temperatures. Thus, in case of changing conditions,

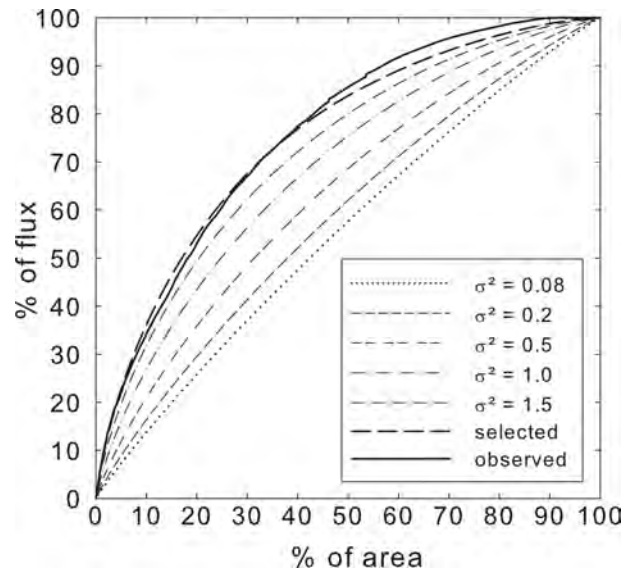


Figure 4.6. Distribution of groundwater flux through the streambed with respect to the streambed area (mean flux of 50 realizations per variance; selected = mean flux of the 10 selected realizations with a mean variance of $\sigma_{\ln(K)}^2 = 2.16$).

the model boundary conditions have to be adjusted to the respective observed conditions and a new relation between the variance of $\ln(K)$ and the variance of the temperature has to be established. However, the resulting controlling variance of $\ln(K)$ should be the same for all boundary conditions.

In future studies, the influence of hydraulic gradient, mean K , and temperature gradient should be investigated. A normalization of the parameters could enable to elaborate general relationships. Furthermore, the assumption of vertical flow through the streambed and the influence of horizontal advective heat transport could be investigated through a three-dimensional model. For natural streams with heterogeneous streambed characteristics, the influence of the streambed on the distribution of groundwater fluxes should be analyzed.

4.7 Summary and conclusion

Small-scale heterogeneities in the aquifer may not be captured by traditional subsurface investigation techniques. Despite a large number of sampling locations, the variance of hydraulic conductivities (K), particularly with respect to the lower permeabilities, could not fully be represented in the present study.

In stream–aquifer systems, a simple methodology may help capture subsurface heterogeneities. Profiles of temperatures were recorded in the streambed. In the presented case of an artificially constructed homogeneous streambed, the heterogeneity of the measured streambed temperatures was interpreted as heterogeneity of the connected aquifer. The stream–aquifer system was represented in a flow and heat transport model including stochastically generated fields of K . These fields were generated from the mean and variance of $\ln(K)$ data obtained from direct-push methods. By varying the input variance of $\ln(K)$ and analyzing the relation between the

4 How streambed temperatures can contribute to the determination of aquifer heterogeneity

variance of streambed temperatures and the variance of $\ln(K)$, the required variance of $\ln(K)$ to cause the observed temperature distribution could be determined with the model. From K -fields generated with the adjusted variance, several realizations could be selected which were suitable to represent the range of observed groundwater fluxes and temperatures. The distribution of groundwater discharge with respect to the streambed area could also be well reproduced with the relatively simple two-dimensional model. The selected K distributions constitute reliable input data sets for the simulation of flow and transport processes between the groundwater and the stream. The mapping of streambed temperatures therefore offers the opportunity to quickly, simply and cheaply obtain parameters for the calibration of groundwater–surface water models and significantly improve model results. This study shows that methods based on temperature as sampling and calibration parameter constitute a valuable supplement to traditional subsurface investigation techniques. The potential of geothermal investigations should be further investigated in applied geophysics.

Influence of aquifer and streambed heterogeneity on the distribution of groundwater discharge

This chapter is published as:

Kalbus, E., Schmidt, C., Molson, J. W., Reinstorf, F., and Schirmer, M. (2009): Influence of aquifer and streambed heterogeneity on the distribution of groundwater discharge. *Hydrology and Earth System Sciences*, 13, 69-77.

Abstract. The spatial distribution of groundwater fluxes through a streambed can be highly variable, most often resulting from a heterogeneous distribution of aquifer and streambed permeabilities along the flow pathways. Using a groundwater flow and heat transport model, we defined four scenarios of aquifer and streambed permeability distributions to simulate and assess the impact of subsurface heterogeneity on the distribution of groundwater fluxes through the streambed: (a) a homogeneous low- K streambed within a heterogeneous aquifer; (b) a heterogeneous streambed within a homogeneous aquifer; (c) a well connected heterogeneous low- K streambed within a heterogeneous aquifer; and (d) a poorly connected heterogeneous low- K streambed within a heterogeneous aquifer. The simulation results were compared with a base case scenario, in which the streambed had the same properties as the aquifer, and with observed data. The results indicated that the aquifer has a stronger influence on the distribution of groundwater fluxes through the streambed than the streambed itself. However, a homogeneous low- K streambed, a case often implemented in regional-scale groundwater flow models, resulted in a strong homogenization of fluxes, which may have important implications for the estimation of peak mass flows. The flux distributions simulated with heterogeneous low- K streambeds were similar to the flux distributions of the base case scenario, despite the lower permeability. The representation of heterogeneous distributions of aquifer and streambed properties in the model has been proven to be beneficial for the accuracy of flow simulations.

5.1 Introduction

Groundwater fluxes at the interface between aquifers and streams can show strong variations in space and time at different scales (e.g., *Ellis et al.*, 2007; *Krause et al.*, 2007). This is important since the magnitude of groundwater discharge across the streambed influences the exchange with and the size of the hyporheic zone (*Boano et al.*, 2008; *Cardenas and Wilson*, 2007) which plays a critical role for the functioning of stream ecosystems (*Brunke and Gonser*, 1997). For example, the exchange of water between aquifers and streams has important implications for the hydrochemistry of the streambed sediments (*Malcolm et al.*, 2003), thus influencing biogeochemical nutrient cycling and habitat quality. A heterogeneous distribution of groundwater fluxes and hyporheic exchange flows leads to a patchy distribution of biogeochemical gradients and interstitial fauna (*Boulton et al.*, 1998; *Malcolm et al.*, 2004).

Spatial heterogeneities of groundwater fluxes through the streambed also impact the fate and transport of contaminants between aquifers and streams (e.g., *Conant et al.*, 2004; *Kalbus et al.*, 2007; *Chapman et al.*, 2007). *Schmidt et al.* (2008b) showed that the highly variable groundwater fluxes observed at a small stream resulted in a significant tailing of contaminant mass flow rates compared to the theoretical homogeneous case.

It is commonly assumed that the groundwater flux across streambeds is controlled by the heterogeneity of the connected aquifer (e.g., *Wondzell and Swanson*, 1996; *Wroblicky et al.*, 1998; *Storey et al.*, 2003; *Conant*, 2004). The properties of the streambed sediments may further contribute to the heterogeneous distribution of groundwater fluxes (*Conant*, 2004; *Ryan and Boufadel*, 2006, 2007). Also, geomorphologic features at different spatial scales were shown to cause variabilities of water exchange across the groundwater – surface water interface (*Kasahara and Wondzell*, 2003; *Cardenas*, 2008). Infiltrating stream water caused by streambed irregularities further leads to a very complex spatial exchange pattern (*Savant et al.*, 1987; *Salehin et al.*, 2004; *Gooseff et al.*, 2006).

Our focus is on the influence of heterogeneous distributions of hydraulic conductivity (K) in the aquifer and the streambed sediments on the spatial distribution of groundwater fluxes across the streambed. In a few recent modelling studies, subsurface heterogeneity was included to simulate stream-aquifer interactions. *Chen and Chen* (2003) considered anisotropic and layered aquifers as well as streambeds with different hydraulic conductivities in their simulations of stream-aquifer interactions, but did not include within-layer heterogeneity. *Bruen and Osman* (2004) studied the effect of spatial variabilities of aquifer K on stream-aquifer seepage flow, but did not consider a separate analysis of the influence of streambed properties. *Cardenas et al.* (2004) simulated the impact of heterogeneous streambed deposits on hyporheic zone geometry, fluxes, and residence time distributions, but did not include the groundwater component. *Fleckenstein et al.* (2006) investigated the effect of aquifer heterogeneity on the distribution of seepage on an intermediate (10^2 m) scale.

The objective of our study was to investigate the potential influence of the heterogeneity of both the aquifer and the streambed sediments on the spatial distribution of fluxes through the streambed on the metre-scale. In numerical simulations we used different combinations of aquifer and streambed heterogeneity to evaluate which of these hydrological units has a stronger influence on the flux distribution. Focussing on spatial variations at fixed boundary conditions, we performed steady-state simulations to look at the flux distribution at a certain point in time. This study is a theoretical investigation of flow processes between aquifers and streams. However, we based the numerical model parameters on measured field data to obtain results in

realistic orders of magnitude.

5.2 Background

Along a 220 m reach of a small stream in Germany, streambed temperatures were mapped with high resolution by *Schmidt et al.* (2006). The stream is a man-made stream which partially penetrates a Quaternary alluvial aquifer. It is about 3 m wide and has an average water depth of 0.6 m. The mean annual discharge is $0.2 \text{ m}^3 \text{ s}^{-1}$ at a gradient of 0.0008 m m^{-1} . The streambed consists of a 0.6 m layer of crushed rock. The interstices of the coarse crushed rock grains are filled with allochthonous, sandy, alluvial material. The connected aquifer is unconfined with a mean saturated thickness of about 8 m and consists of sandy gravel. Further information about the study site can be found in *Schmidt et al.* (2006, 2008b) and *Kalbus et al.* (2007, 2008a).

The streambed temperatures were mapped with a multilevel temperature probe at depths between 0.1 and 0.5 m below the streambed surface. Based on the observed temperature profiles, *Schmidt et al.* (2006) estimated groundwater fluxes through the streambed by applying a one-dimensional analytical solution of the heat-advection-diffusion-equation. From both the temperature observations and the flux calculations, considerable spatial heterogeneity of the groundwater discharge was observed, ranging from no discharge up to a flux of $455 \text{ L m}^{-2} \text{ d}^{-1}$ with a reach-average flux of $58.2 \text{ L m}^{-2} \text{ d}^{-1}$.

The observed spatial heterogeneity was assumed by *Kalbus et al.* (2008a,b) to result from the permeability distribution of the connected aquifer. Even though observed streambed temperatures are temporally highly variable (e.g., *Westhoff et al.*, 2007), the temperature distribution observed at a certain point in time is a consequence of the spatial distribution of subsurface permeabilities and the head and temperature gradient between groundwater and stream at the time of observation. As long as the temperature observations are recorded at a sufficient depth below the streambed surface, they are not influenced by diurnal temperature oscillations in the surface water and the system can be considered to be at a quasi-steady state for the short duration of observation (*Schmidt et al.*, 2007). Focussing on the spatial variabilities, *Kalbus et al.* (2008a,b) simulated groundwater flow and heat transport through the streambed at the stream reach investigated by *Schmidt et al.* (2006). They included stochastically generated fields of K to represent the aquifer properties. The variance of $\ln(K)$, one parameter for the generation of the K -fields, represents the heterogeneity of the aquifer permeability. After developing a relation between this parameter and the variance of observed temperatures, it was calibrated until the simulation results matched the observed distribution of temperatures and groundwater fluxes through the streambed. From 50 realizations of K -fields used for the simulations, 10 were selected which reproduced best the field observations.

Kalbus et al. (2008a,b) assumed in their simulations that the streambed had the same properties as the aquifer and thus they did not parameterize the streambed elements in the model differently from the aquifer elements. However, it is often presumed that streambed sediments are characterized by lower permeabilities due to clogging effects resulting from the deposition of fine-grained sediment and organic matter (e.g., *Sophocleous et al.*, 1995; *Su et al.*, 2004), siltation around macrophytes (e.g., *Wharton et al.*, 2006), or bacterial growth and biofilms (e.g., *Boulton et al.*, 1998; *Pusch et al.*, 1998). These low- K layers could effect the distribution of fluxes across the streambed. Moreover, a heterogeneous streambed with a parameter distribution independent of the aquifer could lead to altered discharge patterns. Therefore, we

performed subsequent simulations with different combinations of aquifer and streambed heterogeneity to identify the roles of the aquifer and the streambed in the generation of heterogeneous flux distributions.

5.3 Methodology

Based on the study by *Kalbus et al.* (2008a,b), we used their model set-up and the 10 *K*-field realizations selected in their study as the base case for subsequent simulations. To evaluate the effect of streambed characteristics, we added different hydraulic conductivity scenarios for the streambed sediments to the model. The results were compared with the base case model results and the observed distribution of groundwater fluxes obtained by *Schmidt et al.* (2006) from mapped streambed temperatures.

5.3.1 Model set-up

A two-dimensional groundwater flow and heat transport model using the model code HEAT-FLOW (*Molson et al.*, 1992; *Molson and Frind*, 2005) was set up according to the model used by *Kalbus et al.* (2008a,b). The conceptual model (Figure 5.1) represents a vertical longitudinal profile along the streambed and within the underlying aquifer, and corresponds to the length of the investigated stream section and the saturated thickness of the aquifer (220 m × 8 m). The upper 0.60 m hydrostratigraphic layer represents the streambed sediments, which corresponds to the thickness of the crushed rock layer at the study site. The model grid consists of 220 × 65 elements with a layer thickness varying from 0.20 m at the bottom to 0.05 m at the top.

Since we look at spatial variations at a certain point in time, the system is assumed to be at steady state. The bottom and top boundaries are constant head boundaries, left and right boundaries are no-flow boundaries, leading to vertical flow through the system. Although the assumption of vertical groundwater discharge seems rigid for complex stream-aquifer systems it is commonly made for the interpretation of groundwater fluxes through the streambed (e.g., *Cardenas and Wilson*, 2007; *Keery et al.*, 2007). The constant head values were chosen such that for each simulation the mean groundwater flux through the model equalled the mean flux through the streambed calculated from the observed temperature profiles ($q_z^{\text{mean}} = 58.2 \text{ L m}^{-2} \text{ d}^{-1}$).

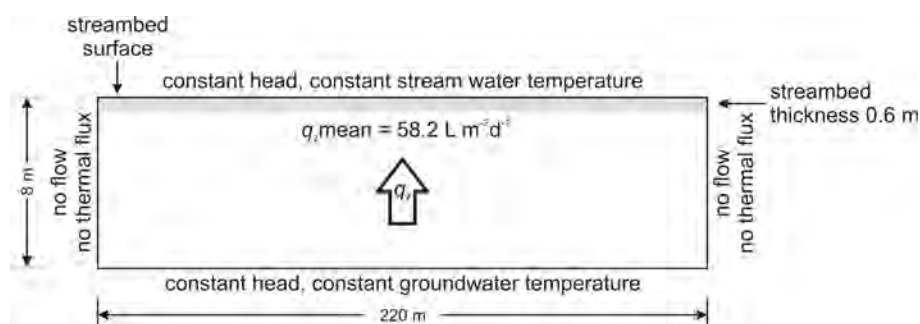


Figure 5.1. Model definition and boundary conditions

Table 5.1. Aquifer and streambed properties of all simulation cases. K = hydraulic conductivity, σ^2 = variance of $\ln(K)$, λ_x and λ_z = correlation lengths in the x- and z-directions.

Scenario	Aquifer properties	Streambed properties
Base Case	Heterogeneous $K_{mean} = 2.1 \times 10^{-04} \text{ m s}^{-1}$ $\sigma^2 = 2.1$ $\lambda_x = 6.0 \text{ m}$ $\lambda_z = 1.5 \text{ m}$	Same as aquifer
Case A	As in base case	Homogeneous $K = 2.1 \times 10^{-06} \text{ m s}^{-1}$
Case B	Homogeneous $K = 2.1 \times 10^{-04} \text{ m s}^{-1}$	As in base case aquifer
Case C	As in base case	As in base case but each streambed element K divided by 100 ($K_{mean} = 2.1 \times 10^{-06} \text{ m s}^{-1}$)
Case D	As in base case	Heterogeneous, independent K -fields with $K_{mean} = 2.1 \times 10^{-06} \text{ m s}^{-1}$ $\sigma^2 = 2.1$ $\lambda_x = 6.0 \text{ m}$ $\lambda_z = 1.5 \text{ m}$

The temperature boundary conditions correspond to the mean stream water temperature during the mapping programme (18.4°C) at the top boundary and the constant deep groundwater temperature (10.9°C) at the bottom boundary. No energy flux is assumed across the left and right boundaries, because in conditions of vertical flow the lateral heat transport by conduction is negligible.

The thermal transport properties were taken from the literature (thermal conductivity of the saturated sediments = $2 \text{ J s}^{-1} \text{ m}^{-1} \text{ }^\circ\text{C}^{-1}$; matrix specific heat = $800 \text{ J kg}^{-1} \text{ }^\circ\text{C}^{-1}$; matrix density = 2630 kg m^{-3} ; specific heat of water = $4174 \text{ J kg}^{-1} \text{ }^\circ\text{C}^{-1}$; density of water = 1000 kg m^{-3}). The thermal conductivity of saturated sediments varies only little between different sediment types and can therefore reliably estimated from literature data (Stonestrom and Constantz, 2003). A porosity of 0.25 was estimated from field data.

A heterogeneous distribution of hydraulic conductivity was achieved by including stochastically generated fields of hydraulic conductivity in the simulations. With the code FGEN (Robin *et al.*, 1993), the K -fields were generated from the mean and variance of $\ln(K)$ and the correlation lengths in each direction (Table 5.1). These data were obtained from field observations of K , except the variance which was calibrated with the observed temperature distribution by Kalbus *et al.* (2008a,b). Ten realizations of the K distribution were used for the simulation of each of the scenarios explained below. The heterogeneous K -fields of the aquifer were identical in all scenarios and the base case.

5.3.2 Scenarios

The case simulated by *Kalbus et al.* (2008a,b) was taken as the base case for comparison with the four streambed scenarios described in the following list. For the base case, the streambed was assumed to be part of the aquifer and have exactly the same permeability characteristics. The K -fields were generated for the entire model domain. Cases A and B were chosen to isolate the influence of the aquifer and the streambed, respectively. Cases C and D were defined to include effects of clogging together with different concepts of streambeds: one considering the streambed as part of the aquifer (Case C) and one considering the streambed as a separate unit (Case D).

Case A: The aquifer was assumed heterogeneous as in the base case, the streambed was assumed homogeneous with K two orders of magnitude less than the mean aquifer K . This scenario was selected to demonstrate the effect of a low- K stream boundary condition using a conductance term as it is often used in regional-scale groundwater flow models. The rather small value of the streambed K was selected to represent a clogged layer and cause clear effects.

Case B: To investigate the potential of the streambed sediment layer alone to cause a heterogeneous distribution of groundwater discharge, the aquifer was assumed homogeneous with the same mean K as in the base case and the streambed was assumed heterogeneous with the same statistical properties as the aquifer in the base case.

Case C represents a naturally developed streambed which basically consists of the same material as the underlying aquifer, but is assumed to have experienced some clogging. The aquifer and streambed were both assumed heterogeneous (using the same variance and correlation lengths as in the base case), while streambed clogging was simulated by dividing the K value of each streambed element by 100. The streambed thus has the same degree of heterogeneity as the aquifer, but the mean K is two orders of magnitude less.

Case D: The streambed properties were assumed to be independent of the aquifer, which may occur for instance in streambeds with high sediment turnover rates or in man-made streams. The connectivity between aquifer and streambed is lower than in Case C, which was achieved by generating new K -fields for the streambed layers only. As in Case C, the mean streambed K was chosen two orders of magnitude less than the mean aquifer K . The other statistical parameters for the K -field generation (variance, correlation lengths) were adopted from the aquifer statistics to enable a direct comparison with Case C.

The aquifer and streambed properties used for the generation of K -fields for the simulations of the base case and the four scenarios are summarized in Table 5.1.

5.4 Results and discussion

The groundwater fluxes simulated in the base case scenario are highly variable with a standard deviation of $\sigma(q) = 63.7 \text{ L m}^{-2} \text{ d}^{-1}$ matching well the observed variation ($\sigma(q) = 65.5 \text{ L m}^{-2} \text{ d}^{-1}$). Homogeneous low- K streambeds (Case A) significantly dampen the groundwater fluxes compared to the base case scenario and result in a relatively uniform spatial pattern of fluxes with a small standard deviation of $\sigma(q) = 6.4 \text{ L m}^{-2} \text{ d}^{-1}$ (Figure 5.2A). The range of fluxes is much smaller than in the base case (Figure 5.3). Homogeneous low- K streambeds thus serve as homogenizing layers which reduce the influence of the aquifer texture. It is highly unlikely that this

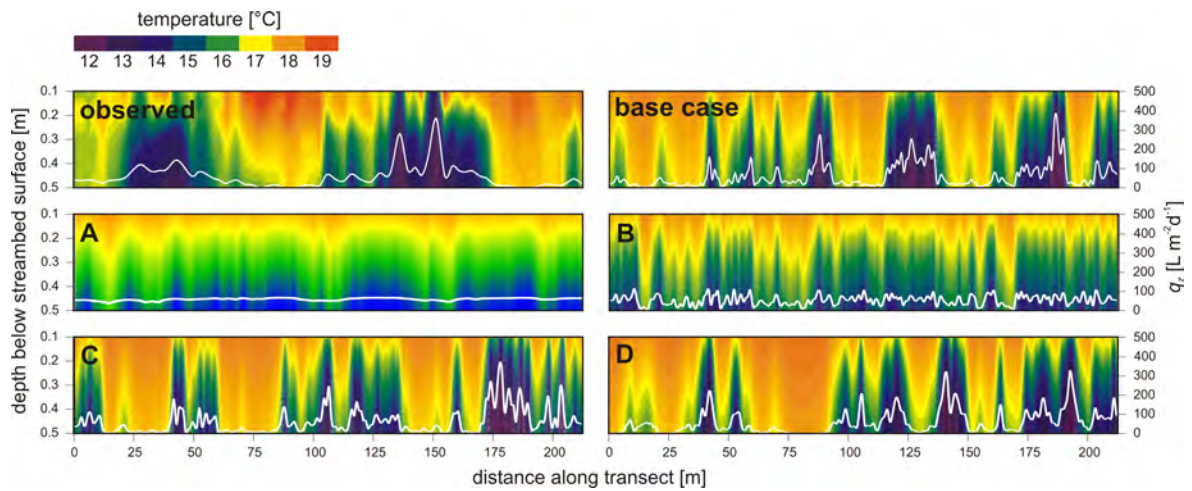


Figure 5.2. Observed (top left; after *Schmidt et al. (2006)*) and simulated (base case and Cases A–D) results showing temperature (colour maps) and flux distributions (white curves) in the streambed (represented by the upper grey zone in Figure 5.1). Temperature data are shown at streambed depths between 0.1 and 0.5 m corresponding to the observations. Simulated results are shown from one example out of ten K -field realizations (the same realization is shown in all scenarios). Vertical exaggeration is approx. 100x.

case occurs in reality, since all naturally developed streambeds as well as artificially constructed streambeds develop some degree of heterogeneity resulting from groundwater fluxes, sediment turnover, hyporheic fluxes, or activities of the interstitial and benthic fauna. Nevertheless, homogeneous low- K streambeds are often implemented in regional-scale groundwater flow models (e.g., *McDonald and Harbaugh, 1988*) and in the analysis of stream flow depletion through pumping (*Chen et al., 2008*) where the stream-aquifer interaction is governed by a conductance term representing the resistance of the streambed (*Rushton, 2007*). This approach may be sufficient for evaluating average water budgets on a regional scale, but prediction accuracies may be low because it would not provide a range of possible fluxes. For a detailed analysis of flow and transport processes, a homogeneous representation of the streambed may not be appropriate. For instance, in cases of contaminated groundwater discharging to a stream, maximum contaminant mass flow rates may be underestimated since areas of high groundwater discharge contribute more mass flow than low-discharge areas. *Schmidt et al. (2008b)* also showed that a heterogeneous distribution of groundwater discharge strongly influences the time scales of contaminant release from a contaminated streambed. Hence, for small-scale investigations of stream-aquifer interactions, a representation of the streambed in flow models using a boundary condition with a uniform conductance term is not recommended. The streambed conductance should rather be resolved on a small scale to cover the range of high- and low-permeability zones and thus the range of high and low groundwater fluxes in the streambed.

In Case B, a heterogeneous streambed on top of a homogeneous aquifer leads to a wider distribution of fluxes than in Case A (Figure 5.2B) with a standard deviation of $\sigma(q) = 22.5 \text{ L m}^{-2} \text{ d}^{-1}$, but the range is still much smaller than in the base case (Figure 5.3). This case is also highly unlikely to occur in reality, since all aquifers show some degree of heterogeneity. Nevertheless, it shows that the streambed alone does not cause the observed distribution of fluxes, at least not for the considered ranges and patterns. We performed some simulations increasing the

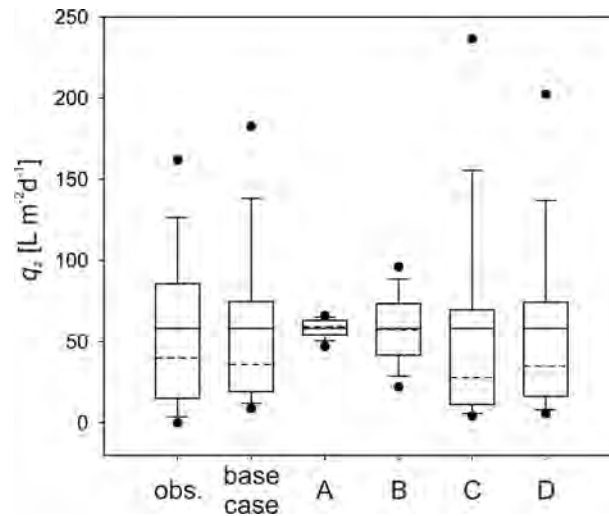


Figure 5.3. Box plots of the groundwater discharge through the streambed showing 95th and 5th percentile (dots), 90th and 10th percentile (error bars), 75th and 25th percentile (box), arithmetic mean (solid line), and median (dashed line). Observed data are complete data of the mapping programme ($n = 140$), simulated data are the complete data set from all 10 realizations ($n = 2200$) for each case.

variance of $\ln(K)$ of the streambed K -fields to see how large it would have to be to cause a flux distribution similar to the base case (data not shown), but we did not get close to the base case flux distribution within a reasonable range of variances. *Gelhar* (1993) gave a range of variances from 0.16 to 4.41 for alluvial aquifers. In our simulations, even with a variance of 10, which is a highly unreasonable value, the simulated range of fluxes was still too small ($\sigma(q) = 33.6 \text{ L m}^{-2} \text{ d}^{-1}$). The passage through the streambed, which is much shorter compared to the passage through the aquifer, seems insufficient to cause highly diverse flow paths. Larger structures are necessary to direct the flow into highly permeable zones resulting in higher flow velocities.

A heterogeneous streambed with a mean K two orders of magnitude less than the mean K of the heterogeneous aquifer (Case C) shows a similar pattern of fluxes to the base case (Figure 5.2C). The high- and low-discharge zones are at the same locations and the range of fluxes is similar to the range of the base case (Figure 5.3). The maximum fluxes are even higher than those of the base case ($\sigma(q) = 89.0 \text{ L m}^{-2} \text{ d}^{-1}$). This is a result of the larger gradient which had to be implemented in the models to achieve the reach-average flux of $58.2 \text{ L m}^{-2} \text{ d}^{-1}$ (average hydraulic gradient = 0.011; base case: 0.002). Within high-permeability zones, this higher gradient leads to increased fluxes compared to the base case with a lower gradient. When reaching the streambed, the short passage through the less permeable streambed does not have much influence on the flow velocities in these zones since the permeability is still higher than in the neighbouring low-discharge zones.

In case of an independent heterogeneity of the streambed (Case D), the pattern is still similar to that of a related heterogeneity as in Case C, but the locations of high- and low-discharge zones have been slightly displaced, some peaks have disappeared, while other peaks have developed (Figure 5.2D). The range of fluxes is almost identical with the range of the base case (Figure 5.3) with a standard deviation of $\sigma(q) = 74.8 \text{ L m}^{-2} \text{ d}^{-1}$. Again, the higher gradient (average hydraulic gradient = 0.014) leads to increased flow velocities through the

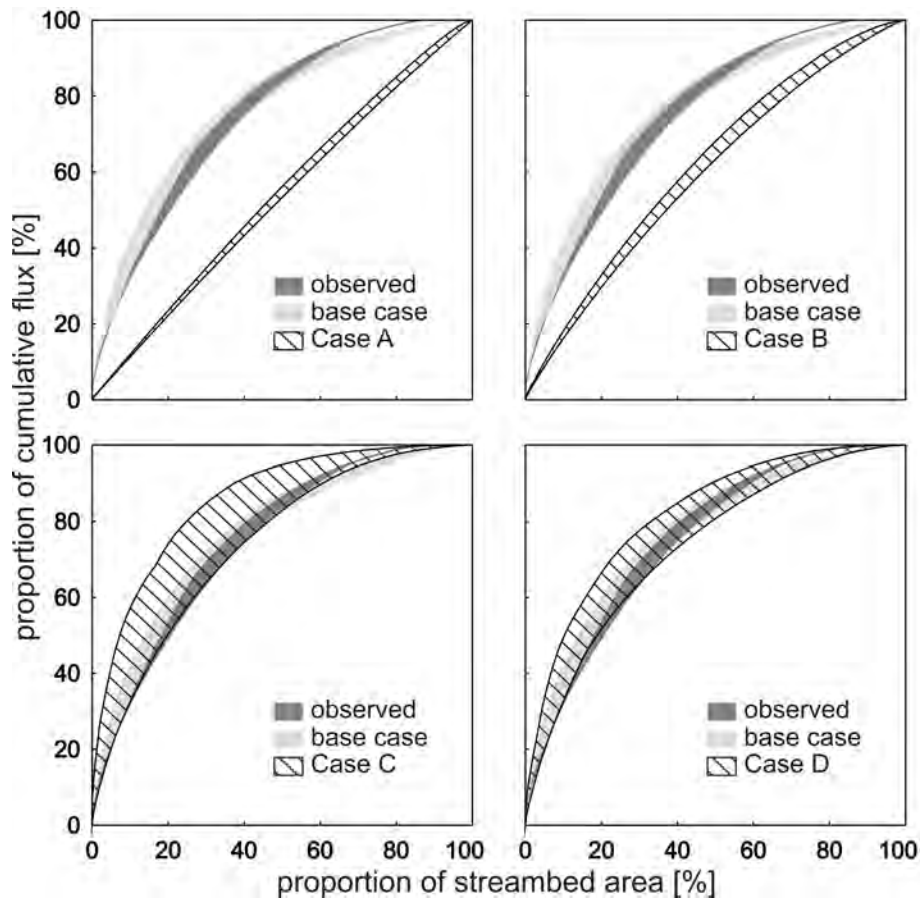


Figure 5.4. Distribution of groundwater fluxes through the streambed in relation to the streambed area. Bands show the full range between maximum and minimum values of observations and modelling results, respectively.

high-permeability zones of the aquifer. As opposed to Case C, however, groundwater flow from high- K zones within the aquifer may now intersect low-permeability zones in the streambed and will thus be diverted to neighbouring zones with higher permeabilities. This attenuates some of the peak flows observed in Case C and creates new peaks at other locations.

Comparing the mean (solid line) and median (dashed line) in Figure 5.3, it becomes apparent that greater spatial heterogeneity mainly leads to an increase in the proportion of high fluxes. Because we assumed vertical flow through the model domain, the fluxes cannot become less than zero, but well connected high-permeability zones can lead to very high fluxes which are concentrated in small areas. This is even more evident from Figure 5.4, which shows the relative contribution of the streambed area to the cumulative flux. In Cases A and B, the band representing the range between maximum and minimum fluxes of all K -field realizations is narrow and almost straight with a slope of 1:1. In these cases, a certain proportion of streambed area thus contributes a similar proportion of cumulative flux. For instance, 20% of the streambed area contributes 22% (Case A) to 30–33% (Case B) of the cumulative flux. In Cases C and D, a much smaller proportion of streambed area contributes a larger proportion of cumulative flux. For instance, in Case C, 20% of the streambed area contributes 50–74% of the cumulative flux

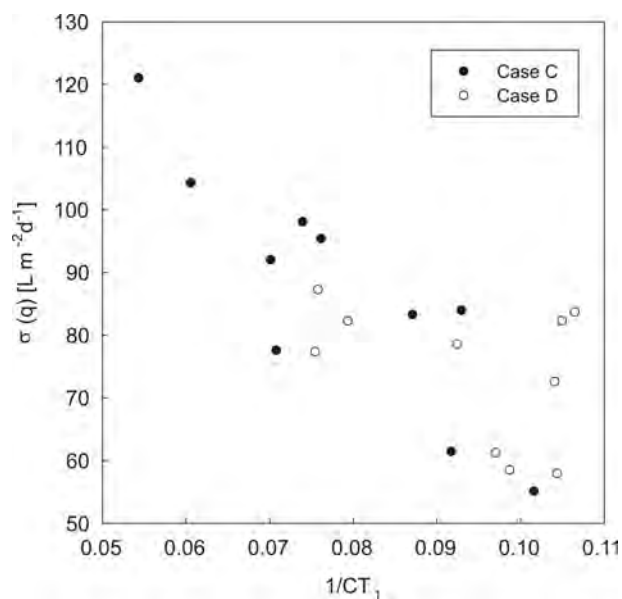


Figure 5.5. Standard deviation of groundwater flux through the streambed, $\sigma(q)$, in relation to the connectivity indicator $1/CT_1$ for Case C and Case D.

along the modelled reach. The band is much wider in Cases C and D, indicating considerable variation between the different K -field realizations. In Case C, the variations are even larger than in Case D, which is a result of a better connectivity between aquifer and streambed.

We used the transport connectivity indicator CT_1 by *Knudby and Carrera* (2005) to analyse the relation between connectivity and discharge variations. CT_1 was defined by *Knudby and Carrera* (2005) as the ratio between the average arrival time t_{AVE} of a solute travelling through the model domain and the time t_5 at which 5% of the solute has arrived. Better connectivity leads to shorter early arrival times. Here we use the reciprocal, $1/CT_1 = t_5/t_{AVE}$, and thus better connectivity results in values of $1/CT_1$ approaching zero.

t_{AVE} was obtained from the domain length in flow direction and the mean flux across the domain. t_5 was determined through particle tracking. 5000 particles were released at the bottom of the model domain and t_5 was determined from the breakthrough curves.

Figure 5.5 shows the standard deviation of the flux across the streambed $\sigma(q)$ in relation to the connectivity indicator $1/CT_1$. It is apparent that a higher connectivity results in a higher variation of discharge rates. In Case C, smaller values of $1/CT_1$ are found than in Case D, which confirms that the larger variations in fluxes observed in Figure 5.4 (Case C) are a result of better connectivities between aquifer and streambed.

5.5 Conclusions

Previous simulations of groundwater flow and heat transport through a streambed have revealed that strong spatial variations in groundwater discharge to a stream are caused by a heterogeneous distribution of aquifer hydraulic conductivity. The influence of the streambed on the distribution of fluxes was investigated in subsequent simulations with different scenarios of

aquifer and streambed hydraulic conductivity. The aquifer was found to have a stronger influence on the spatial distribution of fluxes than the streambed. However, the implementation of a homogeneous low- K streambed within a heterogeneous aquifer caused a significant homogenization of the fluxes. This behaviour should be considered when using the concept of streambed conductance in regional-scale groundwater models. A heterogeneous distribution of hydraulic conductivity only in the streambed was not sufficient to cause strong flux variations. Simulation results with heterogeneous low- K streambeds were similar to the results from the model without a distinction between aquifer and streambed properties. Thus, if streambed clogging, which leads to a reduced permeability of the streambed sediments compared to the aquifer, has to be considered in a model, it might be appropriate to implement a heterogeneous distribution of streambed hydraulic conductivity even at large scales to avoid an underestimation of peak flows. These results also confirm the applicability of the methodology proposed by *Kalbus et al.* (2008a,b) to use measured streambed temperatures for calibration of aquifer properties even without distinguishing between the aquifer and streambed.

Observed distributions of groundwater fluxes through the streambed may often be a result of both aquifer and streambed heterogeneity, with the aquifer having a stronger influence. Numerical model predictions of groundwater flow and solute transport may thus significantly benefit from heterogeneous distributions of aquifer and streambed properties. Since mass fluxes of dissolved compounds across streambeds are governed by the flux of water, the consideration of heterogeneous flux distributions is essential for the prediction of contaminant transport and for biogeochemical modelling at the groundwater – surface water interface.

Summary, conclusions and perspectives

6.1 Summary

Interactions between groundwater and streams play an important role for the functioning of stream ecosystems. Most nutrient cycling and stream metabolism take place in the transition zone between aquifers and streams. Since flow patterns are the major controlling factor for the transformation of substances in the transition zone, the characterization and quantification of flow is an important component for integrated river basin management and the protection of both groundwater and surface water resources.

The flow pathways in the transition zone commonly display a complex pattern, resulting from heterogeneities in the permeability distribution in the aquifer and the streambed sediments. Hyporheic exchange flows through infiltrating stream water further complicate the flow patterns. A careful selection of measuring methods is therefore required to capture the range of flows as a consequence of subsurface heterogeneities and to obtain representative results.

6.1.1 The study site

The study site is located in the industrial area of Bitterfeld/Wolfen, one of the oldest industrial centres of Germany. More than a century of chemical production has resulted in a regional aquifer contamination with an estimated extent of 25 km² directly affecting more than 200 million m³ of groundwater. Several small streams interact with the contaminated groundwater. One of these streams is the Schachtgraben, a man-made stream which had originally been constructed for drainage water discharge from open-cast lignite mines, and later was also used for waste water discharge from the chemical industry. During this time, contaminants in the stream water accumulated in the streambed sediments. Today, the hydraulic gradient is towards the stream and it gains contaminated groundwater.

6.1.2 Objectives

The general objectives of this study were the determination of water and solute fluxes between the contaminated aquifer at the study site and the Schachtgraben and the investigation of the

underlying processes and controlling factors with a focus on subsurface heterogeneity. Appropriate measuring and modelling approaches should be selected and applied which, on the one hand, capture small-scale heterogeneities and allow an assessment of the full range of fluxes between aquifer and stream, and, on the other hand, provide robust and representative flux estimates.

6.1.3 Review of measuring methods

Numerous methods exist to measure interactions between groundwater and surface water which are either applied in the aquifer, in the surface water, or in the transition zone itself.

The methods differ in resolution, sampled volume, and the time scales they represent. Often, the choice of methods constitutes a trade-off between resolution of heterogeneities and sampled subsurface volume. Furthermore, the measurement scale on which a selected technique operates may have a significant influence on the results, leading to differences between estimates obtained from a grid of point measurements and estimates obtained from large-scale techniques. Therefore, a better representation of the local conditions including the effects of scale on measurement results can be achieved by conducting measurements at multiple scales at a single study site.

Attention should be paid to distinguish between groundwater discharge and hyporheic exchange flow. Small-scale flow measurements in the shallow streambed may not suffice to make this distinction, so that additional measurements to identify the water source are recommended.

Characteristics of the study site may exclude the application of some measuring methods. Coarse grain sizes of aquifer and streambed sediments, for instance, can make the insertion of probes or piezometers impossible. Accessibility of the study site and portability of the equipment can also influence the choice of methods.

The study goal plays a decisive role in choosing appropriate methods. For regional investigations, large-scale techniques may be more suitable, whereas process studies may require measurements which enable high resolution. All methods have their limitations and uncertainties. However, a multi-scale approach combining multiple techniques can considerably reduce uncertainties and constrain estimates of fluxes between groundwater and surface water.

6.1.4 Methods applicable at the study site

The streambed of the Schachtgraben consists of coarse crushed rock. Some measuring methods typically applied in the streambed, such as direct groundwater discharge measurements with seepage meters or measurements of vertical hydraulic conductivity with in-situ permeameters, were not applicable in this material. Also mass-balance approaches were not successful, because the groundwater discharge rates were relatively small and the stream discharge rates highly variable. The stream receives drainage water from a landfill, so that the discharge rates are influenced by the pumping schedule of the landfill. Also the runoff from sealed surfaces within the industrial area are discharged into the stream, so that the water level and discharge quickly respond to rainfall events. With respect to the contamination, mass-balance approaches also did not give clear results, because the stream water contains contaminants in highly variable composition and concentrations without any regular pattern, presumably coming from the landfill drainage water.

The measuring methods applicable at the study were therefore limited to methods involving robust equipment that can be hammered into crushed rock, or methods applied in the aquifer to quantify the water and contaminant fluxes which are migrating toward the stream along the regional water table gradient and to determine subsurface properties for assessing the flow distribution.

6.1.5 Contaminant mass fluxes at the stream – aquifer interface

A new methodology was developed to estimate mass fluxes of contaminants between the aquifer and the stream Schachtgraben. Two novel approaches were combined into an efficient methodology to quantify water and solute flows at the stream – aquifer interface: Streambed temperature mapping for determining the spatial distribution and magnitude of groundwater discharge through the streambed, and integral pumping tests (IPT) for the estimation of average contaminant concentrations and mass flow rates in the groundwater migrating toward the stream.

The streambed temperatures were measured during a two-days mapping programme along a longitudinal transect of 60 m in length following the methodology proposed by *Schmidt et al.* (2006). The stream section corresponds to the location where the IPTs were performed as described below. Measurements were spaced at intervals of roughly 3 m in the centre of the channel cross-section. At each location, streambed temperatures were recorded simultaneously at depths of 0.10 m, 0.15 m, 0.20 m, 0.30 m, and 0.50 m below the streambed surface. Stream water and groundwater temperatures were monitored continuously.

By comparing the mapped streambed temperatures with the temperature of the groundwater and the stream water, locations of high or low groundwater discharge could be delineated. Furthermore, an analytical solution of the heat transport equation was applied to calculate the water flux at each location from the measured temperature profile. Calculated groundwater fluxes through the streambed ranged from 0 to $40 \text{ L m}^{-2} \text{ d}^{-1}$ (Figure 3.4, p. 36) with an average of $22.7 \text{ L m}^{-2} \text{ d}^{-1}$. Total daily groundwater discharge over the investigated reach length of 60 m and a stream width of 3 m was 4061 L d^{-1} .

For the determination of contaminant concentrations in the groundwater migrating toward the stream, IPTs were performed. Four wells were drilled along a control plane perpendicular to the mean local groundwater flow direction which was parallel to the stream flow direction. For a time period of five days, groundwater was pumped simultaneously from the four wells with a constant pumping rate. Water samples were taken every three hours from all wells and from the stream. Within 24 h, the samples were analysed for concentrations of mono- (MCB), di- (DCB), tri- and tetrachlorobenzene. Average contaminant concentrations were computed for each well using an analytical solution as a first approximation. This solution is valid, in theory, only for the case of circular isochrones. Therefore, we additionally calculated average contaminant concentrations numerically through the code CSTREAM (*Bayer-Raich*, 2004) which accounts for irregular isochrone shapes. This required a numerical flow model with particle tracking for the definition of the capture zone geometry.

Contaminant concentrations remained quite stable in the four wells during the pumping duration, indicating that the wells were located within a wide plume with an insignificantly varying contaminant concentration. Average contaminant concentrations obtained from the analytical solution and the numerical solution differed by less than 1%, showing that the simple analytical solution produced satisfactory results. Average MCB concentrations ranged from 9.64

to $18.15 \mu\text{g L}^{-1}$, increasing from well W14 to well W11 (Figure 3.4, p. 36). Average DCB concentrations ranged from 2.58 to $3.97 \mu\text{g L}^{-1}$, not showing any directional trend. Tri- and tetrachlorobenzenes were found only in concentrations close to the detection limit.

The potential contaminant mass flux from the aquifer to the stream was calculated from the average contaminant concentrations in the aquifer obtained from the IPT and the groundwater flux to the stream obtained from the temperature observations. It varied between 0 and $496.40 \mu\text{g m}^{-2} \text{d}^{-1}$ for MCB and between 0 and $127.75 \mu\text{g m}^{-2} \text{d}^{-1}$ for DCB (sum of isomers) (Figure 3.4, p. 36), with mean values of $272 \mu\text{g m}^{-2} \text{d}^{-1}$ MCB and $71 \mu\text{g m}^{-2} \text{d}^{-1}$ DCB, respectively.

These calculated mass fluxes are representative only for the time of the streambed temperature mapping campaign. The average contaminant concentrations can be considered representative for a longer time period, because the diffuse contamination extends over a large area in the region and the groundwater flow rates are low (0.1 m d^{-1}). However, the groundwater discharge rates through the streambed depend strongly on the hydraulic gradient between groundwater and stream. In the dry summer of 2006, the groundwater table was very low, resulting in a hydraulic gradient of only 40% of the long-term average gradient. Compared to groundwater discharge rates obtained by *Schmidt et al.* (2006) at an adjacent stream reach one year before, the average groundwater discharge rate over the observed reach length ($q_z = 22.7 \text{ L m}^{-2} \text{d}^{-1}$) was only 40% of the value obtained by *Schmidt et al.* (2006) ($q_z = 58.2 \text{ L m}^{-2} \text{d}^{-1}$), which corresponds to the smaller gradient. In their study, calculated water fluxes ranged from $-10.0 \text{ L m}^{-2} \text{d}^{-1}$ (surface water enters the streambed) to $455.0 \text{ L m}^{-2} \text{d}^{-1}$ (groundwater discharges to the stream), which is more than tenfold the range of our results. When taken their observed range of groundwater fluxes, the potential contaminant mass fluxes could reach up to $8258 \mu\text{g m}^{-2} \text{d}^{-1}$ MCB and $1806 \mu\text{g m}^{-2} \text{d}^{-1}$ DCB, respectively.

6.1.6 Heterogeneity in fluxes through the streambed resulting from aquifer properties

The groundwater discharge rates at the investigated stream reach showed substantial heterogeneity, with fluxes ranging from no discharge up to a flux of $455.0 \text{ L m}^{-2} \text{d}^{-1}$. It is commonly assumed that the groundwater flux across streambeds is predominantly controlled by the heterogeneity of the connected aquifer. Zones of high groundwater discharge in a stream are therefore connected to highly permeable zones in the underlying aquifer.

The distribution of groundwater discharge at the study site has been investigated by measurements of streambed temperatures. In zones of high groundwater discharge, the temperatures in the streambed are close to the groundwater temperature, and in zones of low groundwater discharge, they are close to the stream water temperature. Hence, streambed temperatures close to the groundwater temperature indicate a connection to highly permeable zones in the underlying aquifer and vice versa. This means, the heterogeneity in aquifer permeability may be inferred from spatially highly resolved streambed temperature data.

A two-dimensional groundwater flow and heat transport model of the streambed and the connected aquifer was set up using the finite-element numerical model code HEATFLOW (*Molson et al.*, 1992). The model domain corresponded to the length of the investigated stream section and the saturated thickness of the aquifer ($220 \text{ m} \times 8 \text{ m}$) and represented a vertical longitudinal profile through the streambed to the underlying aquitard (Figure 4.2, p. 45).

A heterogeneous distribution of hydraulic conductivity (K) was achieved by stochastically generating K -fields from the mean and variance of $\ln(K)$ and the correlation lengths in each direction. Aquifer K data were estimated by a combination of direct-push injection logging (DPIL) and slug tests. At 41 sampling locations (Figure 4.1, p. 44), profiles of relative permeability (K_{DPIL} ratio) were recorded. To obtain absolute values of K , direct-push pneumatic slug tests were performed at 2-3 depths at 10 DPIL locations (Figure 4.1, p. 44). The K data obtained from the slug tests were used in a regression analysis between K_{DPIL} ratios and slug-test K estimates to transform all K_{DPIL} ratios into K estimates. From all K estimates, the mean and variance were calculated and the correlation lengths in x -, y -, and z -direction were determined by variogram-analysis. Assuming that the heterogeneity of the groundwater discharge mainly results from the heterogeneity of the aquifer, the streambed was not parametrized separately; it was represented as one unit together with the aquifer.

The model was run with 50 realizations of K -fields generated with the variance of $\ln(K)$ obtained from the DPIL data ($\sigma_{\ln(K)}^2 = 0.08$). It was found that the range of simulated groundwater fluxes and streambed temperatures was much smaller than the observed range of fluxes and temperatures (Figure 4.3, p. 48). We concluded that the variance of $\ln(K)$ obtained from the DPIL data was too small to represent the heterogeneity of the groundwater flux to the stream in the model.

In the next step, K fields with the same mean $\ln(K)$ and correlation lengths as before, but with different variances of $\ln(K)$ were generated. From the simulation results with these K -fields we plotted the variances of $\ln(K)$ versus the variances of the simulated temperatures at a depth of 50 cm (Figure 4.4, p. 49). The plot shows a strong linear relation from which the variance of $\ln(K)$ required to induce the variance of measured temperatures at a depth of 50 cm can be determined ($\sigma_{\ln(K)}^2 = 2.06$).

Subsequently, we selected those realizations for which the simulated results matched best the observed values. Ten realizations remained with which the range of measured groundwater fluxes and streambed temperatures could be well reproduced (Figure 4.5, p. 50). The distribution of the simulated groundwater flux in relation to the streambed area is also in good agreement with the observed distribution (Figure 4.6, p. 51).

The model results show that small variances of $\ln(K)$ lead to a uniform distribution of the groundwater discharge along the streambed area. Thus, the heterogeneity of the aquifer has a significant influence on the heterogeneity of the groundwater discharge through the streambed.

6.1.7 Influence of aquifer and streambed heterogeneity on the distribution of fluxes

In the previous chapter it was shown that the heterogeneity of aquifer permeabilities has a significant influence on the distribution of fluxes through the streambed. It was assumed that the streambed had the same properties as the aquifer and thus the streambed elements in the model were not parameterized differently from the aquifer elements. However, it is often presumed that streambed sediments are characterized by lower permeabilities due to the deposition of fine-grained sediment and organic matter, which could effect the distribution of fluxes across the streambed. Moreover, the permeability distribution in the streambed could be independent of the distribution in the aquifer as a result of sediment turnover, activities of benthic organisms, or in case of a man-made streambed. To investigate the influence of the heterogeneity of both the

aquifer and the streambed sediments on the spatial distribution of fluxes through the streambed, numerical simulations were performed involving different combinations of aquifer and streambed heterogeneity.

We defined four scenarios of aquifer and streambed permeability distributions to simulate and assess the impact of subsurface heterogeneity on the distribution of groundwater fluxes through the streambed: (a) a homogeneous low- K streambed within a heterogeneous aquifer; (b) a heterogeneous streambed within a homogeneous aquifer; (c) a well connected heterogeneous low- K streambed within a heterogeneous aquifer; and (d) a poorly connected heterogeneous low- K streambed within a heterogeneous aquifer. The simulation results were compared with a base case scenario, in which the streambed had the same properties as the aquifer, and with observed data.

The results showed that homogeneous low- K streambeds (Case A) significantly dampen the groundwater fluxes compared to the base case scenario and result in a relatively uniform flux distribution close to the mean (Figure 5.2 A, p. 59). The range of fluxes is much smaller than in the base case (Figure 5.3, p. 60). Homogeneous low- K streambeds thus serve as homogenizing layers which reduce the influence of the aquifer texture.

A heterogeneous streambed on top of a homogeneous aquifer (Case B) leads to a wider distribution of fluxes than in Case A (Figure 5.2 B, p. 59), but the range is still much smaller than in the base case (Figure 5.3, p. 60). This shows that the streambed alone does not cause the observed distribution of fluxes.

A heterogeneous streambed with a mean K two orders of magnitude less than the mean K of the heterogeneous aquifer (Case C) shows a similar pattern of fluxes to the base case (Figure 5.2 C, p. 59). The high- and low-discharge zones are at the same locations and the range of fluxes is similar to the range of the base case (Figure 5.3, p. 60). The short passage through the less permeable streambed does not have much influence on the flow pattern.

In case of an independent heterogeneity of the streambed (Case D), the pattern is still similar to that of a related heterogeneity as in Case C, but the locations of high- and low-discharge zones have been slightly displaced, some peaks have disappeared, while other peaks have developed (Figure 5.2 D, p. 59). The range of fluxes is almost identical with the range of the base case (Figure 5.3, p. 60).

A greater spatial heterogeneity mainly leads to an increase in the proportion of high fluxes, because well connected high-permeability zones can lead to very high fluxes concentrated in small areas. Thus, smaller proportions of streambed area contribute larger proportions of cumulative flux (Figure 5.4, p. 61). A higher connectivity results in a higher variation of discharge rates (Figure 5.5, p. 62).

In conclusion, the aquifer was found to have a stronger influence on the spatial distribution of fluxes than the streambed.

6.2 Conclusions

Many different measuring methods are available to investigate interactions between groundwaters and streams. Due to the various spatial and temporal scales of both processes and methods, it is a critical step to select the most appropriate methods or combine different ap-

proaches into an efficient methodology, including field observations and laboratory experiments as well as modelling efforts.

At the Schachtgraben stream, two novel methods were combined to determine contaminant mass flow rates between aquifer and stream. Mapping of temperatures in the streambed enabled to estimate the range of water fluxes through the streambed. Integral pumping tests gave representative average contaminant concentrations in the aquifer. The combination of both methods has proven to be an efficient methodology to obtain mass fluxes of contaminants between aquifer and stream. Since mass fluxes are controlled by advection, high-discharge zones in the streambed contribute most of the contaminant mass. Therefore, a high-resolution survey of the full range of water fluxes enables a better evaluation of the environmental impact of contaminated aquifers on connected stream ecosystems than an estimation of only reach-average groundwater discharge rates.

The distribution of water fluxes across the streambed commonly displays substantial spatial heterogeneity, which was also observed at the Schachtgraben. The spatial distribution of water flux is governed by the distribution of permeability in the subsurface. Since these variations in groundwater discharge occur on a very small spatial scale, the heterogeneities of the aquifer have to be correspondingly small-scale. A very dense grid of sampling points would be necessary to capture these small-scale changes in aquifer properties, which would require considerable measurement efforts and financial resources. We showed that the degree of heterogeneity of the aquifer can be inferred from measurements of streambed temperatures in coupled stream-aquifer systems. Thus, observations of streambed temperatures offer the opportunity to easily and quickly obtain additional parameters to significantly improve estimations of aquifer heterogeneity from traditional subsurface investigation techniques.

Not only aquifers, but also streambeds are usually characterized by a heterogeneous distribution of permeability. The modelling study comparing different combinations of aquifer and streambed permeability distributions showed that the influence of the aquifer on the distribution of fluxes across the streambed is stronger though, because the longer passage through the aquifer leads to a concentration of flow lines through highly permeable zones. However, the implementation of a homogeneous streambed with a small permeability within a heterogeneous aquifer causes a significant homogenization of the fluxes. This behaviour should be considered when using the concept of streambed conductance in regional-scale groundwater models. Even when streambeds are clogged, which leads to a reduced permeability of the streambed sediments compared to the aquifer, it might be appropriate to implement a heterogeneous distribution of streambed permeability in models even at large scales to avoid an underestimation of peak flows. Numerical model predictions of groundwater flow and solute transport may significantly benefit from heterogeneous distributions of aquifer and streambed properties.

Subsurface heterogeneity was shown to play an important role for interactions between groundwaters and streams. Spatial variations of permeability result in a diversion of flow paths and a highly variable distribution of groundwater discharge rates across the streambed. Dissolved solutes in the groundwater are transported with the water flow, and the solute mass fluxes are controlled by the water fluxes. A detailed investigation of small-scale heterogeneities and the full range of water fluxes is therefore crucial to estimate possible contaminant mass fluxes for an evaluation of the condition of stream and groundwater ecosystems and the prediction of the effects of disturbances or restoration measures.

6.3 Perspectives

In this study, water and contaminant mass fluxes between a contaminated aquifer and a stream were determined. The methods involved the estimation of contaminant concentrations in the groundwater migrating towards the stream, and the investigation of the distribution of water fluxes in the streambed as well as factors influencing this distribution. Several assumptions had to be made in the course of the analysis, which were usually based on results of previous studies or were commonly accepted simplifications. However, some of the processes or factors neglected in this study may have an influence on the results and should be investigated in future studies.

For the calculation of contaminant mass fluxes between aquifers and stream, it was assumed that the contaminants travel through the streambed without experiencing any transformation during the passage. However, streambeds often contain a larger amount of dissolved oxygen than aquifers due to the infiltration of oxygen-rich surface water, which may lead to enhanced biodegradation rates. Furthermore, the amount of organic carbon is also usually higher in streambeds, which may cause a stronger sorption of contaminants to the sediments. These processes may reduce the contaminant mass that is finally discharged to the stream and therefore may contribute to the natural attenuation of contaminants in stream-aquifer systems. The hyporheic zone may thereby play an important role, because it brings together characteristics of both the groundwater and the surface water zone. The permeable sediments provide habitat for microorganisms and the low flow velocities lead to longer residence times compared to the surface water. Compared to groundwater, the hyporheic zone is better supplied with oxygen and nutrients. These factors may lead to an enhanced degradation capacity. The supply of the hyporheic zone with solutes from the surface water as well as the residence time of solutes in the streambed depend strongly on the water flow rates through the sediments. Also the sorption of contaminants at sediments may be influenced by the water flow rates. Future studies should look at the patterns of biodegradation and their dependence on the distribution of water fluxes and heterogeneous flow paths and on the effects on sorption/desorption. This could help identify the potential of the hyporheic zone to attenuate contaminants and its contribution to the self-purification capacity of streams.

The influence of subsurface heterogeneity on the distribution of fluxes across the streambed was analyzed with a two-dimensional groundwater flow and heat transport model. It was assumed that the water flow through the streambed is vertical. However, as flow pathways through aquifers and streambeds are commonly strongly diverted corresponding to the position of permeable zones, it would be interesting to study the system in a three-dimensional model to look at the effects of this assumption and the influence of non-vertical flow. Particularly the effects of hyporheic exchange flows, i.e. surface water entering the streambed and leaving it again at some distance downstream, were not included in this study. Hyporheic flow lines can be directed vertically downwards and thus counteract the discharge of groundwater, and they can also lead to horizontal flow lines, violating the assumption of vertical flow. Underflow corresponding to the slope of the stream may further influence the direction of flow lines in the streambed. Future work is needed to further develop both experimental and modelling approaches to enable a reliable characterization of the flow field in streambeds. Also, the implementation of subsurface heterogeneity of both aquifers and streambeds in coupled stream-aquifer models needs further development. To date, the streambed is often represented by a homogeneous boundary condition, which may lead to an underestimation of peak flows. However, the parametrization of

numerical models is often difficult due to the lack of field data, and future efforts are required to make use of stochastic methods and to deal with uncertainties in the assessment of model results.

Bibliography

- Alyamani, M., and Z. Sen (1993), Determination of hydraulic conductivity from complete grain-size distribution curves, *Ground Water*, 31(4), 551–555.
- Anderson, E. (2005), Modeling groundwater-surface water interactions using the dupuit approximation, *Adv. Water Resour.*, 28(4), 315–327.
- API (2002), Estimating mass flux for decision-making: An expert workshop., *Tech. rep.*, American Petroleum Institute, Washington DC.
- API (2003), Groundwater remediation strategies tool, vol. 4730., *Tech. rep.*, Regulatory Analysis and Scientific Affairs Department, American Petroleum Institute, Washington DC.
- Basu, N. B., P. Rao, I. C. Poyer, M. Annable, and K. Hatfield (2006), Flux-based assessment at a manufacturing site contaminated with trichloroethylene, *J. Contam. Hydrol.*, 86(1-2), 105–127.
- Bauer, S., M. Bayer-Raich, T. Holder, C. Kolesar, D. Müller, and T. Ptak (2004), Quantification of groundwater contamination in an urban area using integral pumping tests, *J. Contam. Hydrol.*, 75, 183–213.
- Baxter, C., F. Hauer, and W. Woessner (2003), Measuring groundwater-stream water exchange: New techniques for installing minipiezometers and estimating hydraulic conductivity, *Trans. Amer. Fisher. Society*, 132(3), 493–502.
- Bayer-Raich, M. (2004), Integral pumping tests for the characterization of groundwater contamination, Ph.D. thesis, Eberhard-Karls-Universität Tübingen, Geowissenschaftliches Institut.
- Bayer-Raich, M., R. Jarsjö, R. Liedl, T. Ptak, and G. Teutsch (2004), Average contaminant concentration and mass flow in aquifers from time-dependent pumping well data: Analytical framework, *Water Resour. Res.*, 40, W08 303, doi:10.1029/2004WR003095.
- Bayer-Raich, M., J. Jarsjö, R. Liedl, T. Ptak, and G. Teutsch (2006), Integral pumping test analyses of linearly sorbed groundwater contaminants using multiple wells: Inferring mass flows and natural attenuation rates, *Water Resour. Res.*, 42(8), W08 411, doi: 10.1029/2005WR004244.
- Becker, M., T. Georgian, H. Ambrose, J. Siniscalchi, and K. Fredrick (2004), Estimating flow and flux of ground water discharge using water temperature and velocity, *J. Hydrol.*, 296(1-4), 221–233.
- Bencala, K. (1993), A perspective on stream-catchment connections., *J. N. Amer. Benthol. Soc.*, 12, 44–47.

- Bencala, K., and R. Walters (1983), Simulation of solute transport in a mountain pool-and-riffle stream: A transient storage model, *Water Resour. Res.*, *19*(3), 718–724.
- Bense, V., and H. Kooi (2004), Temporal and spatial variations of shallow subsurface temperature as a record of lateral variations in groundwater flow, *J. Geophys. Res.*, *109*, B04103, doi:10.1029/2003JB002782.
- Beyer, W. (1964), Zur Bestimmung der Wasserdurchlässigkeit von Kiesen und Sanden aus der Kornverteilungskurve, *Wasserwirtschaft Wassertechnik*, *14*(6), 165–168.
- Béland-Pelletier, C., J. F. Barker, A. Bockelmann, and T. Ptak (2001), Evaluation of two techniques to estimate the mass flux of contaminants in groundwater, in *Joint Can. Geotechn. Soc./Internat. Assoc. Hydrogeologists Conference, Calgary, AB, September 16–19*.
- Boano, F., R. Revelli, and L. Ridolfi (2008), Reduction of the hyporheic zone volume due to the stream-aquifer interaction, *Geophys. Res. Lett.*, *35*, L09401, doi:10.1029/2008GL033554.
- Bockelmann, A., T. Ptak, and G. Teutsch (2001), An analytical quantification of mass fluxes and natural attenuation rate constants at a former gasworks site, *J. Contam. Hydrol.*, *53*(3-4), 429–453.
- Bockelmann, A., D. Zamfirescu, T. Ptak, P. Grathwohl, and G. Teutsch (2003), Quantification of mass fluxes and natural attenuation rates at an industrial site with a limited monitoring network: a case study, *J. Contam. Hydrol.*, *60*(1-2), 97–121.
- Bopp, S. (2004), Development of a passive sampling device for combined chemical and toxicological long-term monitoring of groundwater, Ph.D. thesis, UFZ – Helmholtz Centre for Environmental Research / University of Rostock, Germany.
- Bopp, S., H. Wejá, M. Schirmer, P. Grathwohl, and K. Schirmer (2004), Passive Probennahme in Grund- und Oberflaechenwasser - ein Ueberblick, *Grundwasser*, *9*(2), 109–118.
- Borden, R., R. Daniel, L. Lebrun, and C. Davis (1997), Intrinsic biodegradation of MTBE and BTEX in a gasoline-contaminated aquifer, *Water Resour. Res.*, *33*(5), 1105–1115.
- Boulton, A., S. Findlay, P. Marmonier, E. Stanley, and H. Valett (1998), The functional significance of the hyporheic zone in streams and rivers, *Annu. Rev. Ecol. Syst.*, *29*, 59–81.
- Bouwer, H., and R. Rice (1976), Slug test for determining hydraulic conductivity of unconfined aquifers with completely or partially penetrating wells, *Water Resour. Res.*, *12*(3), 423–428.
- Bravo, H. R., F. Jiang, and R. J. Hunt (2002), Using groundwater temperature data to constrain parameter estimation in a groundwater flow model of a wetland system, *Water Resour. Res.*, *38*(8), 1153, doi:10.1029/2000WR000172.
- Bredehoeft, J., and I. Papadopolus (1965), Rates of vertical groundwater movement estimated from the earth's thermal profile, *Water Resour. Res.*, *1*(2), 325–328.
- Bruen, M. P., and Y. Z. Osman (2004), Sensitivity of stream-aquifer seepage to spatial variability of the saturated hydraulic conductivity of the aquifer, *J. Hydrol.*, *293*(1-4), 289–302.
- Brunke, M., and T. Gonser (1997), The ecological significance of exchange processes between rivers and groundwater, *Freshwater Biol.*, *37*, 1–33.
- Butler, J. (1998), *The Design, Performance, and Analysis of Slug Tests*, CRC Press LLC, Boca Raton, FL.

- Butler, J. J. J., and E. J. Garnett (2000), Simple procedures for analysis of slug tests in formations of high hydraulic conductivity using spreadsheet and scientific graphics software, *Open-File Report 2000-40*, Kansas Geological Survey.
- Butler, J. J. J., A. A. Lanier, J. M. Healey, S. M. Sellwood, W. McCall, and E. J. Garnett (2000), Direct-push hydraulic profiling in an unconsolidated alluvial aquifer, *Open-File Report 2000-62*, Kansas Geological Survey.
- Cardenas, M., and V. Zlotnik (2003), A simple constant-head injection test for streambed hydraulic conductivity estimation, *Ground Water*, 41(6), 867–871.
- Cardenas, M., J. Wilson, and V. Zlotnik (2004), Impact of heterogeneity, bed forms, and stream curvature on subchannel hyporheic exchange, *Water Resour. Res.*, 40(8), W08307, doi:10.1029/2004WR003008.
- Cardenas, M. B. (2008), Surface water-groundwater interface geomorphology leads to scaling of residence times, *Geophys. Res. Lett.*, 35, L08402, doi:10.1029/2008GL033753.
- Cardenas, M. B., and J. L. Wilson (2007), Exchange across a sediment-water interface with ambient groundwater discharge, *J. Hydrol.*, 346(3-4), 69–80.
- Carey, S., and W. Quinton (2005), Evaluating runoff generation during summer using hydro-metric, stable isotope and hydrochemical methods in a discontinuous permafrost alpine catchment, *Hydrol. Proc.*, 19(1), 95–114.
- Carslaw, H., and J. Jaeger (1959), *Conduction of Heat in Solids*, Oxford University Press, New York.
- Carter, R. W., and J. Davidian (1968), *General Procedure for Gaging Streams, Techniques of Water-Resources Investigations*, vol. Book 3, chap. A6, U. S. Geological Survey.
- Castro, N., and G. Hornberger (1991), Surface-subsurface water interactions in an alluviated mountain stream channel, *Water Resour. Res.*, 27(7), 1613–1621.
- Chapman, S. W., B. L. Parker, J. A. Cherry, R. Aravena, and D. Hunkeler (2007), Groundwater-surface water interaction and its role on tce groundwater plume attenuation, *J. Contam. Hydrol.*, 91(3-4), 203–232.
- Chen, X. (2000), Measurement of streambed hydraulic conductivity and its anisotropy, *Environ. Geol.*, 39(12), 1317–1324.
- Chen, X., and X. Chen (2003), Stream water infiltration, bank storage, and storage zone changes due to stream-stage fluctuations, *J. Hydrol.*, 280(1-4), 246–264.
- Chen, X., M. Burbach, and C. Cheng (2008), Electrical and hydraulic vertical variability in channel sediments and its effects on streamflow depletion due to groundwater extraction, *J. Hydrol.*, 352(3-4), 250–266.
- Chow, V. (1952), On the determination of transmissivity and storage coefficients from pumping test data., *Trans. Amer. Geophys. Union*, 33, 397–404.
- Chow, V. (1964), *Handbook of Applied Hydrology*, Mc-Graw Hill, New York.
- Christophersen, N., and R. Hooper (1992), Multivariate-analysis of stream water chemical-data - the use of principal components-analysis for the end-member mixing problem, *Water Resour. Res.*, 28(1), 99–107.
- Clark, I., and P. Fritz (1997), *Environmental Isotopes in Hydrogeology*, CRC Press, Boca Raton.

- COM (2003), Proposal for a directive of the European Parliament and of the Council on the protection of groundwater against pollution., *Tech. Rep. 550 final, 2003/0210/COD*, Commission of the European Communities.
- Conant, B. (2004), Delineating and quantifying ground water discharge zones using streambed temperatures, *Ground Water*, 42(2), 243–257.
- Conant, B., J. Cherry, and R. Gillham (2004), A PCE groundwater plume discharging to a river: influence of the streambed and near-river zone on contaminant distributions, *J. Contam. Hydrol.*, 73(1-4), 249–279.
- Constantz, J. (1998), Interaction between stream temperature, streamflow, and groundwater exchanges in alpine streams, *Water Resour. Res.*, 34(7), 1609–1615.
- Constantz, J., and D. Stonestrom (2003), Heat as a tracer of water movement near streams, in *Heat as a tool for studying the movement of ground water near streams*, edited by D. Stonestrom and J. Constantz, Circular 1260, U.S. Geological Survey.
- Constantz, J., D. Stonestrom, A. Stewart, R. Niswonger, and T. Smith (2001), Analysis of streambed temperatures in ephemeral channels to determine streamflow frequency and duration, *Water Resour. Res.*, 37(2), 317–328.
- Constantz, J., A. Stewart, R. Niswonger, and L. Sarma (2002), Analysis of temperature profiles for investigating stream losses beneath ephemeral channels, *Water Resour. Res.*, 38(12), 1316, doi:10.1029/2001WR001221.
- Cook, P., and A. Herczeg (2000), *Environmental tracers in subsurface hydrology*, Kluwer, Boston.
- Cook, P., G. Favreau, J. Dighton, and S. Tickell (2003), Determining natural groundwater influx to a tropical river using radon, chlorofluorocarbons and ionic environmental tracers, *J. Hydrol.*, 277(1-2), 74–88.
- Cooper, H., and C. Jacob (1946), A generalized graphical method for evaluating formation constants and summarizing well-field history, *Trans. Amer. Geophys. Union*, 27(4), 526–534.
- Cooper, H., I. Papadopoulos, and J. Bredehoeft (1967), Response to a finite-diameter well to an instantaneous charge of water, *Water Resour. Res.*, 3(1), 263–269.
- Coplen, H., A. Herczeg, and C. Barnes (2000), Isotope engineering – using stable isotopes of the water molecule to solve practical problems, in *Environmental tracers in subsurface hydrology*, edited by P. Cook and A. Herczeg, Kluwer, Boston.
- Dahm, C., N. Grimm, P. Marmonier, H. Valett, and P. Vervier (1998), Nutrient dynamics at the interface between surface waters and groundwaters, *Freshwater Biol.*, 40, 427–451.
- D'Angelo, D., J. Webster, S. Gregory, and J. Meyer (1993), Transient storage in appalachian and cascade mountain streams as related to hydraulic characteristics, *J. N. Amer. Benthol. Soc.*, 12(3), 223–235.
- Darcy, H. (1856), *Les fontaines publiques de la Ville de Dijon*, Victon Dalmont, Paris.
- Davie, T. (2002), *Fundamentals of Hydrology*, Routledge, New York.
- De Jonge, H., and G. Rothenberg (2005), New device and method for flux-proportional sampling of mobile solutes in soil and groundwater, *Environ. Sci. Technol.*, 39(1), 274–282.

- Derlien, H., T. Faupel, and C. Nieters (1999), Industriestandort mit Vorbildfunktion? Das ostdeutsche Chemiedreieck, *Discussion Paper FS IV 99-16*, Wissenschaftszentrum Berlin.
- Dietrich, P., J. J. Butler, and K. FaiSS (2008), A rapid method for hydraulic profiling in unconsolidated formations, *Ground Water*, 46(2), 323-328.
- Domenico, P., and F. Schwartz (1998), *Physical and Chemical Hydrogeology*, 2 ed., John Wiley & Sons Inc., New York.
- Eismann, L. (2002), Tertiary and quaternary geology of the Saale-Elbe region of Eastern Germany, *Quatern. Sci. Rev.*, 21(11), 1241-1346.
- Elliott, A., and N. Brooks (1997), Transfer of nonsorbing solutes to a streambed with bed forms: Theory, *Water Resour. Res.*, 33(1), 123-136.
- Ellis, P. A., R. Mackay, and M. O. Rivett (2007), Quantifying urban river-aquifer fluid exchange processes: A multi-scale problem, *J. Contam. Hydrol.*, 91(1-2), 58-80.
- EPA (2003), The DNAPL remediation challenge: Is there a case for source depletion?, *Tech. Rep. EPA/600/R-03/143*, Expert Panel on DNAPL Remediation, U. S. Environmental Protection Agency.
- Ferguson, G. (2007), Heterogeneity and thermal modeling of ground water, *Ground Water*, 45(4), 485-490.
- Fleckenstein, J. H., R. G. Niswonger, and G. E. Fogg (2006), River-aquifer interactions, geologic heterogeneity, and low-flow management, *Ground Water*, 44(6), 837-852.
- Freeze, R., and J. Cherry (1979), *Groundwater*, Prentice Hall, Inc., Upper Saddle River, NJ 07458.
- Gelhar, L. (1993), *Stochastic subsurface hydrology*, Prentice Hall, Englewood Cliffs.
- Genereux, D., and R. Hooper (1998), Oxygen and hydrogen isotopes in rainfall-runoff studies, in *Isotope Tracers in Catchment Hydrology*, edited by C. Kendall and J. McDonnell, Elsevier Science, Amsterdam.
- Gooseff, M., J. Anderson, S. Wondzell, J. LaNier, and R. Haggerty (2006), A modelling study of hyporheic exchange pattern and the sequence, size, and spacing of stream bedforms in mountain stream networks, Oregon, USA, *Hydrol. Proc.*, 20(11), 2443-2457.
- Gutjahr, A. (1989), Fast Fourier transform for random field generation, *Project report for Los Alamos grant, contract 4-r58-2690r*, New Mexico Inst. of Min. and Technol.
- Halford, K., and G. Mayer (2000), Problems associated with estimating ground water discharge and recharge from stream-discharge records, *Ground Water*, 38(3), 331-342.
- Hannula, S., K. Esposito, J. Chermak, D. Runnells, D. Keith, and L. Hall (2003), Estimating ground water discharge by hydrograph separation, *Ground Water*, 41(3), 368-375.
- Hart, D., P. Mulholland, E. Marzolf, D. DeAngelis, and S. Hendricks (1999), Relationships between hydraulic parameters in a small stream under varying flow and seasonal conditions, *Hydrol. Proc.*, 13(10), 1497-1510.
- Harvey, F., D. Lee, D. Rudolph, and S. Frappe (1997), Locating groundwater discharge in large lakes using bottom sediment electrical conductivity mapping, *Water Resour. Res.*, 33(11), 2609-2615.

- Harvey, J., and K. Bencala (1993), The effect of streambed topography on surface-subsurface water exchange in mountain catchments, *Water Resour. Res.*, 29(1), 89–98.
- Harvey, J., and B. Wagner (2000), Quantifying hydrologic interactions between streams and their subsurface hyporheic zones, in *Streams and Groundwaters*, edited by J. Jones and P. Mulholland, Academic Press, San Diego.
- Hatch, C. E., A. T. Fisher, J. S. Revenaugh, J. Constantz, and C. Ruehl (2006), Quantifying surface water-groundwater interactions using time series analysis of streambed thermal records: Method development, *Water Resour. Res.*, 42(10), W10 410, doi:10.1029/2005WR004787.
- Hatfield, K., M. Annable, J. Cho, P. Rao, and H. Klammler (2004), A direct passive method for measuring water and contaminant fluxes in porous media, *J. Contam. Hydrol.*, 75, 155–181.
- Hazen, A. (1892), Some physical properties of sands and gravels., *Tech. Rep. 24th Annual Report*, Mass. State Board of Health.
- Heidrich, S., M. Schirmer, H. Weiss, P. Wycisk, J. Grossmann, and A. Kaschl (2004a), Regionally contaminated aquifers - toxicological relevance and remediation options (Bitterfeld case study), *Toxicology*, 205, 143–155.
- Heidrich, S., H. Weiss, and A. Kaschl (2004b), Attenuation reactions in a multiple contaminated aquifer in Bitterfeld (Germany), *Environ. Pollut.*, 129(2), 277–288.
- Hinkle, S., J. Duff, F. Triska, A. Laenen, E. Gates, K. Bencala, D. Wentz, and S. Silva (2001), Linking hyporheic flow and nitrogen cycling near the Willamette River – a large river in Oregon, USA, *J. Hydrol.*, 244(3-4), 157–180.
- Hlavacova, E., M. Rulik, and L. Cap (2005), Anaerobic microbial metabolism in hyporheic sediments of a gravel bar in a small lowland stream, *River Research and Applications*, 21(9), 1003–1011.
- Hooper, R. P., and C. A. Shoemaker (1986), A comparison of chemical and isotopic hydrograph separation, *Water Resour. Res.*, 22(10), 1444–1454.
- Hornberger, G., J. Raffensperger, P. Wiberg, and K. Eshleman (1998), *Elements of Physical Hydrology*, The John Hopkins University Press, Baltimore.
- Hutchinson, P., and I. Webster (1998), Solute uptake in aquatic sediments due to current-obstacle interactions, *J. Environ. Eng.*, 124(5), 419–426.
- Hvorslev, M. (1951), Time lag and soil permeability in ground-water observations, *Waterways exper. sta. bull*, U.S. Army Corps of Engineers.
- Hyder, Z., J. Butler, C. McElwee, and W. Liu (1994), Slug tests in partially penetrating wells, *Water Resour. Res.*, 30(11), 2945–2957.
- Hynes, H. (1983), Groundwater and stream ecology, *Hydrobiologia*, 100, 93–99.
- Isiorho, S., and J. Meyer (1999), The effects of bag type and meter size on seepage meter measurements, *Ground Water*, 37(3), 411–413.
- ITRC (2003), Assessing the performance of DNAPL source reduction remedies., *Tech. rep.*, Dense Nonaqueous Phase Liquids Team, Interstate Technology and Regulatory Council.
- James, E., M. Manga, T. Rose, and G. Hudson (2000), The use of temperature and the isotopes of O, H, C, and noble gases to determine the pattern and spatial extent of groundwater flow, *J. Hydrol.*, 237(1-2), 100–112.

- Jarsjö, J., M. Bayer-Raich, and T. Ptak (2005), Monitoring groundwater contamination and delineating source zones at industrial sites: Uncertainty analyses using integral pumping tests, *J. Contam. Hydrol.*, 79(3-4), 107–134.
- Jawitz, J. W., A. D. Fure, G. G. Demmy, S. Berglund, and P. S. C. Rao (2005), Groundwater contaminant flux reduction resulting from nonaqueous phase liquid mass reduction, *Water Resour. Res.*, 41(10), W10408.
- Kalbus, E., F. Reinstorf, and M. Schirmer (2006), Measuring methods for groundwater-surface water interactions: a review, *Hydrol. Earth Syst. Sci.*, 10(6), 873–887.
- Kalbus, E., C. Schmidt, M. Bayer-Raich, S. Leschik, F. Reinstorf, G. Balcke, and M. Schirmer (2007), New methodology to investigate potential contaminant mass fluxes at the stream-aquifer interface by combining integral pumping tests and streambed temperatures, *Environ. Pollut.*, 148(3), 808–816.
- Kalbus, E., C. Schmidt, J. W. Molson, F. Reinstorf, and M. Schirmer (2008a), Groundwater-surface water interactions at the contaminated mega-site Bitterfeld, Germany, in *GQ07: Securing Groundwater Quality in Urban and Industrial Environments*, pp. 491–498, IAHS Publication 324.
- Kalbus, E., C. Schmidt, F. Reinstorf, R. Krieg, and M. Schirmer (2008b), Wie Flussbett-Temperaturdaten zur Ermittlung der Aquifer-Heterogenität beitragen können (How streambed temperatures can contribute to the determination of aquifer heterogeneity), *Grundwasser*, 13(2), 91–100.
- Kasahara, T., and S. M. Wondzell (2003), Geomorphic controls on hyporheic exchange flow in mountain streams, *Water Resour. Res.*, 39(1), 1005, doi:10.1029/2002WR001386.
- Keery, J., A. Binley, N. Crook, and J. W. Smith (2007), Temporal and spatial variability of groundwater-surface water fluxes: Development and application of an analytical method using temperature time series, *J. Hydrol.*, 336(1-2), 1–16.
- Kelly, S., and L. Murdoch (2003), Measuring the hydraulic conductivity of shallow submerged sediments, *Ground Water*, 41(4), 431–439.
- Kendall, C., and J. McDonnell (1998), *Isotope tracers in catchment hydrology*, Elsevier Science, Amsterdam.
- Kilpatrick, F. A., and E. D. Cobb (1985), *Measurement of Discharge Using Tracers, Techniques of Water-Resources Investigations*, vol. Book 3, chap. A16, p. 52, U. S. Geological Survey.
- Kilpatrick, F. A., and V. R. Schneider (1983), *Use of Flumes in Measuring Discharge, Techniques of Water-Resources Investigations*, vol. Book 3, chap. A14, p. 46, U. S. Geological Survey.
- Knudby, C., and J. Carrera (2005), On the relationship between indicators of geostatistical, flow and transport connectivity, *Adv. Water Resour.*, 28, 405–421.
- Kot, A., B. Zabiegala, and J. Namiesnik (2000), Passive sampling for long-term monitoring of organic pollutants in water, *Trends Anal. Chem.*, 19(7), 446–459.
- Kraemer, T. (2005), Radium isotopes in Cayuga Lake, New York: Indicators of inflow and mixing processes, *Limnol. Oceanogr.*, 50(1), 158–168.
- Krause, S., A. Bronstert, and E. Zehe (2007), Groundwater-surface water interactions in a North German lowland floodplain - implications for the river discharge dynamics and riparian water balance, *J. Hydrol.*, 347(3-4), 404–417.

- Krupa, S., T. Belanger, H. Heck, J. Brock, and B. Jones (1998), Krupaseep – the next generation seepage meter, in *Special Issue*, vol. 26, pp. 210–213, International Coastal Symposium (ICS 98).
- Ladouche, B., A. Probst, D. Viville, S. Idir, D. Baque, M. Loubet, J. Probst, and T. Bariac (2001), Hydrograph separation using isotopic, chemical and hydrological approaches (Strengbach catchment, France), *J. Hydrol.*, 242(3-4), 255–274.
- Land, L., and C. K. Paull (2001), Thermal gradients as a tool for estimating groundwater advective rates in a coastal estuary: White Oak River, North Carolina, USA, *J. Hydrol.*, 248(1–4), 198–214.
- Landon, M., D. Rus, and F. Harvey (2001), Comparison of instream methods for measuring hydraulic conductivity in sandy streambeds, *Ground Water*, 39(6), 870–885.
- Laudon, H., and O. Slaymaker (1997), Hydrograph separation using stable isotopes, silica and electrical conductivity: an alpine example, *J. Hydrol.*, 201(1-4), 82–101.
- Lücke, E. (2002), Grundwassermanagement am Standort Bitterfeld – Sachstand und Optimierungskonzept, in *Berichte vom 18. Bochumer Altlasten-Seminar 2002 und 13. Leipziger Altlasten-Seminar 2002.*, edited by M. Laßl and S. Scholz, pp. 371–384, Schürmann and Klagges.
- Lee, D. R. (1977), A device for measuring seepage flux in lakes and estuaries, *Limnol. Oceanogr.*, 22(1), 140–147.
- Lee, D. R., and J. A. Cherry (1978), A field exercise on groundwater flow using seepage meters and mini-piezometers, *J. Geol Education*, 27, 6–10.
- Libelo, E. L., and W. G. MacIntyre (1994), Effects of surface-water movement on seepage-meter measurements of flow through the sediment-water interface, *Hydrogeol. J.*, 2(4), 49–54.
- Linsley, R., M. Kohler, and J. Paulhus (1988), *Hydrology for Engineers*, McGraw-Hill Book Company, London.
- Malcolm, I., C. Soulsby, A. Youngson, and J. Petry (2003), Heterogeneity in ground water-surface water interactions in the hyporheic zone of a salmonid spawning stream, *Hydrol. Proc.*, 17(3), 601–617.
- Malcolm, I., C. Soulsby, A. Youngson, D. Hannah, I. McLaren, and A. Thorne (2004), Hydrological influences on hyporheic water quality: implications for salmon egg survival, *Hydrol. Proc.*, 18(9), 1543–1560.
- Mau, D., and T. Winter (1997), Estimating ground-water recharge from streamflow hydrographs for a small mountain watershed in a temperate humid climate, New Hampshire, USA, *Ground Water*, 35(2), 291–304.
- McDonald, M., and A. Harbaugh (1996), User's documentation for MODFLOW-96, an update to the U.S. Geological Survey modular finite difference ground-water flow model, *Open File Report 96-485*, U.S. Geological Survey.
- McDonald, M. G., and A. W. Harbaugh (1988), *A Modular Three-Dimensional Finite-Difference Ground-Water Flow Model*, *Techniques of Water-Resources Investigations*, vol. Book 6, chap. A1, U. S. Geological Survey.
- McDonnell, J. J., M. Bonell, M. K. Stewart, and A. J. Pearce (1990), Deuterium variations

- in storm rainfall: implication for stream hydrograph separation, *Water Resour. Res.*, 26(3), 455–458.
- Meißner, R., T. Neef, M. Rode, and J. Spindler (2005), Stickstofftransport und -umsatz in der gewässernahen und hyporheischen Zone im pleistozänen Tiefland des Elbegebietes – Konzeption und erste Ergebnisse, *Mitteilungen der Deutschen Bodenkundlichen Gesellschaft*, 107(1), 81–82.
- Miall, A. (1996), *The Geology of Fluvial Deposits: Sedimentary Facies, Basin Analysis, and Petroleum Geology*, Springer, Berlin.
- Moench, A. F. (1995), Combining the Neuman and Boulton models for flow to a well in an unconfined aquifer, *Ground Water*, 33(3), 378–384.
- Molson, J., E. Frind, and C. Palmer (1992), Thermal-energy storage in an unconfined aquifer. 2. Model development, validation, and application, *Water Resour. Res.*, 28(10), 2857–2867.
- Molson, J. W., and E. O. Frind (2005), Heatflow, a 3D groundwater flow and thermal energy transport model for porous and fractured porous media, version 2.0, *Tech. rep.*, University of Waterloo.
- Morrice, J., H. Valett, C. Dahm, and M. Campana (1997), Alluvial characteristics, groundwater-surface water exchange and hydrological retention in headwater streams, *Hydrol. Proc.*, 11(3), 253–267.
- Mulholland, P., and D. DeAngelis (2000), Surface-subsurface exchange and nutrient spiraling., in *Streams and groundwaters*, edited by J. Jones and P. Mulholland, pp. 149–164, Elsevier, New York.
- Murdoch, L., and S. Kelly (2003), Factors affecting the performance of conventional seepage meters, *Water Resour. Res.*, 39(6), 1136, doi:10.1029/2002WR001347.
- Mutz, M., and A. Rohde (2003), Processes of surface-subsurface water exchange in a low energy sand-bed stream, *Int. Rev. Hydrobiol.*, 88(3-4), 290–303.
- Mutz, M., E. Kalbus, and S. Meineke (2007), Effect of instream wood on vertical water flux in low-energy sand bed flume experiments, *Water Resour. Res.*, 43, W10 424, doi:10.1029/2006WR005676.
- Namiesnik, J., B. Zabiegala, A. Kot-Wasik, M. Partyka, and A. Wasik (2005), Passive sampling and/or extraction techniques in environmental analysis: A review, *Anal. Bioanal. Chem.*, 381(2), 279–301.
- Negrel, P., E. Petelet-Giraud, J. Barbier, and E. Gautier (2003), Surface water-groundwater interactions in an alluvial plain: Chemical and isotopic systematics, *J. Hydrol.*, 277(3-4), 248–267.
- Neuman, S. (1975), Analysis of pumping test data from anisotropic unconfined aquifers considering delayed gravity response, *Water Resour. Res.*, 11(2), 329–342.
- NRC (2004), Contaminants in the subsurface: Source zone assessment and remediation., *Tech. rep.*, The National Academies Press, Washington DC.
- Paulsen, R., C. Smith, D. O'Rourke, and T. Wong (2001), Development and evaluation of an ultrasonic ground water seepage meter, *Ground Water*, 39(6), 904–911.
- Pinder, G., and J. Jones (1969), Determination of the groundwater component of peak discharge from the chemistry of total runoff, *Water Resour. Res.*, 5(2), 438–445.

- Pitkin, S., J. Cherry, R. Ingleton, and M. Broholm (1999), Field demonstrations using the Waterloo ground water profiler, *Ground Water Monit. Remediat.*, 19(2), 122–131.
- Pollock, D. (1994), User's guide for MODPATH/MODPATH-PLOT, version 3: A particle tracking post-processing package for MODFLOW, the U.S. Geological Survey finite-difference ground-water flow model, *Open File Report 94-464*, U.S. Geological Survey.
- Powell, R. M., and R. W. Puls (1997), Hitting the bull's-eye in groundwater sampling, *Pollut. Eng.*, 29(6), 50–54.
- Ptak, T., R. Schwarz, T. Holder, and G. Teutsch (2000), Ein neues integrales Verfahren zur Quantifizierung der Grundwasserimmission, Teil II: Numerische Lösung und Anwendung in Eppelheim, *Grundwasser*, 4, 176–183.
- Ptak, T., M. Piepenbrink, and E. Martac (2004), Tracer tests for the investigation of heterogeneous porous media and stochastic modelling of flow and transport—a review of some recent developments, *J. Hydrol.*, 294(1-3), 122–163.
- Pusch, M., and J. Schwoerbel (1994), Community respiration in hyporheic sediments of a mountain stream (Steina, Black Forest), *Arch. Hydrobiol.*, 130, 35–52.
- Pusch, M., D. Fiebig, I. Brettar, H. Eisenmann, B. K. Ellis, L. A. Kaplan, M. A. Lock, M. W. Naegeli, and W. Traunspurger (1998), The role of micro-organisms in the ecological connectivity of running waters, *Freshwater Biology*, 40(3), 453–495.
- Rügner, H., T. Holder, U. Maier, M. Bayer-Raich, P. Grathwohl, and G. Teutsch (2004), Natural Attenuation-Untersuchungen "ehemalige Abfalldeponie Osterhofen", *Grundwasser*, 9(2), 98–108.
- Robin, M. J. L., A. L. Gutjahr, E. A. Sudicky, and J. L. Wilson (1993), Cross-correlated random-field generation with the direct fourier-transform method, *Water Resour. Res.*, 29(7), 2385–2397.
- Rodgers, P., C. Soulsby, J. Petry, I. Malcolm, C. Gibbins, and S. Dunn (2004), Groundwater-surface-water interactions in a braided river: a tracer-based assessment, *Hydrol. Proc.*, 18(7), 1315–1332.
- Rosenberry, D., and R. Morin (2004), Use of an electromagnetic seepage meter to investigate temporal variability in lake seepage, *Ground Water*, 42(1), 68–77.
- Rovey, C., and D. Cherkauer (1995), Scale dependency of hydraulic conductivity measurements, *Ground Water*, 33(5), 769–780.
- Rubin, Y., S. S. Hubbard, A. Wilson, and M. A. Cushey (1999), Aquifer characterization, in *The Handbook of Groundwater Engineering*, edited by J. W. Delleur, CRC Press, Boca Raton.
- Runkel, R. (1998), One-dimensional transport with inflow and storage (otis): A solute transport model for streams and rivers, *Water Resources Investigations Report 98-4018*, U.S. Geological Survey.
- Runkel, R., D. McKnight, and H. Rajaram (2003), Modeling hyporheic zone processes, *Adv. Water Resour.*, 26(9), 901–905.
- Rushton, K. (2007), Representation in regional models of saturated river-aquifer interaction for gaining/losing rivers, *J. Hydrol.*, 334(1-2), 262–281.
- Ryan, R., and M. Boufadel (2007), Evaluation of streambed hydraulic conductivity heterogeneity in an urban watershed, *Stoch. Environ. Res. Risk Assess.*, 21(4), 309–316.

- Ryan, R. J., and M. C. Boufadel (2006), Influence of streambed hydraulic conductivity on solute exchange with the hyporheic zone, *Environ. Geol.*, *V51*(2), 203–210.
- Salehin, M., A. Packman, and M. Paradis (2004), Hyporheic exchange with heterogeneous streambeds: Laboratory experiments and modeling, *Water Resour. Res.*, *40*(11), W11504, doi:10.1029/2003WR002567.
- Savant, S., D. Reible, and L. Thibodeaux (1987), Convective transport within stable river sediments, *Water Resour. Res.*, *23*(9), 1763–1768.
- Scanlon, B., R. Healy, and P. Cook (2002), Choosing appropriate techniques for quantifying groundwater recharge, *Hydrogeol. J.*, *10*(1), 18–39.
- Schaelchli, U. (1993), Berechnungsgrundlagen der inneren Kolmation von Fließgewässersohlen, *Wasser, Energie, Luft*, *85*, 321–331.
- Schirmer, M., S. Bopp, and K. Schirmer (2005), Depth-specific passive groundwater sampling for chemical and toxicological analyses of contaminants, *Zentralblatt fuer Geologie und Palaeontologie, Teil I*(1/2), 167–174.
- Schlichter, C. (1905), Field measurements of the rate of movement of underground waters., *Water Supply Paper 140*, U.S. Geological Survey.
- Schmidt, C., M. Bayer-Raich, and M. Schirmer (2006), Characterization of spatial heterogeneity of groundwater-stream water interactions using multiple depth streambed temperature measurements at the reach scale, *Hydrol. Earth Syst. Sci.*, *10*, 849–859.
- Schmidt, C., B. Conant Jr., M. Bayer-Raich, and M. Schirmer (2007), Evaluation and field-scale application of an analytical method to quantify groundwater discharge using mapped streambed temperatures, *J. Hydrol.*, *347*(3-4), 292–307.
- Schmidt, C., E. Kalbus, R. Krieg, M. Bayer-Raich, S. Leschik, F. Reinstorf, M. Martienssen, and M. Schirmer (2008a), Schadstoffmassenströme zwischen Grundwasser, Flussbettsedimenten und Oberflächenwasser am regional kontaminierten Standort Bitterfeld, *Grundwasser*, *13*(3), 133–146.
- Schmidt, C., E. Kalbus, M. Martienssen, and M. Schirmer (2008b), The influence of heterogeneous groundwater discharge on the timescales of contaminant mass flux from streambed sediments – field evidence and long-term predictions, *Hydrol. Earth Sys. Sci. Discuss.*, *5*(2), 971–1001.
- Schwarz, R. (2002), Grundwasser-Gefährdungsabschätzung durch Emissions- und Immissionsmessungen an Deponien und Altlasten, Ph.D. thesis, Eberhard-Karls-Universität Tübingen, Zentrum für angewandte Geowissenschaften.
- Schwarz, R., T. Ptak, T. Holder, and G. Teutsch (1998), Groundwater risk assessment at contaminated sites: a new investigation approach., in *GQ '98 Groundwater Quality: Remediation and Protection*, edited by M. Herbert and K. Kovar, pp. 68–71, IAHS Publication 250.
- Schwoerbel, J. (1961), Ueber die Lebensbedingungen und die Besiedlung des hyporheischen Lebensraumes, *Archiv fuer Hydrobiologie, Suppl.* *25*, 182–214.
- Shepherd, R. (1989), Correlations of permeability and grain-size, *Ground Water*, *27*(5), 633–638.
- Sholkovitz, E., C. Herbold, and M. Charette (2003), An automated dye-dilution based seep-

- age meter for the time-series measurement of submarine groundwater discharge, *Limnol. Oceanogr. Methods*, 1, 16–28.
- Silliman, S., J. Ramirez, and R. McCabe (1995), Quantifying downflow through creek sediments using temperature time series: One-dimensional solution incorporating measured surface temperature, *J. Hydrol.*, 167, 99–119.
- Sophocleous, M. (2002), Interactions between groundwater and surface water: the state of the science, *Hydrogeol. J.*, 10, 52–67.
- Sophocleous, M., A. Koussis, J. L. Martin, and S. P. Perkins (1995), Evaluation of simplified stream-aquifer depletion models for water rights administration, *Ground Water*, 33(4), 579–588.
- Springer, A., W. Petroustson, and B. Semmens (1999), Spatial and temporal variability of hydraulic conductivity in active reattachment bars of the Colorado River, Grand Canyon, *Ground Water*, 37(3), 338–344.
- Stallman, S. (1965), Steady one-dimensional fluid flow in a semi-infinite porous medium with sinusoidal surface temperature, *J. Geophys. Res.*, 70(12), 338–344.
- Stonestrom, D., and J. Constantz (2004), Using temperature to study stream-ground water exchanges, *Fact Sheet 2004-3810*, U. S. Geological Survey.
- Stonestrom, D. A., and J. Constantz (2003), Heat as a tool for studying the movement of ground water near streams, *Circular 1260*, U. S. Geological Survey.
- Storey, R., K. Howard, and D. Williams (2003), Factors controlling riffle-scale hyporheic exchange flows and their seasonal changes in a gaining stream: A three-dimensional groundwater flow model, *Water Resour. Res.*, 39(2), 1034, doi:10.1029/2002WR001367.
- Stuer-Lauridsen, F. (2005), Review of passive accumulation devices for monitoring organic micropollutants in the aquatic environment, *Environ. Pollut.*, 136(3), 503–524.
- Su, G. W., J. Jasperse, D. Seymour, and J. Constantz (2004), Estimation of hydraulic conductivity in an alluvial system using temperatures, *Ground Water*, 42(6-7), 890–901.
- Suzuki, S. (1960), Percolation measurements based on heat flow through soil with special reference to paddy fields, *J. Geophys. Res.*, 65(9), 2883–2885.
- Taniguchi, M., and Y. Fukuo (1993), Continuous measurements of groundwater seepage using an automatic seepage meter, *Ground Water*, 31(4), 675–679.
- Taniguchi, M., W. Burnett, J. Christoff, C. Smith, R. Paulsen, D. O'Rourke, and S. Krupa (2003), Spatial and temporal distributions of submarine groundwater discharge rates obtained from various types of seepage meters at a site in the Northeastern Gulf of Mexico, *Biogeochem.*, 66(1-2), 35–53.
- Terzaghi, K. (1925), *Erdbaumechanik auf bodenphysikalischer Grundlage.*, Deuticke, Wien.
- Teutsch, G., T. Ptak, R. Schwarz, and T. Holder (2000), Ein neues integrales Verfahren zur Quantifizierung der Grundwasserimmission, Teil I: Beschreibung der Grundlagen, *Grundwasser*, 4, 170–175.
- Theis, C. (1935), The relation between the lowering of the piezometric surface and the rate and duration of discharge of a well using groundwater storage., *Trans. Amer. Geophys. Union*, 16, 519–524.

- Thibodeaux, L., and J. Boyle (1987), Bedform-generated convective transport in bottom sediments, *Nature*, 325, 341–343.
- Todd, D., and L. Mays (2005), *Groundwater Hydrology*, vol. 3, Wiley, Hoboken, NJ.
- Tóth, J. (1963), A theoretical analysis of groundwater flow in small drainage basins, *J. Geophys. Res.*, 68, 4785–4812.
- Triska, F., V. Kennedy, R. Avanzino, G. Zellweger, and K. Bencala (1989), Retention and transport of nutrients in a third-order stream in northwestern California: hyporheic processes, *Ecology*, 70(6), 1893–1905.
- Triska, F. J., J. H. Duff, and R. J. Avanzino (1993), The role of water exchange between a stream channel and its hyporheic zone in nitrogen cycling at the terrestrial-aquatic interface, *Hydrobiologia*, 251(1), 167–184.
- Turcotte, D. L., and G. Schubert (1982), *Geodynamics: Applications of Continuum Physics to Geological Problems*, John Wiley & Sons, New York.
- Vrana, B., G. Mills, I. Allan, E. Dominiak, K. Svensson, J. Knutsson, G. Morrison, and R. Greenwood (2005), Passive sampling techniques for monitoring pollutants in water, *TrAC, Trends Anal. Chem.*, 24(10), 845–868.
- Walkow, F. (2000), The dioxin pollution of Bitterfeld – site description., in *Consoil 2000: Bitterfeld/Spittelwasser site case study – Comparison of solutions for a large contamination based on different national policies*, Conference on Contaminated Soil 2000, Leipzig, Germany.
- Weiss, H., et al. (2001), Sanierungsforschung in regional kontaminierten Aquiferen (SAFIRA) - 1. Information zum Forschungsschwerpunkt am Standort Bitterfeld, *Grundwasser*, 6(3), 113–122.
- Westhoff, M. C., H. H. G. Savenije, W. M. J. . Luxemburg, G. S. Stelling, N. C. van de Giesen, J. S. Selker, L. Pfister, and S. Uhlenbrook (2007), A distributed stream temperature model using high resolution temperature observations, *Hydrol. Earth Syst. Sci.*, 11(4), 1469–1480.
- Wharton, G., J. Cotton, R. Wotton, J. Bass, C. Heppell, M. Trimmer, I. Sanders, and L. Warren (2006), Macrophytes and suspension-feeding invertebrates modify flows and fine sediments in the Frome and Piddle catchments, Dorset (UK), *J. Hydrol.*, 330, 171–184.
- Winter, T. C., J. W. Harvey, O. L. Franke, and W. M. Alley (1998), Ground water and surface water : A single resource, *Circular 1139*, U. S. Geological Survey.
- Woessner, W. (2000), Stream and fluvial plain ground water interactions: Rescaling hydrogeologic thought, *Ground Water*, 38(3), 423–429.
- Woessner, W., and K. Sullivan (1984), Results of seepage meter and mini-piezometer study, Lake Mead, Nevada, *Ground Water*, 22(5), 561–568.
- Wondzell, S., and F. Swanson (1996), Seasonal and storm dynamics of the hyporheic zone of a 4th-order mountain stream. 1. Hydrologic processes, *J. N. Amer. Benthol. Soc.*, 15(1), 3–19.
- Wroblicky, G., M. Campana, H. Valett, and C. Dahm (1998), Seasonal variation in surface-subsurface water exchange and lateral hyporheic area of two stream-aquifer systems, *Water Resour. Res.*, 34(3), 317–328.
- Wu, Y., X. Wen, and Y. Zhang (2004), Analysis of the exchange of groundwater and river water

Bibliography

by using radon-222 in the middle Heihe Basin of northwestern China, *Environ. Geol.*, 45(5), 647–653.

Yehdeghoa, B., K. Rozanski, H. Zojer, and W. Stichler (1997), Interaction of dredging lakes with the adjacent groundwater field: an isotope study, *J. Hydrol.*, 192(1-4), 247–270.

Zellweger, G. (1994), Testing and comparison of 4 ionic tracers to measure stream-flow loss by multiple tracer injection, *Hydrol. Proc.*, 8(2), 155–165.

Acknowledgements

I would like to express my sincere gratitude to all the people who contributed to the success of this work:

Prof. Mario Schirmer, my supervisor, for the possibility to work at the UFZ, for his helpful advice, and valuable comments during the course of this project. His door was always open for all kinds of problems.

The professors F. Zwahlen, D. Hunkeler and P. Engesgaard for being members of the evaluation committee.

Prof. Frido Reinstorf for his critical reviews of my manuscripts and for fruitful discussions about concepts, processes and modelling.

Christian Schmidt for endless inspiring discussions and lots of fun during the field work. I really enjoyed writing publications and attending conferences together.

Ronald Krieg for his excellent preparation and incredible efforts during the field programmes.

Prof. John Molson for proof-reading and the support and hospitality during my stay in Canada.

The colleagues at the Department of Hydrogeology for the pleasant working environment, nice lunch and coffee breaks, support during the field programmes, and fruitful discussions.

The colleagues at the Department of Monitoring and Exploration Technologies for providing the direct-push equipment and support.

The colleagues at the Department of Groundwater Remediation for the help with the local authorities at the study site.

The local authorities for permission of drilling and sampling programmes.

My friends at the UFZ for nice parties and other social and cultural events.

My WG for making me feel at home in our flat and in Leipzig.

My dear family and friends for their enduring patience and support.

Florian for love and inspiration.

This work was supported by the European Union FP6 Integrated Project AquaTerra (Project no. GOCE 505428) under the thematic priority "'sustainable development, global change and ecosystems"'.

Annex 1 – Integral Pumping Test Data

Table A1-1. Parameters and contaminant concentrations measured during the integral pumping test at W11

Date and Time	pH	T [°C]	EC [$\mu\text{S cm}^{-1}$]	O ₂ [mg L^{-1}]	MCB [$\mu\text{g L}^{-1}$]	1,2-DCB [$\mu\text{g L}^{-1}$]	1,3-DCB [$\mu\text{g L}^{-1}$]	1,4-DCB [$\mu\text{g L}^{-1}$]
24.10.2005 09:10	6.3	11.0	1461	2.6	12.89	1.27	1.35	0.45
24.10.2005 12:00	6.3	11.2	1465	2.5	17.58	1.76	1.93	0.70
24.10.2005 15:00	6.3	11.1	1455	2.0	14.70	1.38	1.47	0.54
24.10.2005 18:00	6.3	11.2	1452	2.6	16.24	1.57	1.78	0.60
24.10.2005 21:00	6.3	11.1	1446	2.1	14.51	1.28	1.40	0.57
25.10.2005 00:00	6.3	11.1	1438	2.6	14.91	1.52	1.59	0.67
25.10.2005 03:00	6.2	11.1	1436	1.8	15.21	1.53	1.59	0.65
25.10.2005 06:00	6.3	11.2	1432	0.8	12.84	1.14	1.24	0.38
25.10.2005 09:00	6.3	11.2	1425	0.2	11.76	1.08	1.21	0.07
25.10.2005 12:00	6.3	11.3	1424	0.2	12.81	1.19	1.25	0.24
25.10.2005 15:00	6.4	11.3	1426	0.2	13.56	1.21	1.29	0.51
25.10.2005 18:00	6.3	11.3	1423	0.2	14.65	1.34	1.41	0.59
25.10.2005 21:00	6.4	11.3	1422	0.2	12.62	1.21	1.22	0.61
26.10.2005 00:00	6.3	11.3	1418	0.1	13.85	1.25	1.29	0.59
26.10.2005 03:00	6.3	11.2	1417	0.3	14.54	1.34	1.39	0.61
26.10.2005 06:00	6.3	11.1	1416	0.3	15.72	1.45	1.53	0.53
26.10.2005 09:00	6.3	11.2	1413	0.4	15.77	1.51	1.54	0.48
26.10.2005 12:00	6.3	11.4	1420	0.4	16.74	1.62	1.83	0.65
26.10.2005 15:00	6.3	11.3	1405	0.5	15.21	1.45	1.49	0.51
26.10.2005 18:00	6.4	11.2	1404	0.5	13.79	1.25	1.16	0.76
26.10.2005 21:00	6.4	11.1	1404	0.5	17.48	1.52	1.57	0.66
27.10.2005 00:00	6.3	11.2	1406	0.5	17.31	1.50	1.62	0.70
27.10.2005 03:00	6.4	11.2	1405	0.5	19.09	1.79	1.88	0.80
27.10.2005 06:00	6.3	11.1	1406	0.5	15.45	1.45	1.44	0.49
27.10.2005 09:00	6.3	11.3	1402	0.5	16.90	1.59	1.72	0.67
27.10.2005 12:00	6.4	11.9	1399	0.4	16.64	1.61	1.62	0.68
27.10.2005 15:00	6.4	11.6	1400	0.4	16.54	1.50	1.56	0.62
27.10.2005 18:00	6.4	11.3	1403	0.5	18.47	1.70	1.69	0.58
27.10.2005 21:00	6.3	11.4	1397	0.4	17.71	1.65	1.59	0.60
28.10.2005 00:00	6.3	11.3	1398	0.4	17.93	1.66	1.65	0.58
28.10.2005 03:00	6.3	11.3	1398	0.4	17.46	1.59	1.70	0.50
28.10.2005 06:00	6.4	11.2	1411	0.5	18.98	1.69	1.87	0.62
28.10.2005 09:00	6.4	11.3	1393	0.3	18.57	1.73	1.68	0.64
28.10.2005 12:00	6.4	11.5	1394	0.4	18.47	1.59	1.62	0.66
28.10.2005 15:00	6.4	11.6	1396	0.4	20.99	1.92	2.01	0.68
28.10.2005 18:00	6.4	11.3	1396	0.5	20.27	1.81	1.78	0.60
28.10.2005 21:00	6.4	11.3	1398	0.5	19.81	1.84	1.75	0.57
29.10.2005 00:00	6.4	11.2	1384	0.4	19.78	1.74	1.84	0.55
29.10.2005 03:00	6.4	11.3	1396	0.5	21.68	2.00	1.94	0.61
29.10.2005 06:00	6.4	11.3	1397	0.3	20.56	1.86	1.94	0.65
29.10.2005 09:00	6.3	11.2	1396	0.3	21.91	1.97	2.00	0.64

Annex 1 – Integral Pumping Test Data

Table A1-2. Parameters and contaminant concentrations measured during the integral pumping test at W12

Date and Time	pH	T [°C]	EC [$\mu\text{S cm}^{-1}$]	O ₂ [mg L^{-1}]	MCB [$\mu\text{g L}^{-1}$]	1,2-DCB [$\mu\text{g L}^{-1}$]	1,3-DCB [$\mu\text{g L}^{-1}$]	1,4-DCB [$\mu\text{g L}^{-1}$]
24.10.2005 09:10	6.2	10.8	1523	2.3	9.76	1.02	1.19	0.30
24.10.2005 12:00	6.2	11.2	1523	2.8	10.22	1.08	1.12	0.30
24.10.2005 15:00	6.2	11.0	1508	2.0	10.18	1.06	1.16	0.32
24.10.2005 18:00	6.3	11.1	1474	1.8	10.88	1.03	1.12	0.26
24.10.2005 21:00	6.2	10.9	1504	1.4	11.95	1.17	1.33	0.41
25.10.2005 00:00	6.2	10.9	1493	1.6	12.47	1.24	1.35	0.36
25.10.2005 03:00	6.3	11.0	1488	1.3	11.71	1.01	1.20	0.52
25.10.2005 06:00	6.2	10.9	1480	0.1	12.60	1.33	1.53	0.34
25.10.2005 09:00	6.3	10.8	1488	0.2	12.52	1.23	1.33	0.35
25.10.2005 12:00	6.3	10.9	1485	0.2	12.36	1.19	1.34	0.34
25.10.2005 15:00	6.3	10.9	1484	0.2	13.09	1.31	1.44	0.35
25.10.2005 18:00	6.3	11.2	1483	0.2	14.36	1.28	1.56	0.57
25.10.2005 21:00	6.3	11.9	1480	0.1	12.05	1.08	1.21	0.35
26.10.2005 00:00	6.3	10.9	1477	0.1	12.43	1.08	1.21	0.36
26.10.2005 03:00	6.3	10.8	1475	0.1	12.50	1.22	1.23	0.56
26.10.2005 06:00	6.3	10.8	1473	0.2	12.56	1.17	1.29	0.38
26.10.2005 09:00	6.3	10.9	1471	0.7	13.80	1.33	1.47	0.44
26.10.2005 12:00	6.3	11.1	1477	0.5	13.49	1.26	1.35	0.46
26.10.2005 15:00	6.3	11.0	1463	0.5	13.33	1.18	1.32	0.45
26.10.2005 18:00	6.3	10.8	1460	0.5	13.08	1.18	1.25	0.60
26.10.2005 21:00	6.3	10.8	1462	0.5	13.12	1.21	1.27	0.45
27.10.2005 00:00	6.3	10.8	1462	0.4	13.00	1.13	1.27	0.55
27.10.2005 03:00	6.3	10.8	1459	0.4	12.86	1.12	1.26	0.53
27.10.2005 06:00	6.3	10.7	1460	0.3	11.95	1.17	1.26	0.45
27.10.2005 09:00	6.3	10.9	1457	0.4	11.74	1.12	1.18	0.48
27.10.2005 12:00	6.3	11.2	1452	0.4	11.62	1.11	1.24	0.36
27.10.2005 15:00	6.3	11.2	1453	0.4	11.59	1.07	1.10	0.35
27.10.2005 18:00	6.4	10.9	1444	0.5	12.47	1.14	1.37	0.23
27.10.2005 21:00	6.3	10.8	1449	0.3	11.80	1.04	1.14	0.23
28.10.2005 00:00	6.3	10.9	1445	0.5	12.24	1.11	1.32	0.23
28.10.2005 03:00	6.3	10.9	1448	0.4	12.81	1.15	1.21	0.26
28.10.2005 06:00	6.3	10.8	1443	0.3	12.09	1.15	1.22	0.38
28.10.2005 09:00	6.3	11.0	1442	0.3	12.31	1.27	1.25	0.36
28.10.2005 12:00	6.3	11.1	1442	0.3	12.42	1.15	1.18	0.36
28.10.2005 15:00	6.3	11.2	1438	0.4	12.57	1.16	1.27	0.34
28.10.2005 18:00	6.3	10.9	1439	0.5	12.82	1.25	1.39	
28.10.2005 21:00	6.3	10.9	1440	0.3	12.48	1.18	1.21	0.33
29.10.2005 00:00	6.3	10.9	1428	0.3	13.19	1.26	1.40	0.33
29.10.2005 03:00	6.3	10.9	1435	0.2	12.38	1.06	1.14	0.43
29.10.2005 06:00	6.3	10.9	1436	0.2	12.75	1.18	1.17	0.45
29.10.2005 09:00	6.3	10.9	1437	0.3	12.05	1.19	1.13	0.25

Table A1-3. Parameters and contaminant concentrations measured during the integral pumping test at W13

Date and Time	pH	T [°C]	EC [$\mu\text{S cm}^{-1}$]	O ₂ [mg L^{-1}]	MCB [$\mu\text{g L}^{-1}$]	1,2-DCB [$\mu\text{g L}^{-1}$]	1,3-DCB [$\mu\text{g L}^{-1}$]	1,4-DCB [$\mu\text{g L}^{-1}$]
24.10.2005 09:10	6.0	11.1	1523	2.2	10.26	1.25	1.40	0.38
24.10.2005 12:00	6.3	11.7	1490	3.4	10.67	1.14	1.23	0.34
24.10.2005 15:00	6.3	11.3	1512	4.6	10.13	0.99	1.18	0.44
24.10.2005 18:00	6.2	11.2	1502	2.6	10.21	0.95	1.14	0.52
24.10.2005 21:00	6.3	11.0	1500	2.3	10.22	0.96	1.14	0.52
25.10.2005 00:00	6.2	11.0	1492	2.5	11.93	1.24	1.53	0.54
25.10.2005 03:00	6.2	11.0	1486	1.6	11.35	1.26	1.47	0.48
25.10.2005 06:00	6.2	11.3	1485	0.8	9.35	0.91	1.08	0.36
25.10.2005 09:00	6.2	11.3	1482	0.3	9.88	1.04	1.13	0.29
25.10.2005 12:00	6.2	11.4	1480	0.2	10.27	1.06	1.15	0.50
25.10.2005 15:00	6.3	11.3	1483	0.2	10.48	1.04	1.15	0.48
25.10.2005 18:00	6.2	11.3	1483	0.5	10.71	1.07	1.22	0.46
25.10.2005 21:00	6.2	11.3	1482	0.1	11.78	1.01	1.06	0.58
26.10.2005 00:00	6.2	11.2	1480	0.1	10.87	1.03	1.22	0.59
26.10.2005 03:00	6.3	11.2	1478	0.2	10.24	0.95	1.14	0.65
26.10.2005 06:00	6.3	11.2	1478	0.1	11.22	1.15	1.30	0.66
26.10.2005 09:00	6.2	11.2	1478	0.6	15.42	1.01	1.24	0.35
26.10.2005 12:00	6.2	11.5	1483	0.5	8.20	0.83	1.06	0.22
26.10.2005 15:00	6.2	11.3	1471	0.3	9.95	1.01	1.12	0.49
26.10.2005 18:00	6.3	11.1	1471	0.4	11.53	1.13	1.34	0.69
26.10.2005 21:00	6.3	11.1	1472	0.5	11.00	1.13	1.23	0.57
27.10.2005 00:00	6.2	11.0	1473	0.5	10.58	1.03	1.30	0.21
27.10.2005 03:00	6.2	11.0	1470	0.6	11.20	1.10	1.26	0.29
27.10.2005 06:00	6.2	11.1	1472	0.3	9.78	1.00	1.11	0.40
27.10.2005 09:00	6.2	11.2	1471	0.4	9.91	1.05	1.14	0.48
27.10.2005 12:00	6.2	11.5	1469	0.4	9.84	1.04	1.12	0.60
27.10.2005 15:00	6.3	11.5	1465	0.4	10.17	1.11	1.29	0.29
27.10.2005 18:00	6.3	11.1	1459	0.5	9.19	0.94	0.99	0.39
27.10.2005 21:00	6.2	10.9	1454	0.4	11.09	1.01	1.29	0.23
28.10.2005 00:00	6.3	11.1	1464	0.5	9.64	1.04	1.12	0.24
28.10.2005 03:00	6.2	11.1	1467	0.5	9.83	0.94	1.07	0.23
28.10.2005 06:00	6.3	11.1	1461	0.5	10.45	1.15	1.25	0.41
28.10.2005 09:00	6.2	11.3	1459	0.5	10.03	1.07	1.16	0.49
28.10.2005 12:00	6.2	11.4	1460	0.3	9.70	1.03	1.08	0.49
28.10.2005 15:00	6.3	11.5	1461	0.3	9.43	1.01	1.19	0.11
28.10.2005 18:00	6.2	11.2	1460	0.4	8.42	0.93	0.85	0.22
28.10.2005 21:00	6.2	11.1	1461	0.3	10.01	1.05	1.13	0.45
29.10.2005 00:00	6.2	11.2	1450	0.3	10.38	1.10	1.08	0.30
29.10.2005 03:00	6.2	11.2	1455	0.4	10.07	1.03	1.14	0.48
29.10.2005 06:00	6.2	11.1	1457	0.3	10.24	1.04	1.10	0.44
29.10.2005 09:00	6.2	11.1	1458	0.4	9.96	1.03	1.10	0.28

Annex 1 – Integral Pumping Test Data

Table A1-4. Parameters and contaminant concentrations measured during the integral pumping test at W14

Date and Time	pH	T [°C]	EC [$\mu\text{S cm}^{-1}$]	O ₂ [mg L^{-1}]	MCB [$\mu\text{g L}^{-1}$]	1,2-DCB [$\mu\text{g L}^{-1}$]	1,3-DCB [$\mu\text{g L}^{-1}$]	1,4-DCB [$\mu\text{g L}^{-1}$]
24.10.2005 09:10	6.2	11.2	1460	2.6	13.70	4.71	2.25	0.68
24.10.2005 12:00	6.2	13.0	1431	2.7	11.14	1.75	1.72	0.63
24.10.2005 15:00	6.2	11.6	1483	3.7	12.46	1.80	1.82	0.71
24.10.2005 18:00	6.2	11.2	1480	2.5	9.37	1.37	1.45	0.55
24.10.2005 21:00	6.3	11.1	1443	3.4	9.66	1.55	1.47	0.60
25.10.2005 00:00	6.3	11.1	1448	3.3	9.56	1.39	1.43	0.60
25.10.2005 03:00	6.2	11.1	1460	2.0	9.80	1.50	1.56	0.64
25.10.2005 06:00	6.3	11.3	1450	0.6	9.58	1.40	1.47	0.75
25.10.2005 09:00	6.2	11.3	1394	0.2	9.68	1.45	1.50	0.60
25.10.2005 12:00	6.3	11.4	1393	0.2	9.62	1.33	1.45	0.74
25.10.2005 15:00	6.3	11.4	1392	0.1	9.04	1.43	1.34	0.69
25.10.2005 18:00	6.3	11.3	1387	0.1	8.44	1.28	1.33	0.65
25.10.2005 21:00	6.3	11.3	1383	0.1	8.54	1.22	1.23	0.53
26.10.2005 00:00	6.3	11.3	1380	0.1	9.51	1.35	1.31	0.58
26.10.2005 03:00	6.2	11.3	1376	0.1	9.33	1.30	1.49	0.59
26.10.2005 06:00	6.3	11.3	1372	0.1	9.63	1.43	1.43	0.76
26.10.2005 09:00	6.2	11.4	1369	0.5	12.81	1.55	1.60	0.81
26.10.2005 12:00	6.2	11.6	1392	0.5	11.53	1.76	1.88	1.27
26.10.2005 15:00	6.2	11.4	1362	0.3	9.40	1.45	1.43	0.80
26.10.2005 18:00	6.2	11.2	1362	0.5	9.02	1.38	1.43	0.78
26.10.2005 21:00	6.2	11.2	1360	0.4	8.90	1.33	1.31	0.49
27.10.2005 00:00	6.2	11.1	1361	0.4	8.97	1.32	1.50	0.50
27.10.2005 03:00	6.2	11.2	1356	0.4	8.76	1.29	1.33	0.51
27.10.2005 06:00	6.2	11.1	1354	0.3	7.45	1.11	1.07	0.62
27.10.2005 09:00	6.3	11.3	1351	0.3	9.63	1.48	1.53	0.65
27.10.2005 12:00	6.2	11.6	1349	0.3	7.49	1.19	1.17	0.60
27.10.2005 15:00	6.3	11.6	1345	0.3	7.72	1.14	1.05	0.46
27.10.2005 18:00	6.2	11.3	1342	0.3	9.80	1.51	1.52	0.60
27.10.2005 21:00	6.2	11.3	1345	0.5	9.65	1.56	1.53	0.62
28.10.2005 00:00	6.2	11.2	1346	0.4	9.42	1.45	1.38	0.55
28.10.2005 03:00	6.2	11.3	1343	0.4	9.98	1.62	1.57	0.70
28.10.2005 06:00	6.2	11.3	1336	0.3	7.86	1.53	1.50	0.66
28.10.2005 09:00	6.2	11.5	1334	0.3	9.29	1.40	1.37	0.58
28.10.2005 12:00	6.2	11.6	1335	0.3	10.02	1.61	1.60	0.58
28.10.2005 15:00	6.2	11.6	1334	0.3	9.61	1.54	1.47	0.59
28.10.2005 18:00	6.2	11.3	1334	0.3	10.24	1.56	1.54	0.68
28.10.2005 21:00	6.2	11.3	1334	0.4	10.30	1.52	1.43	0.65
29.10.2005 00:00	6.2	11.2	1325	0.2	7.94	1.15	1.10	0.47
29.10.2005 03:00	6.2	11.3	1329	0.2	10.32	1.48	1.38	0.46
29.10.2005 06:00	6.2	11.3	1327	0.2	9.98	1.35	1.29	0.56
29.10.2005 09:00	6.2	11.3	1328	0.2	10.39	1.53	1.44	0.61

Table A1-5. Parameters and contaminant concentrations measured during the integral pumping test in the Schachtgraben

Date and Time	pH	T [°C]	EC [$\mu\text{S cm}^{-1}$]	O ₂ [mg L^{-1}]	MCB [$\mu\text{g L}^{-1}$]	1,2-DCB [$\mu\text{g L}^{-1}$]	1,3-DCB [$\mu\text{g L}^{-1}$]	1,4-DCB [$\mu\text{g L}^{-1}$]
24.10.2005 09:10	7.2	15.5	2510	4.3	10.71	0.46	3.06	1.32
24.10.2005 12:00	7.1	15.0	2430	3.7	24.37	2.69	3.78	1.43
24.10.2005 15:00	7.1	15.3	2290	4.5	22.76	2.79	4.33	1.63
24.10.2005 18:00	7.1	15.5	2290	3.7	25.90	3.00	4.64	1.70
24.10.2005 21:00	7.1	14.9	2470	5.1	19.92	2.85	3.04	1.22
25.10.2005 00:00	7.1	14.6	2150	5.4	74.19	4.61	2.78	1.67
25.10.2005 03:00	7.1	15.7	2430	5.6	23.25	1.14	4.16	1.52
25.10.2005 06:00	7.1	14.2	2200	5.1	18.58	2.29	3.08	1.51
25.10.2005 09:00	7.1	14.8	1819	4.2	30.95	1.78	5.09	2.36
25.10.2005 12:00	7.1	15.3	1817	4.7	22.17	0.95	4.16	1.95
25.10.2005 15:00	7.1	15.1	2260	5.1	23.57	2.36	3.52	1.75
25.10.2005 18:00	7.1	14.7	2380	3.9	28.28	2.78	4.16	1.82
25.10.2005 21:00	7.1	15.2	1913	2.9	29.03	1.17	6.01	2.32
26.10.2005 00:00	7.1	14.5	2520	4.7	17.07	0.10	2.79	0.00
26.10.2005 03:00	7.1	14.4	2650	4.9	23.38	0.09	2.77	0.02
26.10.2005 06:00	7.1	15.4	2610	5.0	46.49	3.32	5.66	2.80
26.10.2005 09:00	7.1	15.4	2380	3.1	29.92	0.95	5.74	2.41
26.10.2005 12:00	7.2	14.9	2180	3.9	15.54	1.09	2.79	1.47
26.10.2005 15:00	6.9	15.5	2080	4.2	12.53	0.10	5.91	2.63
26.10.2005 18:00	7.0	15.0	2470	4.7	14.68	0.89	3.31	1.18
26.10.2005 21:00	7.0	14.2	2400	5.2	19.69	1.71	4.02	1.71
27.10.2005 00:00	6.9	15.0	2260	5.1	29.81	1.95	4.68	2.13
27.10.2005 03:00	7.0	14.3	2550	4.9	10.38	0.91	1.04	0.09
27.10.2005 06:00	6.9	14.4	2480	5.8	21.77	1.78	3.99	1.83
27.10.2005 09:00	6.9	15.3	2170	5.4	23.03	1.36	4.69	1.91
27.10.2005 12:00	6.9	15.3	2450	4.7	23.10	1.55	3.97	1.59
27.10.2005 15:00	6.8	16.2	2390	5.3	7.72	1.14	1.05	0.46
27.10.2005 18:00	6.8	14.8	2450	5.3	14.23	0.91	3.77	1.57
27.10.2005 21:00	6.8	13.5	2400	5.9	21.65	2.31	3.23	1.42
28.10.2005 00:00	6.7	14.4	1997	4.6	26.83	2.64	4.52	1.72
28.10.2005 03:00	6.6	14.8	2460	4.9	23.55	3.10	4.39	1.72
28.10.2005 06:00	6.9	14.4	2560	5.4	15.28	2.01	3.46	1.56
28.10.2005 09:00	6.9	14.7	2410	3.7	24.09	1.69	4.97	1.90
28.10.2005 12:00	6.8	15.8	2420	4.4	25.06	4.27	5.12	2.02
28.10.2005 15:00	6.8	15.5	2450	5.0	30.46	4.80	4.93	1.89
28.10.2005 18:00	6.9	15.1	2420	4.5	31.17	5.46	4.45	1.80
28.10.2005 21:00	6.8	14.6	2210	3.8	40.01	9.98	6.54	2.41
29.10.2005 00:00	7.0	14.3	1988	5.6	22.03	5.29	3.69	1.46
29.10.2005 03:00	6.8	14.4	2220	4.5	32.70	8.08	5.81	2.20
29.10.2005 06:00	6.8	15.2	2540	5.7	26.88	6.23	4.89	1.89
29.10.2005 09:00	6.7	14.8	2530	4.9	31.15	4.94	4.20	1.72

Annex 2 – Injection Logs and Slug Tests

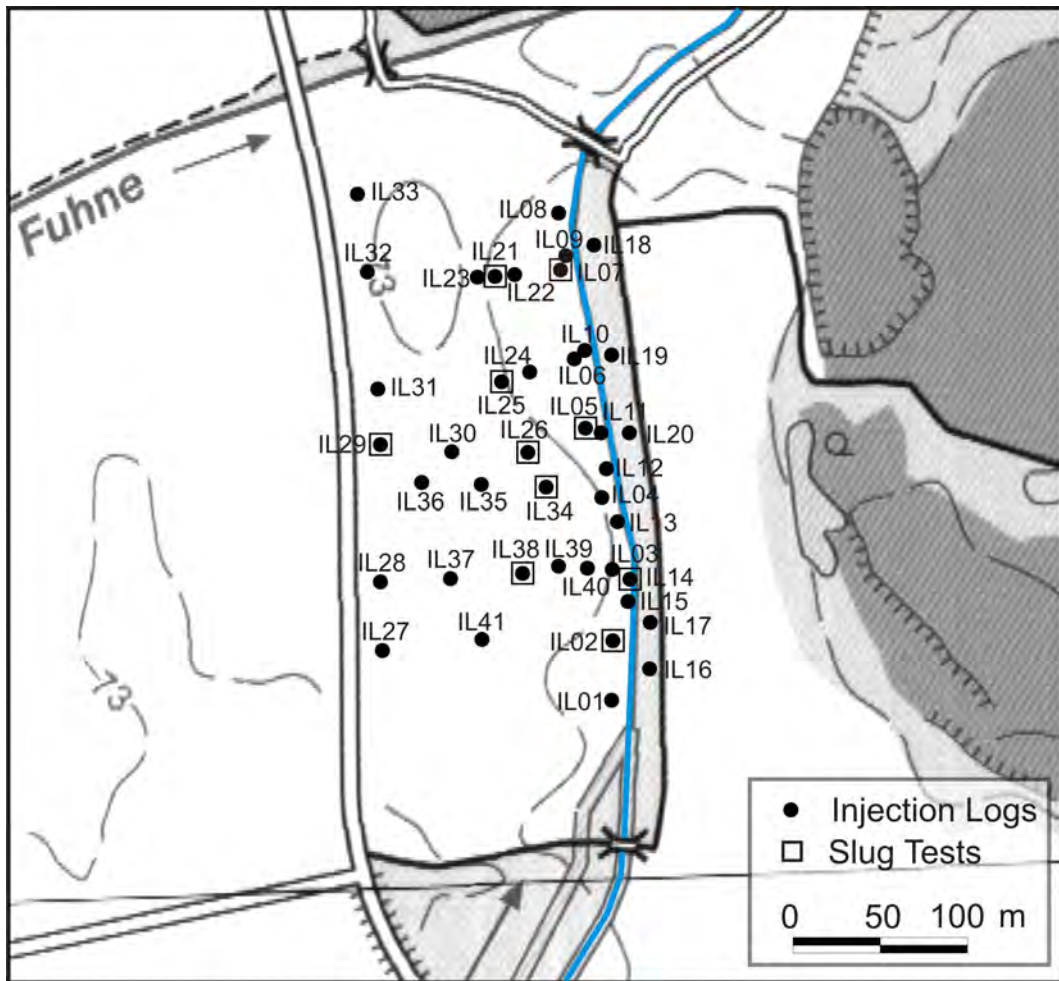


Figure A2-1. Overview of injection log and slug test locations.

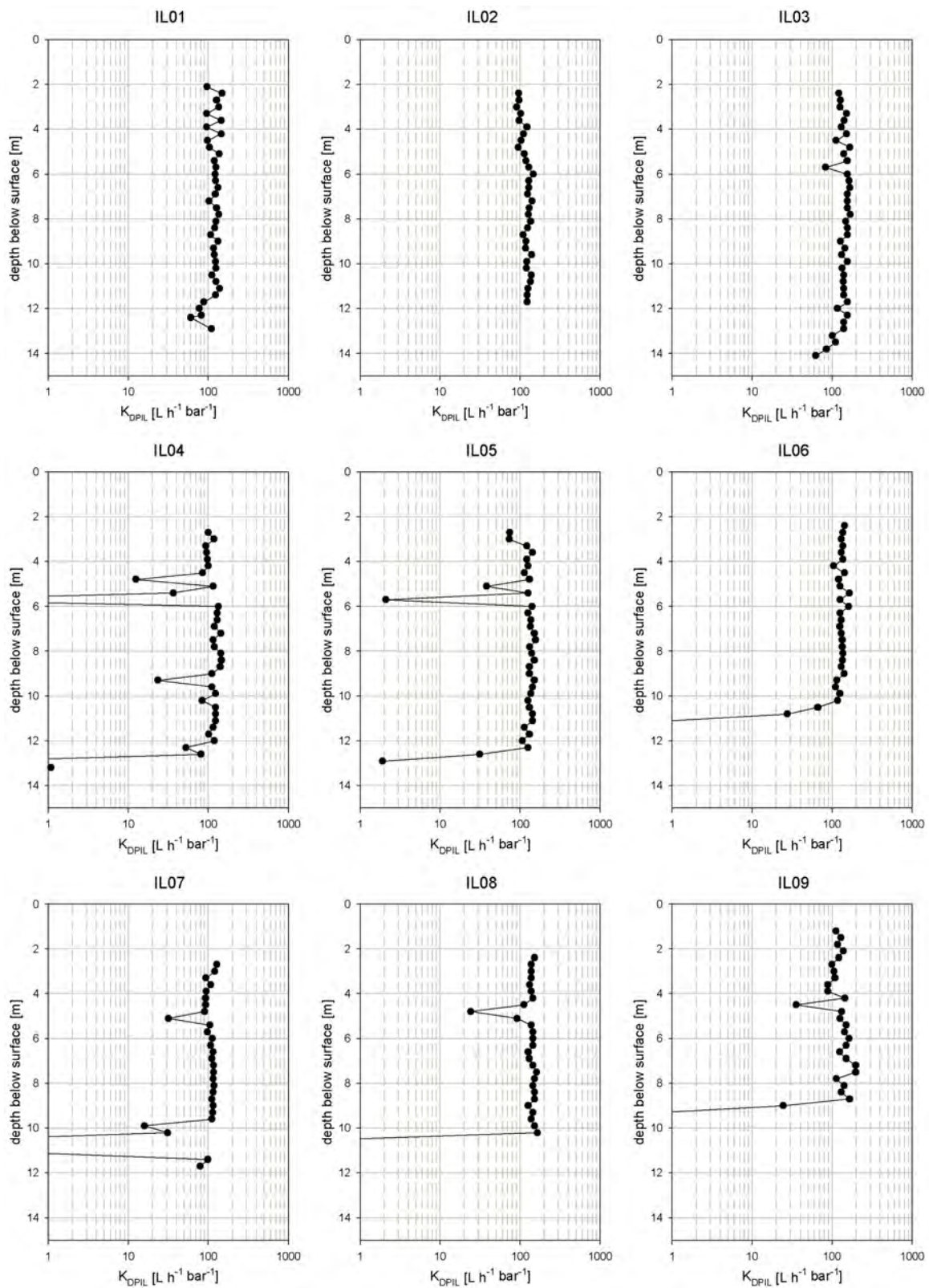


Figure A2-2. Injection logs IL01–IL09

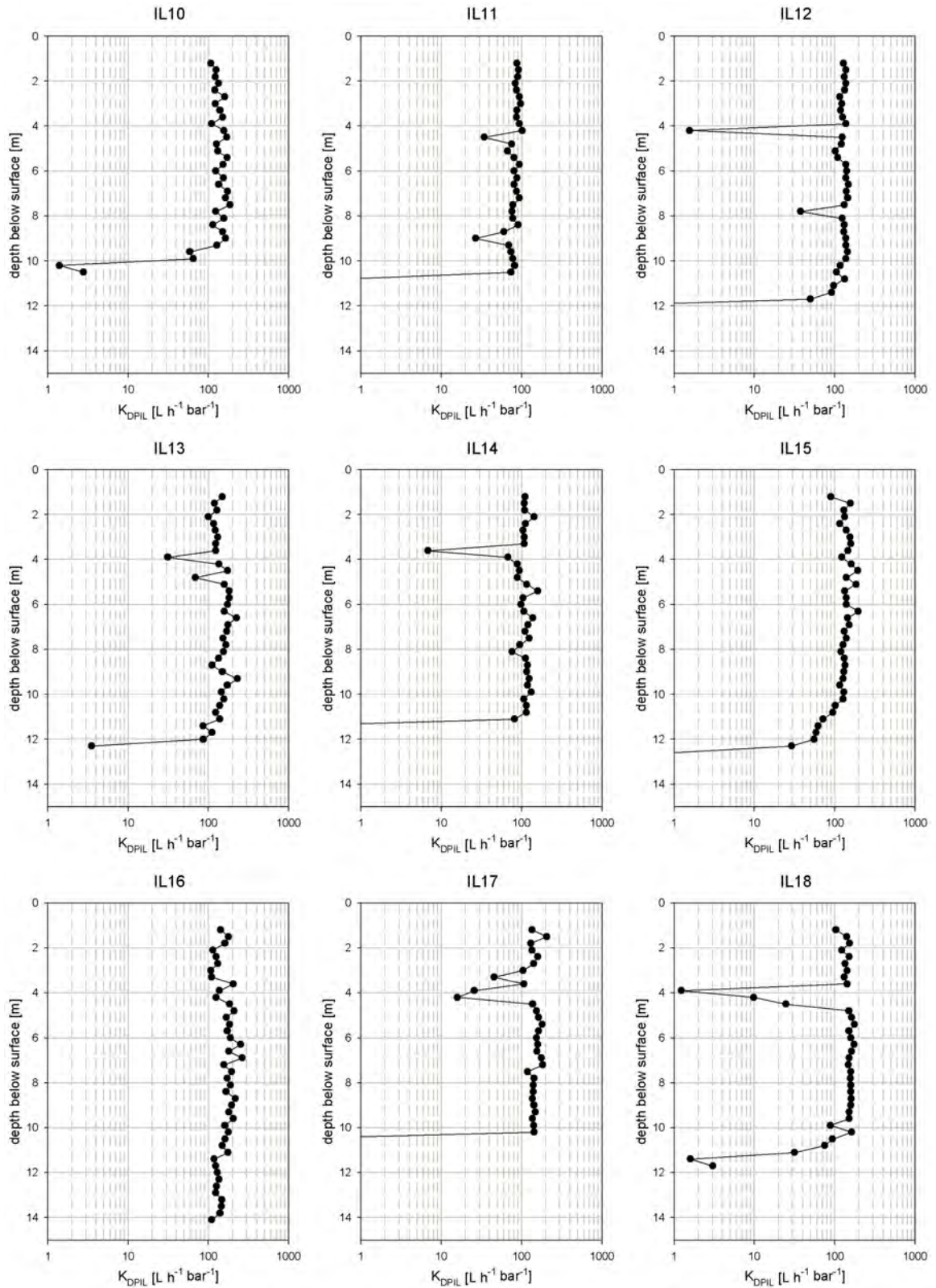


Figure A2-3. Injection logs IL10–IL18

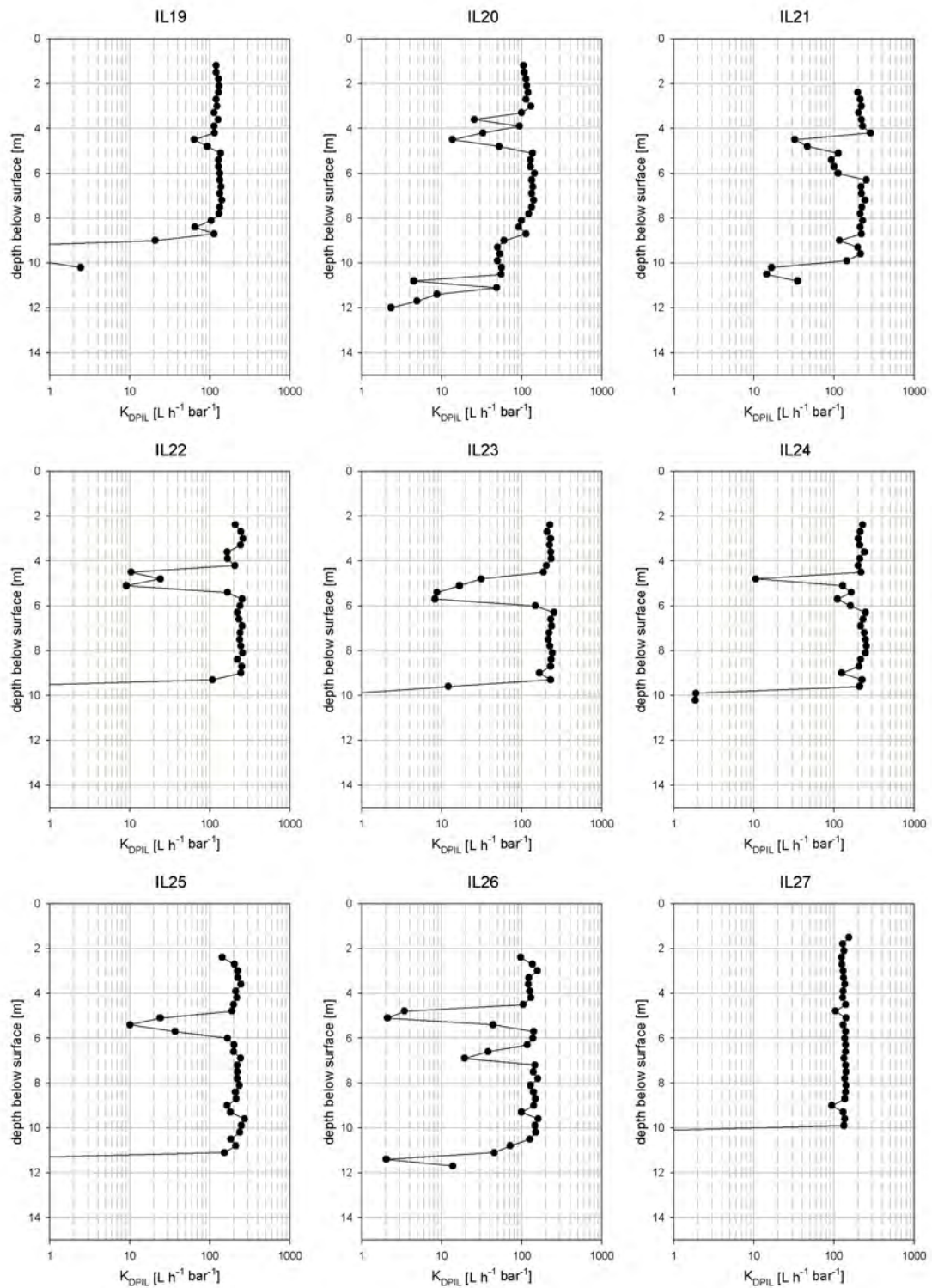


Figure A2-4. Injection logs IL19–IL27

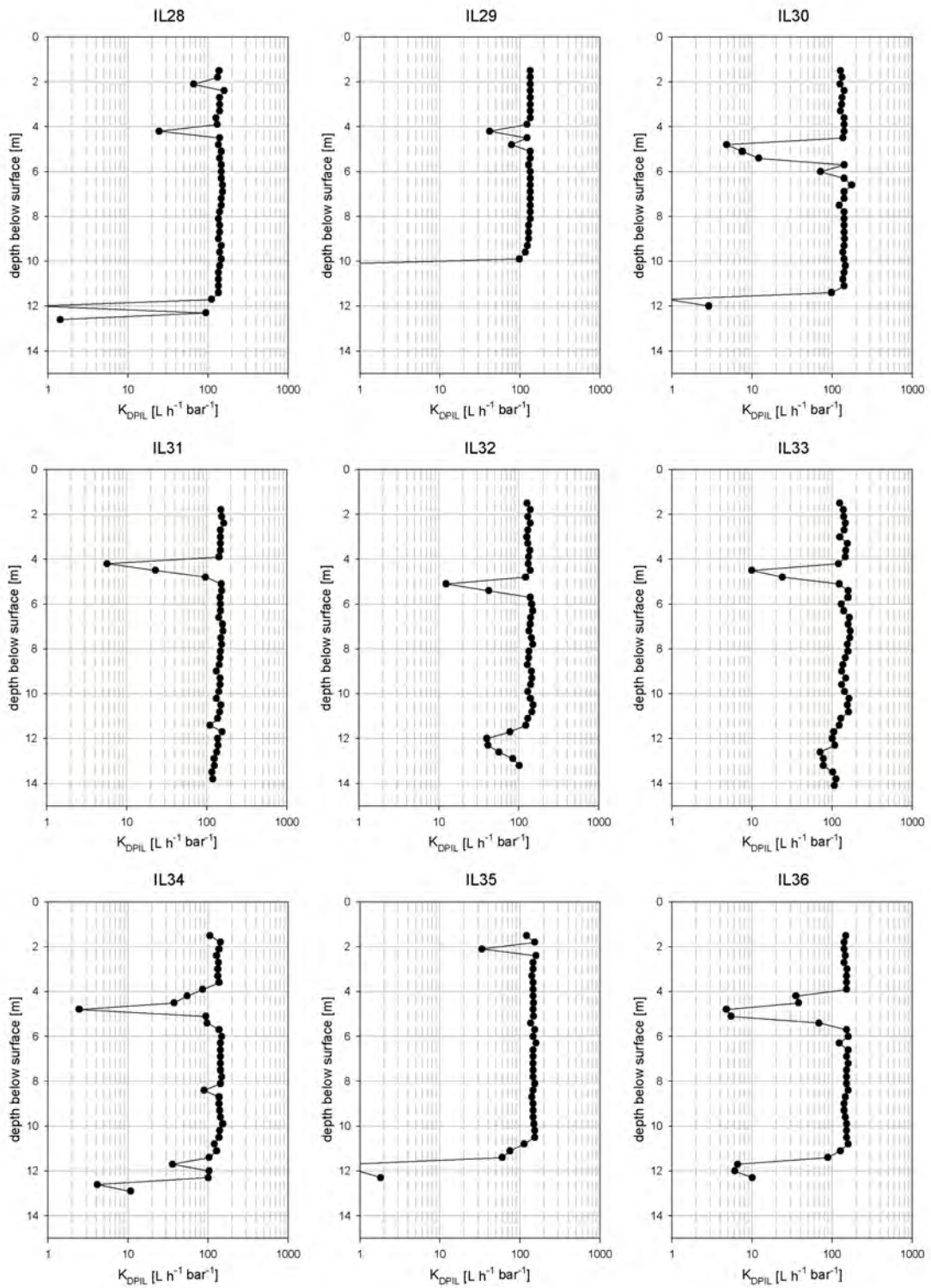


Figure A2-5. Injection logs IL28–IL36

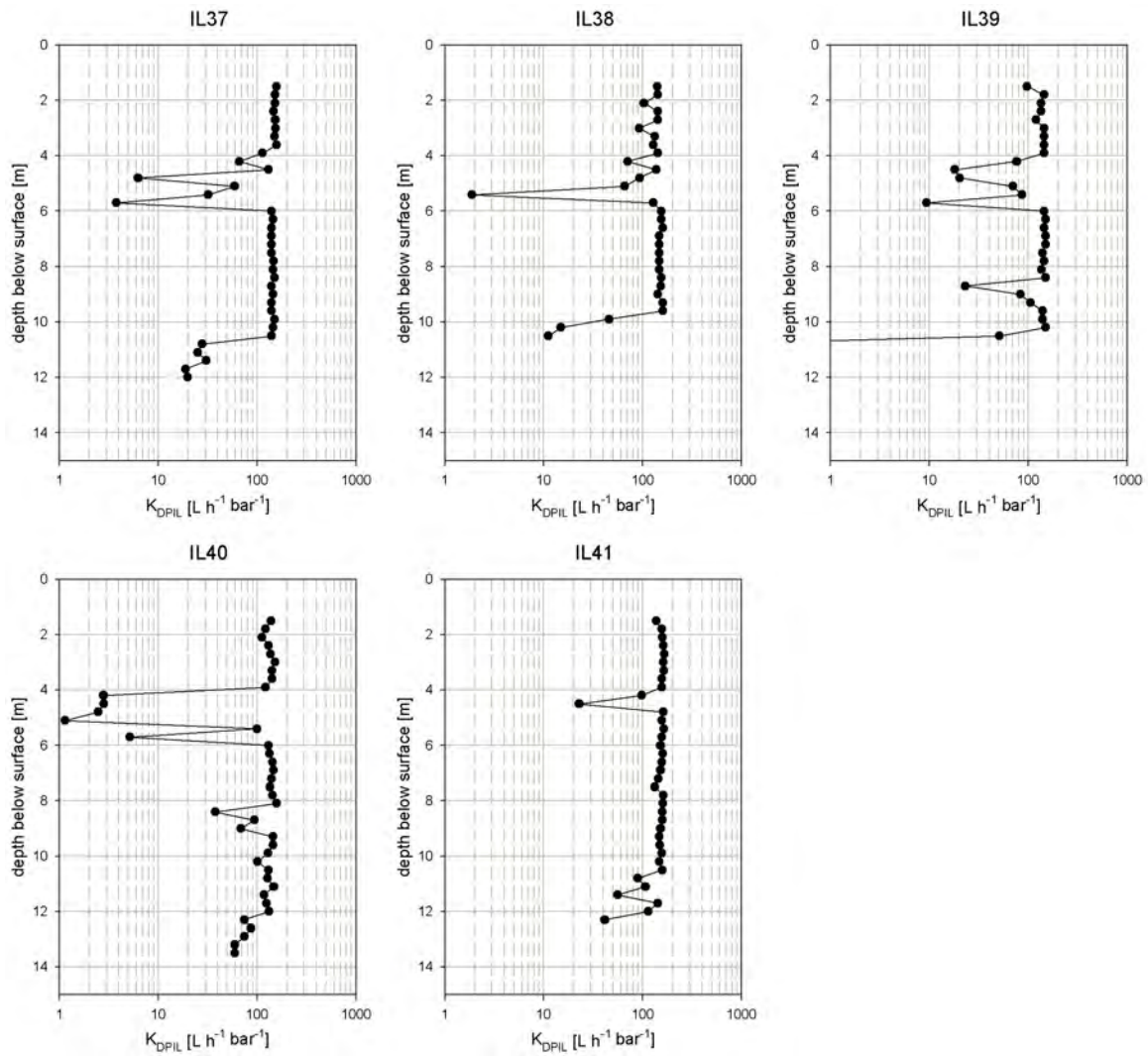


Figure A2-6. Injection logs IL37–IL41

Table A2-1. Hydraulic conductivity (K) estimates from slug tests at injection log (IL) sampling locations

IL Nr.	depth below surface [m]	K [m s^{-1}]	geometric mean K [m s^{-1}]
IL02	4.30	failed	-
	9.00	3.01E-04	3.65E-04
		3.69E-04	
		4.36E-04	
IL05	3.75	failed	-
	5.75	failed	-
	9.45	failed	-
IL07	4.20	failed	-
	5.40	failed	-
	7.20	1.73E-04	1.61E-04
		1.65E-04	
IL14	3.90	failed	-
	6.00	5.14E-04	4.62E-04
		4.42E-04	
IL22	2.50	failed	-
	5.40	9.87E-05	9.67E-05
		9.48E-05	
	7.20	3.41E-04	3.51E-04
		3.73E-04	
3.41E-04			
IL25	4.00	1.19E-04	1.32E-04
		1.10E-04	
		1.74E-04	
	5.70	failed	-
	8.00	6.02E-04	6.00E-04
6.02E-04			
IL26	3.50	9.09E-05	9.18E-05
		9.22E-05	
		9.22E-05	
	5.40	6.16E-05	6.63E-05
		7.43E-05	
		6.38E-05	
	6.00	2.82E-04	2.60E-04
		2.57E-04	
		2.43E-04	
	8.40	5.49E-04	5.34E-04
		5.88E-04	
		4.71E-04	

Table A2-1 (cont). Hydraulic conductivity (K) estimates from slug tests at injection log (IL) sampling locations

IL Nr.	depth below surface [m]	K [m s^{-1}]	geometric mean K [m s^{-1}]
IL29	3.05	2.05E-04	1.70E-04
		1.90E-04	
		1.26E-04	
	4.25	7.03E-05	2.21E-05
		1.41E-05	
		1.10E-05	
	6.95	2.10E-04	2.20E-04
		1.84E-04	
		2.77E-04	
IL34	3.30	3.76E-05	4.07E-05
		4.17E-05	
		4.29E-05	
	5.00	2.74E-04	4.98E-04
	7.00	4.94E-04	
		5.01E-04	
		5.00E-04	
IL38	4.20	failed	-
	5.70	failed	-
	7.20	8.41E-04	9.29E-04
		9.06E-04	
		1.05E-03	

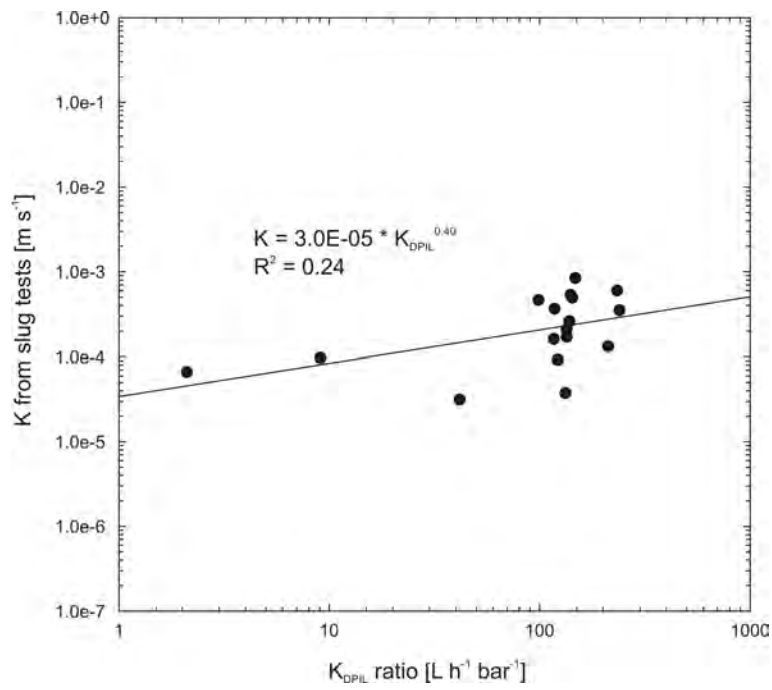


Figure A2-7. Regression analysis of K_{DPIL} ratio vs. K values obtained from slug tests.